Phenol oxidation using ruthenium and iridium catalysis

By

Huda Ramadan Aamara

A Thesis Submitted to
Saint Mary's University, Halifax, Nova Scotia
in Partial Fulfillment of the Requirements for the
Degree of Master of Science in Applied Science

April 2017, Halifax, Nova Scotia

Approved: Dr. Kai Ylijoki
Supervisor
Department of Chemistry

Approved: Dr. Marc Lamoureux
Committee Member
Department of Chemistry

Approved: Dr. Susan Bjornson
Committee Member
Department of Biology

Approved: Dr. Matthew Lukeman
External Examiner
Department of Chemistry

April 2017

ABSTRACT

Phenol oxidation using ruthenium and iridium catalysis

By

Huda Ramadan Aamara

We synthesised 4 different tri-substituted phenols: A (2-(pent-4-en-1-yl)phenol, B (4-methoxy-2-(pent-4-en-1-yl)phenol, C (curcuphenol), and D (curcuphenol). While phenols A, B, and C possessed terminal olefins, phenol D possessed a di-methyl substituted olefin. In order to catalyse the photochemical cycloaddition of these phenols, $[Ir(dF(CF_3)ppy)_2(dtbbpy)(PF_6)$**,** $Ru(bpy)_3(BF_4)_2$, and $Ru(bpy)_3Cl_2$ catalysts were synthesised. Subsequently, we explored the Ir and Ru catalysed photochemical oxidation of each phenol, with the aim of synthesising [5 + 2] cycloaddition bridged bicyclic systems. While cycloadducts were not observed, it became apparent that the reduction of the metal centre before interaction with the phenol might not be a plausible pathway. Thus, future endeavours will include the use of cationic moieties and salts, to elicit metal oxidation prior to phenol-metal interaction in order to foster the formation of a pentadienyl radical cation intermediate. It is envisaged that this pathway will favour cycloaddition.

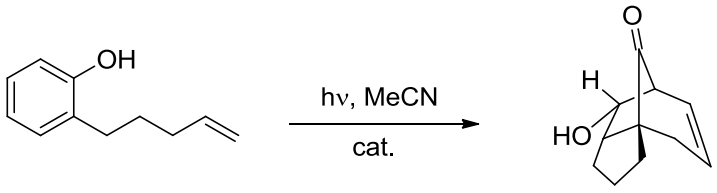

April 2017

ACKNOWLEDGEMENTS

The past two years have been a great learning experience for me in many ways. Firstly, I would like to thank Professor Kai Ylijoki for giving me the opportunity to advance my chemical knowledge and laboratory skills. His advice has helped me to improve my presentation skills and confidence. Most importantly, I thank him for always believing in me even when I did not. He's given me the chance to work with such an enthusiastic supervisor, who has provided me with endless encouragement and advice. My deepest gratitude is extended to Dr. Jetsuda Areephong. I could match this document in length with the thanks I owe her for the opportunities given and the great memories shared. Without her understanding, support, and drive I would never have reached this stage.

I would like to thank my committee members Professors Marc Lamoureux, and Susan Bjornson, for their helpful comments during my annual meetings and for their words of encouragement. I would also like to thank my external supervisor Dr. Matthew Lukeman for unselfishly taking the time from his busy schedule to help me achieve this goal. Also, I would like to thank Professor Christa Brosseau to give me a chance to do some electrochemical experiments in her laboratory. The Ylijoki Group has always been an intelligent and supportive bunch and I'm sure that will continue given the people coming through the ranks. Special thanks are extended to Darlene Goucher, Alyssa Doue' and Elizabeth McLeod for keeping the wheels of research in motion, Gratitude must also be extended to the faculty and staff of the Chemistry Department at Saint Mary's University. This work could not been completed without the use of NMRs at Saint Mary's University. To my lovely husband Reda I owe more than thanks, I owe everything. You give me support and encouragement, giving me the distractions I needed to stay in touch with reality and you are the most beautiful person in all regards. To my kids Rayan, Retag, and Rofana: Please know that I love and will always love you, and I hope I have made you proud.

CONTENTS

Page

List of Figures

Figure **page**

List of Schemes

Structure **Page**

List of Tables

Table **Page**

List of Abbreviations

Ag/AgCl	Silver Chloride Electrode
br	Broad (NMR)
BH_3Me_2S	Borane Dimethyl Sulfide
Brine	Saturated NaCl Solution
Boc_2O	Di-tert-butyl Dicarbonate
CAN	Ceric Ammonium Nitrate
Cat.	Catalyst
˚C	Degrees Celsius
$CHCl_3$	Chloroform
CH_2Cl_2	Dichloromethane
$(CH_3COO)_2Pb.PbO$	Lead Acetate Basic
CV	Cyclic Voltammetry or Voltammogram
d	Doublet
DCM	Dichloromethane
dd	Doublet of Doublet (NMR)
dt	Doublet of Triplet (NMR)
dF(CF3)ppy	2-(2,4-difluorophenyl)-5-trifluromethylpyridine
dtbbpy	4,4-di-tert-butyl-2,2-bipyridine
DMAP	4-Dimethylaminopyridine
DMSO	Dimethysulphoxide
mCPBA	meta-chloroperbenzoic acid
EC-SERS	Electrochemical Surface-Enhanced Raman Spectroscopy
Et_3N	Triethylamine
EtOAc	Ethyl Acetate

EtOH	Ethanol
equiv.	Equivalent
H	Hour
HCl	Hydrochloric Acid
NH_4Cl	Ammonium Chloride
HOMO	Highest Occupied Molecular Orbital
H_2O	Water
H_3PO_2	Phosphinic Acid
Hz	Hertz
IR	Infrared
J	Coupling Constant (NMR)
L	Ligand
LRMS	Low Resolution Mass Spectrometry
LUMO	Lowest Unoccupied Molecular Orbital
m	Multiple (NMR)
m-CPBA	*meta*-Chloroperoxybenzoic acid
MeCN	Acetonitrile
MeOH	Methanol
min	Minute
MLCT	Metal-to-Ligand Charge Transfer
mol	Mole
MS	Mass Spectrometry
NH_3	Ammonia
NMR	Nuclear Magnetic Resonance
ppm	Parts per Million
Py	Pyridine

quint	Quintet (NMR)
quart	Quartet (NMR)
rt	Room Temperature
s	Singlet (NMR)
SET	Singlet-electron transfer
t	Triplet (NMR)
THF	Tetrahydrofuran
TLC	Thin-layer Chromatography
UV	Ultraviolet Light
2,2-bpy	2,2-bipyridine
δ	Chemical Shift (NMR)

Chapter 1

1.1 Objectives of this Thesis

The objective of this thesis is to perform [5+2] cycloaddition reactions by oxidizing phenol compounds via ruthenium and iridium photocatalysis. As a light source choice, LED light has some considerable advantages over UV lamp. LED light is readily produced from small bulbs, while UV lamp requires larger equipment. In addition, LED bulbs require less energy consumption, while UV lamps use a relatively large amount of energy. Although UV light is generally required in everyday organic photochemical syntheses, it has an increased possibility of dangerous side effects. Also it is harder and more expensive to perform UV-based large-scale photochemical reactions due to the need for more photoreactors. By adopting wavelengths of the visible spectrum (for example, blue light), clean and more efficient methods of photochemistry are promoted.

1.2 Scope of this Thesis

This thesis consists of four chapters. Chapter 1 introduces the objectives and states the scope of this thesis. It also features a review of the two forms of ring formation, namely cycloaddition and cyclization, with some examples. Section 1.2 gives an introduction of photochemistry and a brief history of the concept of light in addition to important laws in the field of photochemistry. Section 1.3 provides background theory including NMR spectroscopy, infrared (IR) spectroscopy, mass spectrometry (MS), Raman spectroscopy, and the electrochemical process of cyclic voltammetry because they

are the main characterization methods in the analyses of compounds that are used in this thesis.

Experimental procedures are presented in Chapter 2. This chapter encompasses the preparation of phenol compounds A, B, C, and D as well as those of the ruthenium catalysts, $Ru(bpy)_3Cl_2$ and $Ru(bpy)_2BF4$, and the iridium catalyst, $[Ir(dF(CF_3)ppy)_2(dtbbpy)(PF_6)$. In addition, Chapter 2 presents the results of the electrochemical methods, CV and EC-SERs which were used to perform various tests on phenol compound A. Chapter 3 is the results and discussion, including important details on the synthesis and characterisation. Lastly, the conclusion and future work are presented in Chapter 4.

1.3 Introduction

The investigation and development of new synthetic strategies is very important because these methods can later be applied to the construction of desirable bioactive natural products and some types of drugs. Ring systems are a key aspect of these natural products, which is why an in-depth knowledge of their synthesis is important. Recent studies indicate that of all the anti-cancer drugs made available since the 1940s,[1] about fifty-percent either were natural products or directly derived natural products. When looking at natural products, a large number of them contain rings of various sizes as shown in Figure 1-1. The anti-cancer agent (+)-ptaquiloside bears three, five, and six-membered rings, [1] sesquiterpenoid (+/-)-lasidiol contains five and seven membered rings,[2] and the antibiotic macrolide roxaticin is an example of a 30-membered macrocycle.[3]

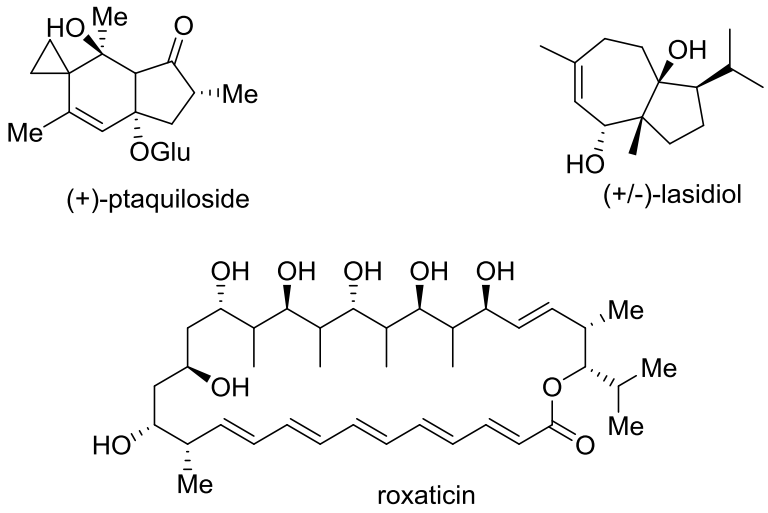

Figure 1.1: Examples of rings in natural products

1.4 Ring Formation

The two main strategies used to form rings in organic chemistry are cyclization and cycloaddition. A cycloaddition reaction occurs when two (or more) unsaturated molecules or parts of the same molecule combine to form a cyclic adduct, in a [m + n] fashion, resulting in a [m + n]-membered ring.[1] A cyclization reaction is defined as the connection of two functional groups to form rings of varying sizes.[2]

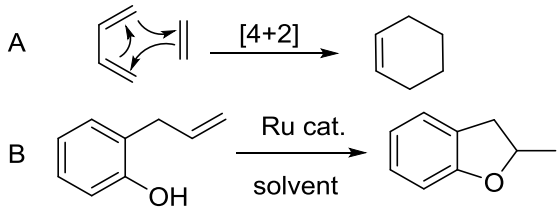

Scheme 1.1: Simple schemes of cycloaddition (A) and cyclization (B) reactions

1.4.1 Cycloaddition Reactions

Cycloaddition reactions have gained importance in synthetic organic chemistry because these reactions allow multiple carbon-carbon bonds to be formed in a single step. While cycloaddition pathways leading to four, five, and six-membered rings have been extensively explored in the past, the synthesis of seven-membered rings resulting from [5 + 2] cycloaddition reactions, has yet to be investigated in depth. Due to continuous discovery of seven-membered carbocycles in bioactive natural products, the preparation of these compounds via traditional organic synthesis has gained popularity despite difficult synthetic procedures.[3] Chemists have become interested in studying phenol oxidation as a starting point to explore this challenge. Phenols participate in a rich variety of oxidatively induced transformations,[4] which can produce a number of complex structures commonly found in bioactive molecules, for example, terpenoids and neolignans.[5] Although oxidized phenol compounds have been used to produce cyclic compounds in the past, the yields were low.[6] This chapter gives an overview of important reactions which have used electrochemical methods to oxidize phenols.

The perezone-pipitzol transformation, performed in 1885, was the first example of a [5 + 2] cycloaddition.[7] This synthesis was carried out by Anschutz and Leather via the reaction of the perezone silver salt with ethylene bromide (Scheme 1.2). However, it was not until 1965 that Joseph-Nathan and co-workers determined the structure of the products from this reaction.[8] Although the incorrect characterisation of the perezone

initially led to a wrong mechanistic proposal, Joseph-Nathan and co-workers later corrected their error and deduced the proper structure of perezone. This allowed for the right elucidation of the mechanism to show that a concerted [5+2] cycloaddition was responsible.

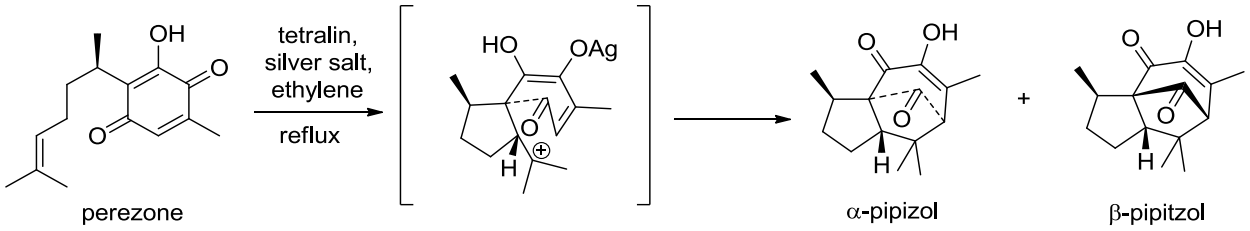

Scheme 1.2: The Perezone-Pipitzol Rearrangement

Yamamura and co-workers have also synthesized some bioactive natural products using electrochemical methods such as terpenoids, neolignans, and futoenone, which were used as potential chemopreventive and therapeutic agents in liver cancer.[9,10,11,12] They reported that the anodic oxidation of 3,4-dimethoxyphenols with different side chains produced both intramolecular [5 + 2] cycloaddition products and spiro compounds with a low yield of only 22% (Scheme 1.3).

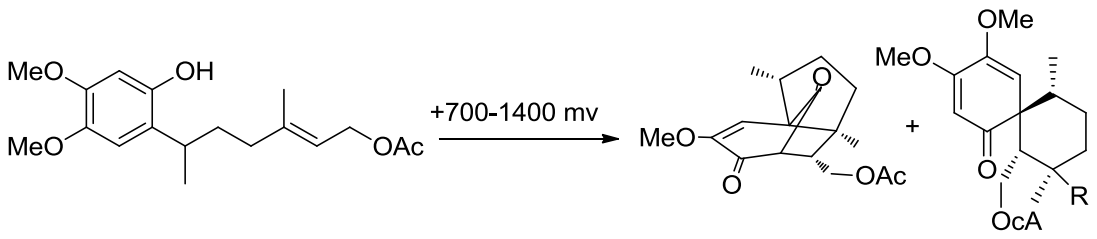

Scheme 1.3: Yamamura's [5 + 2] cycloaddition and spiro compounds

More recently, Pettus and co-workers reported an intramolecular [5 + 2] cycloaddition achieved by oxidizing curcuphenol to make α-cedrene, α-pipitzol, and sec-cedrenol. However, their yields were also low (Scheme 1.4).[13] This reaction proceeded with good diastereoselectivity in comparison to the work of Yamamura.

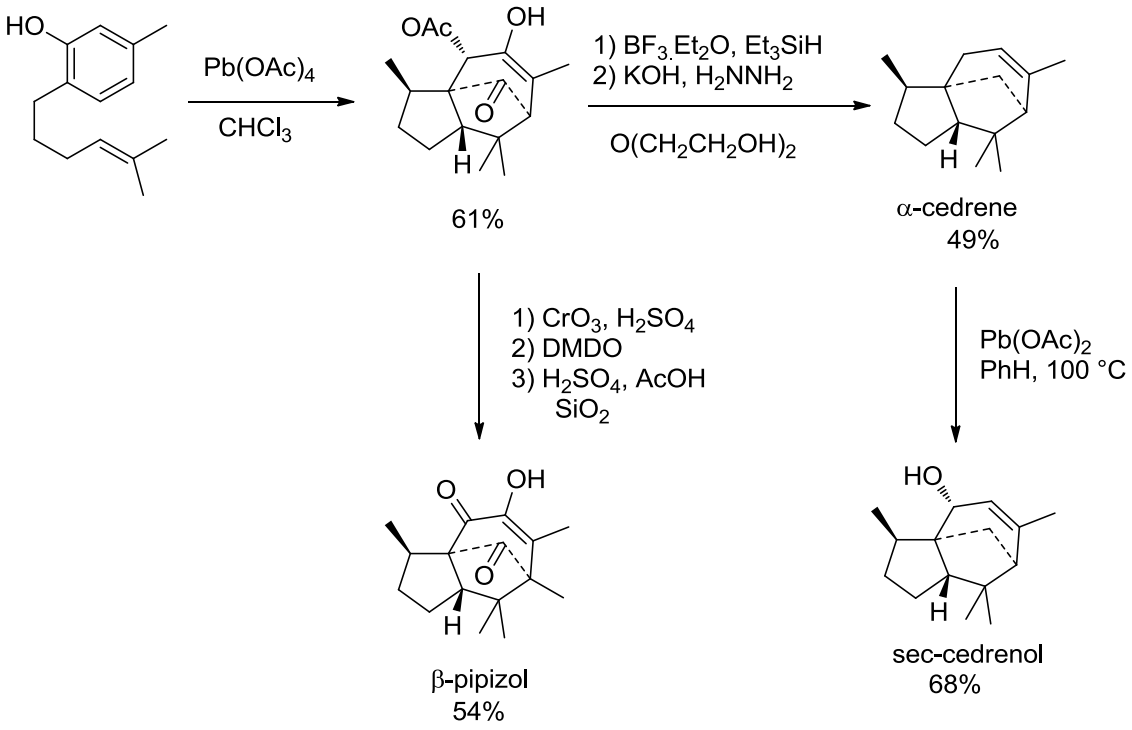

Scheme 1.4: Pettus' dearomatization with successive [5+2] cycloaddition reaction

1.4.2 Cyclization Reactions

The products of cyclization reactions are usually synthetically useful compounds that can be created using side chains of the reactant. For example, the work of Ito and co-

workers demonstrates how an intramolecular cyclization of 2-allyl phenol yields 2,3-dihydro-2-methylbenzofuran (Scheme 1.5). Although this reaction created a cyclic product with an excellent yield of 90% when using the copper catalyst $Cu(OTf)_2$, the yield was low when using a ruthenium catalyst ($RuCl_3.nH_2O$).[14]

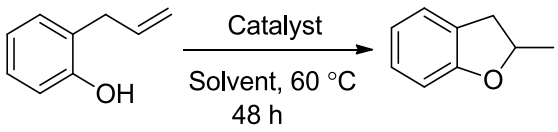

Scheme 1.5: Cyclization reaction of phenol compound

The synthesis of seven-membered rings is difficult to perform via non-catalysed means, as the transition states of such reactions are generally destabilized by the presence of non-bonding interactions, and the reaction itself is unfavorable from an entropic standpoint. These energy barriers can be overcome via low energy transition metal catalysis. Seven-membered carbocycles are found in a large number of natural products, such as the fondosin family,[15] phoorbol esters,[16] guanacasterpenes,[17] and ingenol.[18] Strategies for the synthesis of such structural motifs are therefore wide-ranging, from metathesis reactions,[19] and transitions metal-catalyzed cyclization [20] and cycloadditions.[21]

These examples give a brief introduction to the importance of rings in organic chemistry and the synthesis of natural products. This work will focus on Ru and Ir catalyzed [5+2] cycloaddition reactions of phenol compounds (Scheme 1.6). In the metal-catalyzed reaction, the transition metal oxidizes the phenol compound to form a

pentadienyl cation ring compound, which reacts with a tethered olefin to form a seven-membered ring, which can be complete in single step.

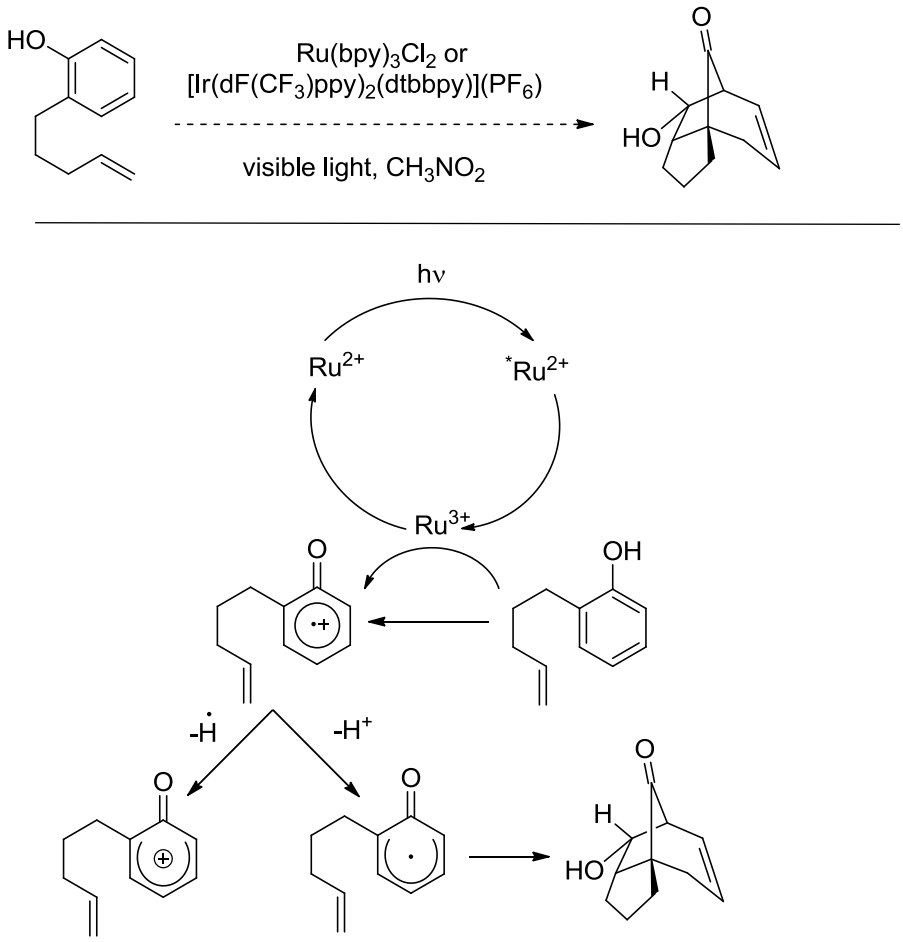

Scheme 1.6: Proposed mechanism of phenol oxidation using ruthenium and iridium catalysts

1.5 Photochemistry in Organic Chemistry

Since the dawn of photochemistry, scientists have been interested in light as an energy source for chemical reactions. By absorbing light, molecules reach an electronically excited state. The chemical properties and the reactivity of the excited state molecules changes and the reaction spectrum of a family of compounds is broadened considerably. In some instances, using photochemical steps significantly shorten a total synthesis, and complex, polycyclic, or highly functionalized structures can frequently be obtained from simple substrates. This section will give a brief historical overview of light as an energy source and will discuss important laws in the field of photochemistry.

1.5.1 A brief history of the concept of light

The first theories about light came from the ancient Greeks who conceived of light as a ray, a straight line moving from one point to another. Pythagoras proposed that vision results from light rays emerging from a person's eye and striking an object.[22] Epicurus argued the opposite, stating that objects produce light rays that then travel to the eye. Other Greek philosophers like Euclid used ray diagrams to show how light bounces off a smooth surface or bends as it passes from one transparent medium to another. Geometrical optics, which has led to products like mirrors, lenses, and prisms, were later developed by Arab scholars.[23] Ibn al-Haytham (Alhacen), who lived in present-day Iraq between 965 and 1039, is considered the father of modern optics and ophthalmology. He

identified the optical components of the human eye and correctly described vision as a process involving light rays bouncing from an object to a person's eye.

In 1695, Christiaan Huygens proposed the existence of some invisible medium (luminiferous aether) filling all empty space between objects.[24] He further speculated that light forms when a luminous body causes a series of waves or vibrations in this aether. Those waves then advance forward until they encounter an object. If that object is an eye, the waves stimulate vision. In 1900, Max Planck, attempting to explain black body radiation, suggested that although light was a wave, these waves could gain or lose energy only in finite amounts related to their frequency. Planck called these "lumps" of light energy "quanta". In 1905, Albert Einstein used the idea of light quanta, later called photons, to explain the photoelectric effect.[25] The concept of a photon allowed photochemistry to emerge from its empirical stage. When it became clear that absorption of light corresponds to the capture of a photon by an atom or a molecule, Johannes Stark and Albert Einstein independently formulated one of the two laws that form the basis of the field of photochemistry between 1908 and 1913.[26]

1.5.2 Fundamentals of photochemistry

Photochemistry utilizes electromagnetic radiation to bring about chemical change in a molecule. This change results from the absorption of a photon,[27] which transforms a molecule from the ground state into an electronically excited state. The reactivity of a molecule in a photochemical reaction is governed by two laws. According to the first law, known as the Grotthuss-Draper Law, light must be absorbed by a compound in order for

a photochemical reaction to take place.[28] The second law, known as the Stark-Einstein Law, states that each photon absorbed leads only to one photochemical activation.

To explain these laws, it can be shown that the absorption of a photon by an organic molecule creates an electronically excited state. This gain in energy promotes an electron from the highest occupied molecular orbital (HOMO) to the lowest unoccupied molecular orbital (LUMO). Once a molecule is in the excited state, the excited electron can cause a number of different processes that can be divided into two categories: non-radiative and radiative processes. Non-radiative decay processes describe the conversion of one electronic state into another without the emission of light. In contrast, radiative processes return the electron to the ground state with the emission of a photon as shown in the Jablonski diagram (Figure 1-2), which details S_0 as the singlet ground state, S_1 as the singlet excited state (pair of electrons with opposite spins but each in a different orbital), and T_1 as the triplet excited state (pair of electrons with parallel spins in different orbital). When a molecule is exposed to light or radiation it may absorb energy and subsequently re-emit the energy, via the process of fluorescence. Some molecules, which continue to glow for some time even after external light has ceased, continue to emit energy via phosphorescence.

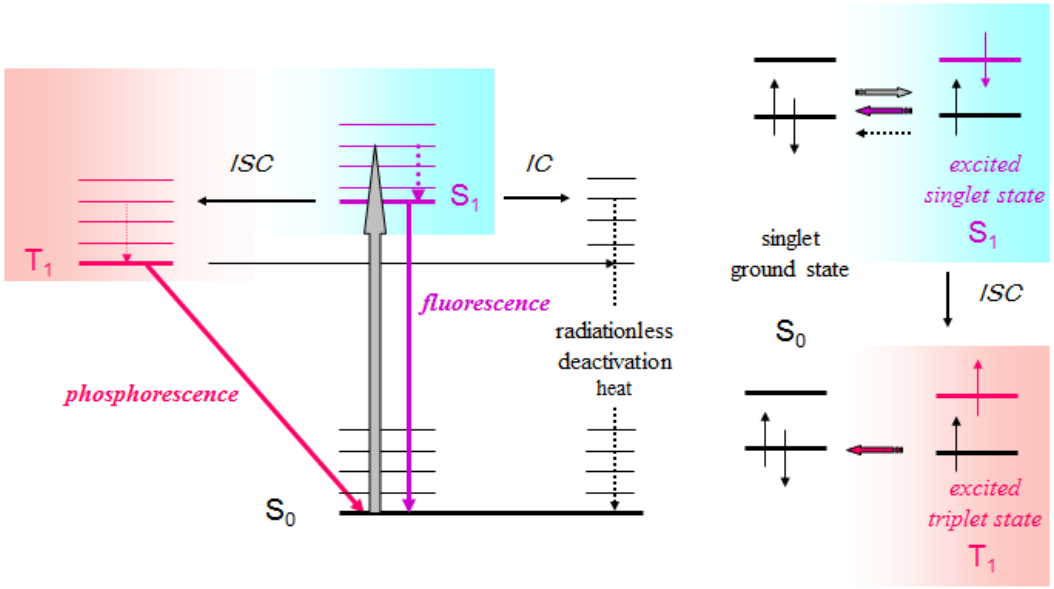

Figure 1.2: Jablonski diagram (Adepted from ref 26)

Once a molecule is excited, there are many ways to dissipate the energy produced. The first is through vibration relaxation, a non-radiative process, which can be seen in the Jablonski diagram arrow between vibration levels. Vibrational relaxation is where the energy deposited by the photon to the electron is given away to other vibrational modes as active energy. This active energy may stay in the same molecule, or may be transferred to other molecules around the excited molecule depending on the phase of the sample. The excited molecule can transition from a vibration level in one electronic state to another vibration level in a lower electronic state, which is called internal conversion, and is identical to vibration relaxation. This internal conversion occurs because of the overlap of vibrational and electronic energy state. As energies increase, the manifold of

vibrational and electronic eigenstates becomes even closer distributed. At energy levels greater than the first excited state, the manifold of vibrational energy level strongly overlaps with the electronic levels. Subsequently, the overlap gives a higher degree of probability that the electron can transition between vibrational levels that will lower the electronic state.[29,30,31,32,33,34,35]

Another path a molecule may take in the dissipation of energy is called fluorescence, which is shown in a Jablonski diagram as a straight line going down on the energy axis between electronic states. Fluorescence is most often observed between the first excited electron state and the ground state for any particular molecule because at higher energies it is more likely that energy will be dissipated through internal conversion and vibrational relaxation. The energy of the photon emitted in fluorescence is always less than the exciting photon because energy is lost in internal conversion and vibrational relaxation. Intersystem crossing is another path a molecule may take in the dissipation of energy. In this way, the electron changes from an excited singlet state to an excited triplet state, which can show as an arrow from one column to another.[36]

1.6 Photoredox catalysts

1.6.1 Introduction

Photosynthesis, which is the fuel of life, is the best example of how light can propagate chemical reactions, whereby during the day, plants absorb light to generate molecules. Based on this process, photochemistry involves the transfer of single electrons and uses light-activated catalysts to generate electron transfer. In 1912, Ciamician proposed using photocatalysts to mediate chemical reactions.[37] Since then, efforts have been made to use catalysts and different metals that are able to absorb light to produce pharmaceutical compounds and other materials.[38,39,40] In the field of synthetic chemistry, the process of mediating organic transformations by using visible light has been promoted as being environmentally-friendly by several like MacMillan,[41] Yoon,[42] Stephenson,[43] and many other researchers.[44]

The most famous photoredox catalysts include ruthenium polypyridine complexes and iridium complexes, which have been shown to be strong tools for oxidation and reduction reactions because of their ability to mediate single electron transfer. This ability of both catalysts have attracted the attention of many researchers, who are interested in developing new types of reactions in green chemistry. Since 2008, this kind of research has represented one of the new trends in organic chemistry and it is still expanding.[45] While photoredox processes of Ru and Ir polypyridine complexes take place at room temperature, these catalysts are excited by visible light (e.g. sun light), which is considered a mild and abundant stimulus. Another irradiation source is the light bulb,

which has important advantages over the high-energy ultraviolet (UV) light. It is important to note that most organic molecules do not absorb visible light, so there is little potential for side reactions that might be caused by photoexcitation itself. [46]

1.6.2 $[Ru(bpy)_3]^{2+}$

In 1936, Burstall reported the first successful synthesis of $[Ru(bpy)_3]^{2+}$ by reacting $[RuCl_3].H_2O$ with excess 2,2-bipyridine (bpy), using ethanol (EtOH) as a reaction solvent. The Ru(II) center is a stable low-spin d^6 species and it forms an octahedral coordination complex with diamagnetic t_{2g}^6 electronic formations (Figure 1.3).[47] Since then, there has been an increasing interest in using this type of complex in photoreactions. $[Ru(bpy)_3]Cl_2$ has become the standard reference for comparing other ruthenium polypyridyl systems because its photochemical and photophysical properties are well documented. [48,49,50,51,52]

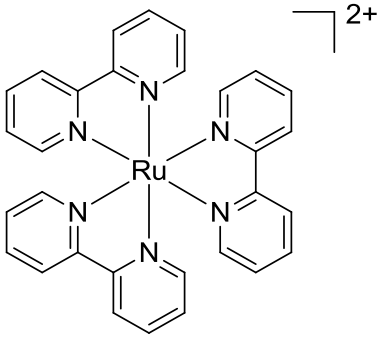

Figure 1.3: Octahedral structure of $[Ru(bpy)_3]^{+2}$

1.6.2 Mechanism of photocatalysis

Ruthenium $[Ru(bpy)_3]^{2+}$ complex is a famous photoredox catalyst because it has some interesting properties. Firstly, it absorbs a photon in the visible light range around 450 nm, and the photoexcitation can be performed using LED lamps, UV light or even natural sunlight. The electron transfers from π orbital of the ruthenium center to the π^* orbital of the 2,2-bipyridine ligand (MLCT) resulting in $Ru(bpy)_3^{2+*}$. Subsequently, intersystem crossing is fast enough for chemical transformations to proceed. Thirdly, the triplet excited state $[Ru(bpy)_3]^{2+*}$ undergoes single-electron-transfer (SET) to/from external organic molecules to serve as either a single electron oxidant or reluctant. Therefore, Ru catalysts have become popular for redox reactions. (Figure 1.4).

After light absorption, photoexcited species performing redox reactions thought two pathways, which are dependent on the reaction conditions employed. The first redox reaction pathway involves the oxidative cycle from the photoexcited species $[^*Ru(bpy)_3^{2+}]$. The $[^*Ru(bpy)_3^{2+}]$ excited species is initially oxidized by an electron donate to give $[Ru(bpy)_3^{3+}]$ The oxidized photosensitizer can be reduced by an electron except to complete the catalytic cycle and regenerate the $[Ru(bpy)_3^{2+}]$. The second redox reaction pathway is reductive cyclic of the excited state $[^*Ru(bpy)_3^{2+}]$ via an electron donating to yield $[Ru(bpy)_3^{+}]$. The reduced species can undergo oxidation in the presence of suitable electron withdrawing groups to regenerate the original $[Ru(bpy)_3^{2+}]$ complex and complete the catalytic cycle.

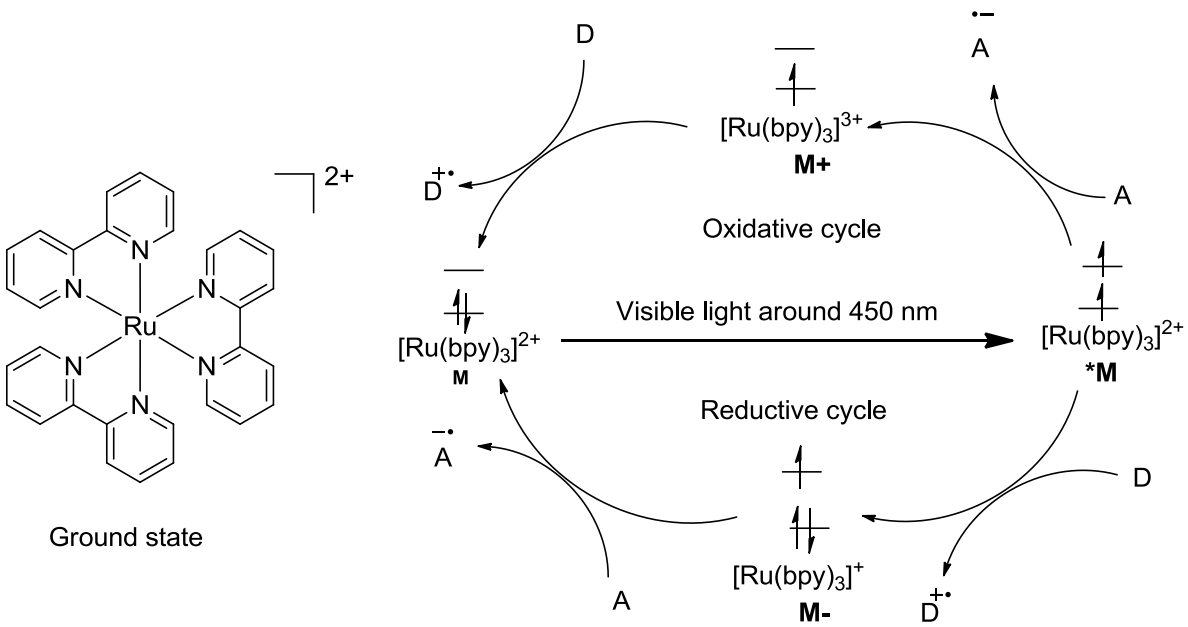

Figure 1.4: Oxidative and reductive quenching cycles for $[Ru(bpy)_3]^{2+}$ (Adapted from ref. 36)

1.7 Photoredox catalysis for organic synthesis

Most of the photoredox mediated synthetic transformations described in this section use transition metal-ligand complexes, especially those with ruthenium and iridium as the transition metal of choice. This is because these catalysts have a higher ability to perform oxidation and reduction reactions in their excited states compared to those of other metal-ligand complexes.

1.7.1 Ruthenium photoredox catalysts

The single electron oxidation pathway has become a very common method for photoredox catalysis. In 1984, Cano-Yelo and Deronzier reported the first photocatalytic Pschorr reaction for the synthesis of phenanthrene.[53] The Pschorr reaction is the arylation of a diazonium salt by using visible light, a ruthenium catalyst, and the solvent acetonitrile to produce phenanthrene carboxylic acids in good yield.[54,55] Some other oxidation reactions of aryldiazonium have been reported by Toste and co-workers.

The proposed mechanism of this reaction shown in (Scheme 1.7) is proceeded by the excitation of $Ru(bpy)_3^{2+}$ by visible light to generate $Ru(bpy)_3^{2+*}$, which transfers an electron to the diazonium to produce an aryl radical, which undergoes in intramolecular arylation. Following intramolecular radical arylation, $Ru(bpy)_3^{3+}$ oxidizes the radical, and final deprotonation yields phenanthrene carboxylic acids, whit regenerating the catalyst $Ru(bpy)_3^{2+}$.

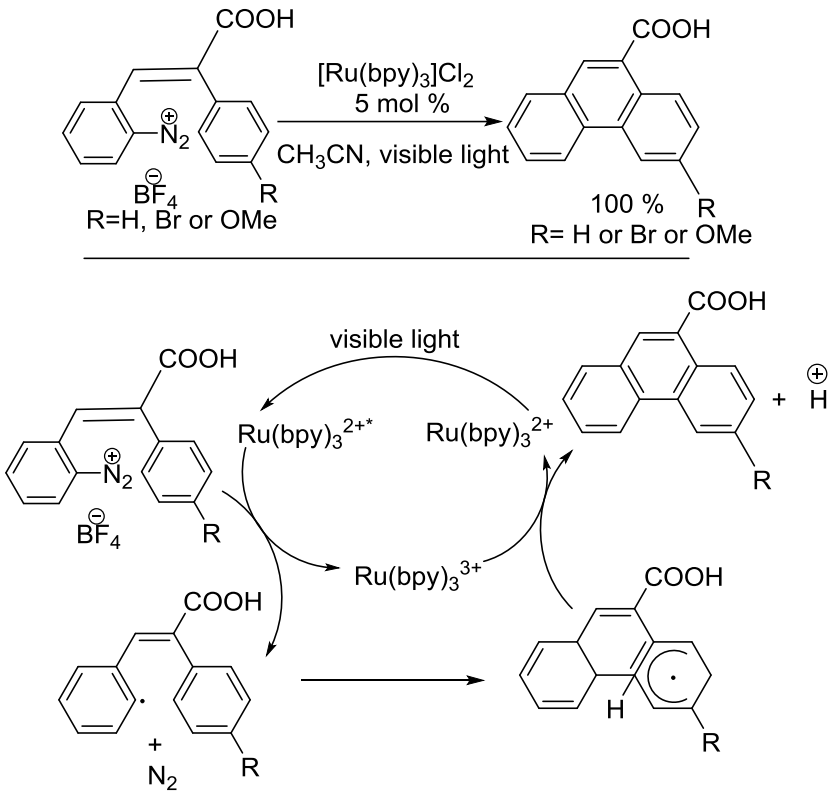

Scheme 1.7: Photocatalytic Pschorr reaction

In the same year, inspired by their first success, Cano-Yelo and Deronzier reported using a ruthenium photoredox catalyst, $[Ru(bpy)_3]Cl_2$, an aryl diazonium salt and MeCN in the oxidation of a benzylic alcohol to produce an aldehyde (Scheme 1.8).[56] The authors proposed a mechanism started by the use of aryldiazonium ion to generate $Ru(bpy)_3^{3+}$ and aryl radical. Following the single electron oxidation by $Ru(bpy)_3^{3+}$, benzylic alcohol forms a radical cation also regenerating $Ru(bpy)_3^{2+}$. The hydrogen atom of the radical cation is abstracted by the aryl radical followed by deprotonation to form aldehydes in a yield of 90%.

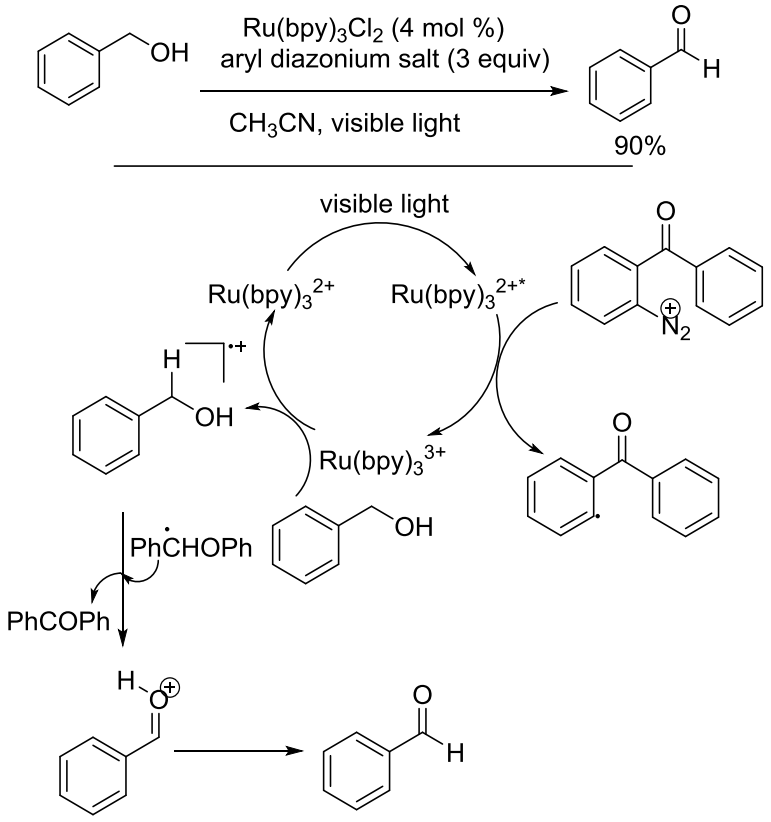

Scheme 1.8: Oxidation of benzylic alcohols using photocatalysis

The formation of carbocycles from photochemical [2 + 2] cycloaddition reactions has been common since 2008.[57,58] Yoon and co-workers reported the [2 + 2] cycloaddition reaction of enone compounds (Scheme 1.9).[59,60] The researchers reported that the excitation of $Ru(bpy)_3^{2+}$ by visible light generates the photoexcited state $Ru(bpy)_3^{2+*}$, which is followed by a single electron transfer from $^{i}Pr_2NEt$ to form $Ru(bpy)_3^{+}$. This $Ru(bpy)_3^{+}$ complex is a powerful reducing agent that can transfer an

electron to the lithium-activated enone to produce a radical compound, which finally leads to the formation of cyclobutane with a yield of 89%.

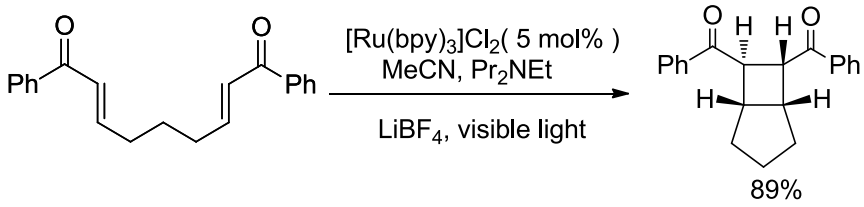

Scheme 1.9: Visible light photocatalyzed [2 + 2] cycloaddition

1.7.2 Iridium photoredox catalysts

Iridium complexes have been used as catalysts for many types of reactions. These reactions include homogeneous hydrogenation,[61,62] asymmetric ring opening reactions,[63] and cycloadditions.[64,65] In this section, only the Ir-catalyzed cycloaddition reactions will be discussed.

Iridium complexes have the same character as ruthenium polybipyridine complexes, so the field of reactions in organic synthesis that can be caused by excited-state iridium complexes, mirrors that of ruthenium complexes. In some cases, the replacement of the ruthenium complexes with iridium complexes has made a difference in organic reactions. In 2016, Lu and co-workers successfully performed [4 + 2] cycloaddition reactions using both ruthenium and iridium catalysts in separate instances (Scheme 1.10). In these reactions, indole-derived bromide and phenylacetylene were

made to react in the presence of iridium and ruthenium as photocatalysts with blue LEDs as a light source. These reactions, which were conducted at room temperature, also included sodium hydrogen phosphate (Na_2HPO_4) as the base and DMF as a solvent, and in each of the Ir and Ru catalyzed reactions, carbazole was synthesised in a 42% yield and 39% yield respectively.[66]

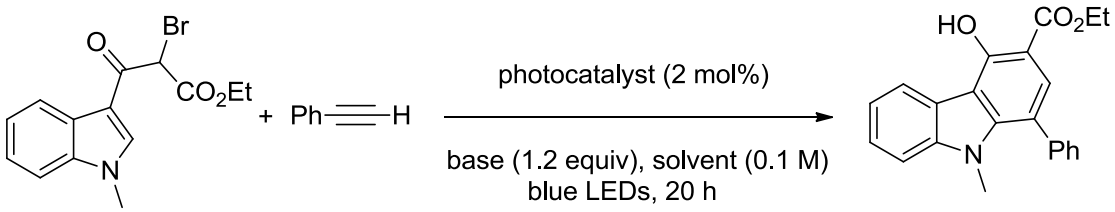

Scheme 1.10: Visible light-photocatalysed carbazole synthesis

Photoredox catalysis with Ru and Ir as photoredox catalysts has become a powerful tool in the formation of new compounds in synthetic chemistry. Products resulting from Ru and Ir catalyzed reactions are generated without any excess amount of oxidation or reduction. The key for the increased use of these catalysts is their ability to work as strong oxidants or reductants through a single-electron transfer. Especially in the last few years, these two groups of catalysts have caused a shift in synthetic approaches with respect to the way chemists apply photochemistry to the synthesis of compounds. Novel characterization techniques are pertinent to the identification of compounds resulting from Ru and Ir catalyzed reactions. Thus, advancements in the efficient

synthesis and identification of novel carbocycles, are dependent upon the synergy of photoredox reactions and characterization techniques.

1.8 Advanced characterization methods for the analysis of phenolic compounds, catalysts, and cycloaddition products.

In organic chemistry, every compound has features that distinguish it from all others. The use of spectroscopic techniques can provide information about the molecular structure of compounds and the purity of the samples. Phenolic compounds, catalysts, and cycloaddition products are usually extracted with alcohol, acetone, benzene, or water mixtures. The crude extract may be purified by solvent extractions while the proper purification and isolation procedure is commonly achieved by column chromatographic methods such as silica gel chromatography. This section discusses nuclear magnetic resonance (NMR) spectroscopy, infrared (IR) spectroscopy, mass spectrometry (MS), Raman spectroscopy, and the electrochemical process of cyclic voltammetry because these are the main characterization methods employed in the analyses of the compounds that were synthesised in this project.

1.8.1 Nuclear magnetic resonance (NMR) spectroscopy.

NMR spectroscopy is the most powerful tool for determining the structure of compounds in organic chemistry. ^{1}H and ^{13}C NMR provide information on the chemical environment of the hydrogen and carbon atoms respectively in the molecule being

analyzed. “While no single form of spectroscopy is currently capable of resolving all structural problems, NMR spectroscopy is probably the technique of paramount importance” Snyder et al. The NMR technique depends on the ability of certain atomic nuclei to receive electromagnetic energy at a characteristic frequency, supplied by radio frequency pulses in a static magnetic field.[67] The exact resonance frequency of each nucleus is dependent on the chemical environment of that nucleus. The difference in the resonance frequency of the nucleus and a standard is called the chemical shift (δ/ppm).

The ^{1}H NMR spectra of phenols contain resonances of aromatic protons at chemical shifts (δ) of between 6 to 12 ppm, unless the ring is fully substituted. Isolated olefinic protons resonate approximately at the same frequency. Different homonuclear coupling constants of ortho- ($^{3}J \sim 8$ Hz), meta- ($^{4}J \sim 2$ Hz), and para- ($^{5}J < 1$ Hz) coupled aromatic protons reveal the relationships of the protons.[68] On an isolated olefinic system, trans-coupled protons ($^{3}J = 15-18$ Hz) have larger coupling constants than *cis*-coupled protons ($^{3}J = 8-12$ Hz). The ^{13}C NMR spectra of an aromatic compound are between δ 120−160 ppm.[67]

1.8.2 Infrared spectroscopy (IR)

Infrared spectroscopy is involves infrared region of the electromagnetic spectrum. Infrared light has a longer wavelength and lower frequency than visible light. In IR, light from 3500 cm^{-1} to 200 cm^{-1} is passed through the sample to give a spectrum. IR is specially used for identifying functional groups. One of the great advantages of IR spectroscopy is that it has the ability to examine any type of sample including liquids,

powders, and solids. It is a fast, easy, and very sensitive technique that can be used to detect micrograms of materials. For single bonds like C-C or C-O the IR spectrum ranges approximately from 400 cm^{-1} to 1600 cm^{-1}, for double bonds like C=O or C=C it ranges from 1500 cm^{-1} to 1660 cm^{-1}, for bonds with hydrogen atoms like O-H or C-H it ranges from 2700 cm^{-1} to 4000 cm^{-1}. Alcohol compounds show a strong broad band for the O-H which stretches from 2300-3400 cm^{-1}, which is one of the most recognizable IR bands.[69, 70]

1.8.3 Mass spectromerty (MS)

Mass spectrometry is a sensitive technique used to determine the mass of as well as to probe the chemical structure of a molecule. The most valuable information is the molecular formula of the molecule, when identifying the structure of an unknown organic molecule. The molecular formula portrays the types and number of atoms in a molecule. Mass spectrometry can be used to determine the molecular mass of a compound, and this technique is advantageous, as it requires only minute quantities of the analyte.[71, 72]

1.8.4 Raman Spectroscopy and Surface-Enhanced Raman Spectroscopy (SERS) for analysis of samples

Raman spectroscopy has some important advantages, such as the ability to analyze aqueous samples without significant spectral interference from water. Accordingly, various techniques have been developed to improve the weak Raman signal, which is called Surface-Enhanced Raman Spectroscopy (SERS).[73] The Raman scattering

of monochromatic light is usually obtained by a laser in the visible, near-infrared or near-ultraviolet range of electromagnetic spectra.

Surface-Enhanced Raman Spectroscopy gives the same information as normal Raman spectroscopy, but with a stronger signal. It was discovered in 1974 by Fleischmann, Hendra and Mcquillan when they tried to do Raman with pyridine (Py) on the silver (Ag) electrode.[74] The primary idea was to generate a high surface area on the metal surface, but the Raman spectrum obtained was of unexpectedly high quality. The main advantages of the SERS technique are summarized as follows: it is highly surface-sensitive, non-destructive to the sample, and it can be employed on small samples with good results. Since SERS activity strongly depends on the nature of the metal surface, the two most common SERS active substrates are metal electrodes of Au and Ag used to create electrochemical oxidation-reduction cycles.[73]

Figure 1.5: DeltaNu 785 nm Raman spectroscopy

This research uses a DeltaNu Advantage 785 Raman Spectrometer produced by DeltaNu in Laramine, WY, USA Figure 1-4. This instrument uses a laser light with a wavelength of 785 nm as the excitation source, and the laser power ranges from 2.93 to 55.9 mW. It is connected to a laptop computer, which uses NuSpec software for signal processing and the setting of spectral information. When photons in laser light interact with a sample then the photons are absorbed by the sample and then emitted. The frequency of the emitted photons that are shifted up or down are compared with the organic frequency, which is called the Raman Effect. This shift effect gives information about the transition of molecules. Raman spectroscopy can be used to study different types of samples including solids or liquids.[74]

1.8.5 Cyclic voltammetry

Cyclic voltammetry (CV) is a type of electrochemical measurement involving the cycling of the potential of silver-silver chloride (Ag/AgCl) an electrode, which is set linearly against time. The controlling potential, which is applied across these two electrodes, can considered as an excitation signal. The excitation signal for CV is a linear potential scan with a triangular waveform is shown in (Figure 1-6). This triangular potential excitation signal sweeps the potential of the electrode between two values, which are called the switching potentials.[75] The excitation signal first causes the potential to scan negatively (Figure 1-7), which is the reduction state of the compound. The point

of the scan direction is then reversed, causing a positive scan, which is the oxidation state of the compound.

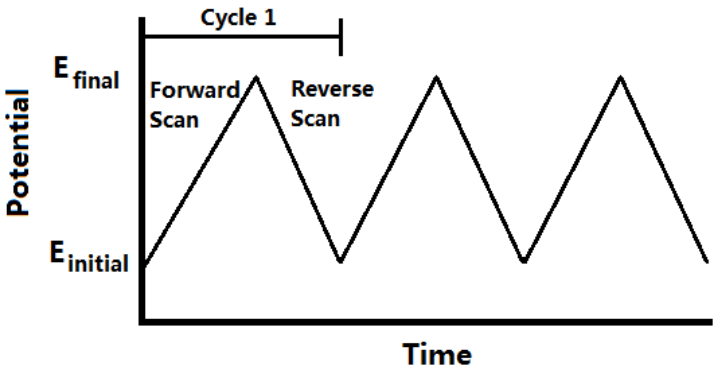

Figure 1.6: Triangular waveform of a potential-time excitation signal in a cyclic voltammetry measurement. (Adepted from ref 73)

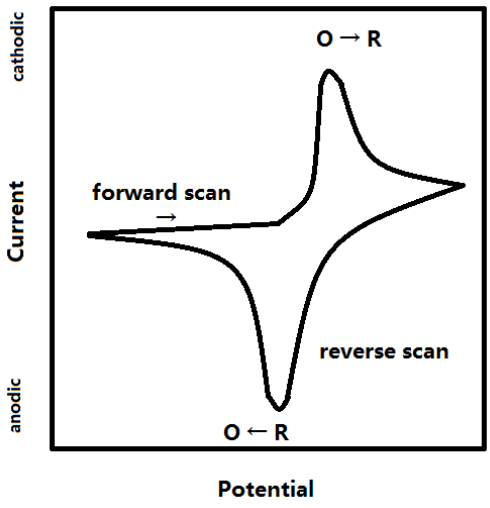

Figure 1.7: Typical cyclic voltammogram for a reversible oxidation/reduction reaction. (Adepted from ref 73)

Chapter 2: Experiments

2.1 General information

All reactions were carried out under an atmosphere of dry nitrogen unless otherwise stated. All glassware were oven-dried and purged with nitrogen. All air- and moisture-sensitive reactions were performed in flasks flame-dried under a positive flow of nitrogen and conducted under an atmosphere of nitrogen. Column chromatography was performed on 230-400 mesh silica gel, and analytical thin-layer chromatography (TLC) was performed on silicycle precoated silica gel F_{254} plates, visualized under UV light.

Chemical shifts for ^{1}H and ^{13}C NMR spectra are reported in parts per million (ppm) from tetramethylsilane with the solvent $CDCl_3$, using a Bruker Avance 300 NMR Spectrometer operating at 300 MHz (^{1}H NMR) and 75 MHz (^{13}C NMR), (Saint Mary's University NMR spectroscopy facility). All reaction solvents (except CH_3NO_2) were saturated with N_2 via a solvent purification system (MBRAUN), and dried with either drying agents or via the alumina columns of the solvent purification system (in Dr. Ylijoki's laboratory). In addition, low-resolution mass spectra, Infrared (IR) spectra were obtained from the Organic Chemistry Laboratory, Saint Mary's University, and IR frequencies (Bruker Alpha FTIR spectrometer) are reported in reciprocal centimeters (cm^{-1}). Low-resolution mass spectrometer, performed by Ms. Patricia Granados at Saint Mary's University (Agilent, 1100 Series LC, MSD Trap, m/z 50-2200, resolution 0.1 a.m.u).

2.2 Synthesis of Phenol Compound: 2-(pent-4-en-1-yl) phenol complex (A)

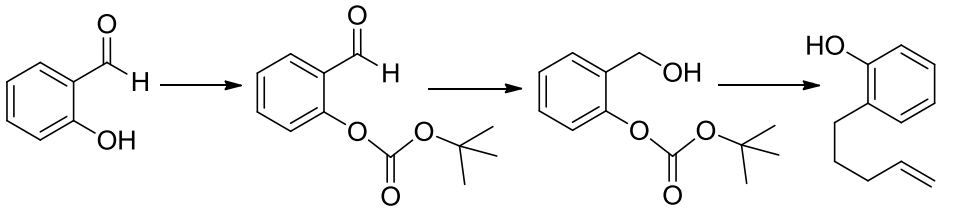

A1 **A2** **A**

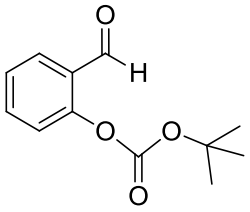

A1

In an oven-dried Schlenk flask, salicylaldeyde (1.63g, 12.02mmol, 1equiv), di-tert-butyl dicarbonate (2.752 g, 12.623 mmol, 1.05 equiv), *N*,*N*-diisopropylethylamine (1.47 mL, 8.415 mmol, 0.7 equiv), and 4-(dimethylamino)-pyridine (0.147 g, 1.202 mmol, 0.10 equiv) were sequentially added to CH_2Cl_2 (12 mL). The solution was stirred for 3 hours before quenching with saturated aqueous NH_4Cl. The solution was extracted with CH_2Cl_2, and the combined organic solution was dried with brine followed by Na_2SO_4. The resulting solution was filtered before removing the solvent in *vacuo*. The crude residue was purified by column chromatography (SiO_2, eluent: 95% hexanes 5% ethyl acetate) to afford **A1** (1.376 g, 6.19 mmol, 80%).[13]

^{1}H NMR (300 MHz, $CDCl_3$): δ 10.10 (s, 1H), 7.76 (dd, *J* =7.8, 7.62 Hz, 1H), 7.19 (t, *J*, 7.9, Hz, 1H), 7.42 (t, *J*, 7.8, Hz, 1H), 7.06 (d, *J*, 8.3, Hz, 1H), 1.57 (s, 9H).

^{13}C NMR (75 MHz, $CDCl_3$): δ 152.3, 129.53, 128.9, 126.5, 121.9, 83.9, 60.4, 61.3, 31.1, 27.7

IR (neat) cm^{-1} 2850, 1760, 1690, 1614, 1230, 1140.

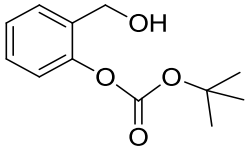

A2

$BH_3.Me_2S$ (1.97 mL, 20.7 mmol, 1.05 equiv) was added at 0 °C to **A1** (4.4 g, 19.8 mmol, 1 equiv) in THF (25 mL, 0.1 M). The reaction was allowed to warm to room temperature over 3 hours before quenching with 0.1 M aqueous HCl. The solution was extracted with ethyl acetate and the combined organic solution was dried with brine followed by Na_2SO_4. The resulting solution was filtered and the solvent was removed in *vacuo*. The crude residue was purified by column chromatography (SiO_2, eluent: 95% hexanes 5% ethyl acetate) to afford **A2** (2g, 13.213mmol, 87%).[13]

^{1}H NMR (300 MHz, $CDCl_3$): δ 7.49 (d, *J* = 7.7 Hz, 1H), 7.34 (t, *J* = 7.7 Hz, 1H), 7.28 (t, *J* = 8.1 Hz, 1H), 7.12 (d, *J* = 7.8 Hz, 1H), 4.58 (d, *J* = 6.2 Hz, 2H), 2.6 (br, 1H), 1.57 (s, 9H).

^{13}C NMR (125 MHz, $CDCl_3$): δ 152.8, 148.9, 139.6, 130.0, 129.8, 127.4, 122.7, 84.0, 60.5, 27.8, 21.2, 14.19.

IR (neat) cm^{-1} 2982, 1761, 1614, 1234, 1144.

LRMS calculated for $C_{12}H_{16}O_4$: 224.25; found –MS 222.8

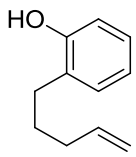

A

A2 (1g, 6.1mmol, 1 equiv) was added to a dry a Schlenk flask, and dissolved in THF (10 mL) the mixture was cooled at -78 ^{o} C then the Grignard reagent $BrMgCH(CH_2)_3$ (prepared by stirring 0.65g of Mg powder and 1.36 ml 4-brom-1-butene, in 10 ml of THF, under an N_2 atmosphere, at room temperature for 1 h) was added dropwise via a syringe. The solution was allowed to warm to room temperature over 1 hour before quenching with saturated aqueous NH_4Cl. The solution was extracted with Et_2O, and the combined organic solution was dried with brine followed by Na_2SO_4. The resulting solution was filtered and the solvent was removed in *vacuo* and the residue was purified by column chromatography (SiO_2, 98% hexanes 2% ethyl acetate) to afford **A** (0.417 g, 2.75 mmol, 75 %).[13]

^{1}H NMR (300MHz, $CDCl_3$): δ 7.13 (d, *J* = 7.6 Hz, 1H), 7.20 (d, *J* = 7.8 Hz, 1H), 6.90 (t, *J* = 7.3 Hz, 1H), 6.80 (d, *J* = 7.8 Hz, 1H), 5.87 (m, 1H), 5.16 (t, *J* = 8.1 Hz, 2H), 3.8 (br, 1H), 2.63 (t, *J* = 7.7, 2H), 2.14 (quint, *J* = 7.2, 2H), 1.74 (quint, *J* = 7.6, 2H).

^{13}C NMR (75 MHz, $CDCl_3$): δ 153.5, 138.8, 130.4, 128.3, 127.3, 120.9, 115.4, 115.0, 33.5, 29.4, 29.0.

IR (neat) cm^{-1} 3308 (br), 2928, 2859, 1639, 1591, 1502, 1454.

LRMS calculated for $C_{11}H_{14}O$: 162.10: found – MS, 160.8

2.3 Synthesis of 4-methoxy-2-(pent-4- en-1-yl) phenol complex B

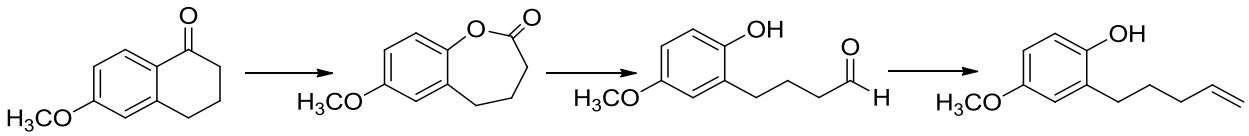

B1 **B2** **B**

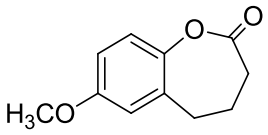

B1

6-methoxy-1-tetralone (0.5g, 2.83mmol, 1 equiv), was added to a round-bottom flask, followed by DCM (5. 68 ml, 0.5 M) and a Teflon stir bar. MCPBA (0.88g, 5.1mmol, 1.8 equiv) was then added to the resulting solution was stirred at room temperature, until dissolution. The flask was fitted with a condenser open to air and the solution was heated to reflux and allowed to stir for 72 h. Afterwards, the reaction was cooled in an ice bath and quenched with saturated aqueous sodium bisulfite solution. After quenching, the solution was transferred to an appropriate separatory funnel and the organic layer was washed with 10% aqueous NaOH (x5), then collected and dried using $MgSO_4$.[76] Afterwards, the organic layer was filtered and concentrated In *vacuo* to afford the crude lactone (0.2g, 1.23mmol, 80%).

^{1}H NMR (300MHz, $CDCl_3$) : δ 7.1 (d, *J* = 8.1 Hz, 1H), 6.76 (dd, *J* = 9.9 Hz, 2H), 3.80 (s, 3H), 2.78 (t, *J* = 7.3 Hz, 2H), 2.46(t, *J* = 7.1 Hz, 2H), 2.20-2.05 (quint, *J* = 6.7 Hz, 2H).

^{13}C NMR (75 MHz, $CDCl_3$): δ 172.1, 157.1, 145.3, 131.1, 119.9, 115.0, 112.4, 55.5, 30.9,8.4, 26.2.

IR (neat) cm^{-1}: 2943, 1759,1673,1448,1342.

LRMS calculated for $C_{11}H_{12}O_3$: 192.08: found – MS, 19

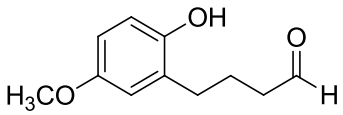

B2

A Teflon stir bar, **B1** (0.2g, 1.23mmol, 1 equiv), and previously dried toluene was added to dry Schlenk flask (12.3 mL, 0.1 M). The reaction was cooled to -78 ^{0}C, and then DIBAL-H (0.2mL, 1.35mmol, 1.1 equiv) was added dropwise and the solution was stirred. The reaction was monitored by TLC analysis and upon completion 5 h, it was quenched with sat.aq Rochelle's salt (potassium sodium tartrate). The solution was allowed to stir overnight at room temperature. Afterwards, the solution was extracted with EtOAc (x3), and the combined organic solution was dried with brine followed by $MgSO_4$. The resulting solution was filtered and concentrated in *vacuo* to yield the crude aldehyde. The aldehyde was purified via column chromatography (SiO_2, 5-10 % ethyl acetate / hexanes) to afford **B2** (0.1 g, 0.514 mmol) with a 75 % yield.[76]

^{1}H NMR (300MHz, $CDCl_3$) : δ 9.70 (t, *J* = 3.1 Hz, 1H), 6.73 (s, 1H), 6.66 (quint, *J* = 8.5 Hz, 3H), 3.75 (t, *J* = 5.1 Hz, 3H), 2.65(t, *J* = 8.1 Hz, 2H), 2.50 (t, *J* = 6.7, 6.5 Hz, 2H), 1.96 (quint, *J* = 7.5 Hz, 2H).

^{13}C NMR (75 MHz, $CDCl_3$): δ 203.6, 153.4, 148.0, 128.3, 116.1, 115.8, 112.2, 55.7, 42.9, 29.9, 22.1.

IR (neat) cm^{-1}: 3336, 2862, 1712, 1504, 1449.

LRMS calculated for $C_{11}H_{14}O_3$:194.09: found – MS, 192.8.

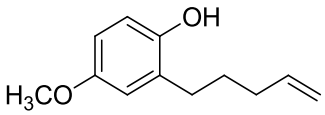

B

Ph_3PCH_3Br (0.78 g, 2.05 mmol, 4 equiv), was added to a dried a schlenk flask with a Teflon stir bar in dry THF (5.1 mL, 0.1 M), and the flask was placed in an ice bath followed by the addition of KOtBu (0.22 g, 0.2004 mmol, 3.9 equiv). The reaction was allowed to stir for 1h, then the aldehyde (0.1 g, 0.514 mmol, 1 equiv) in THF (0.1 M) was added via syringe and allowed to stir 3h. The reaction was quenched with sat.aq NH_4Cl and then transferred to separator funnel. The aqueous layer was extracted with Et_2O (x3), and the combined organic solution was dried using $MgSO_4$, filtered and concentrated under reduced pressure. The crude reaction mixture was purified using flash column chromatography (5-10% EtOAc/Hexanes) providing the corresponding phenol compound **B** (0.01 g, 0.05 mmol) with a yield of 70 %.[76]

^{1}H NMR (300MHz, $CDCl_3$): δ 6.71-6.67 (m, 2H), 6.63 (dd, J = 9.0 Hz, 3.0 Hz, 1H), 5.85 (ddt, J = 17.0, 10.0, 6.5 Hz, 1H), 5.05 (d, J = 17.0 Hz, 1H), 5.00 (d, J = 10.0 Hz, 1H), 4.36 (s, 1H), 3.76 (s, 3H), 2.59 (ap. t, J = 7.8 Hz, 2H), 2.13 (q, J = 7.2 Hz, 2H), 1.72 (quint, J = 7.5 Hz, 2H.)

^{13}C NMR (75 MHz, $CDCl_3$): δ 153.8, 147.6, 138.8. 129.6, 115.9, 115.8, 114.8, 111.7, 55.9, 33.5, 29.7, 28.8.

IR (neat) cm^{-1} 3372 (br), 2948, 2860, 2842, 1505, 1434.

LRSM calculated for $C_{12}H_{16}O_2$: 192.08: found – MS, 190.8

2.4 Synthesis of curcuphenol complex C1

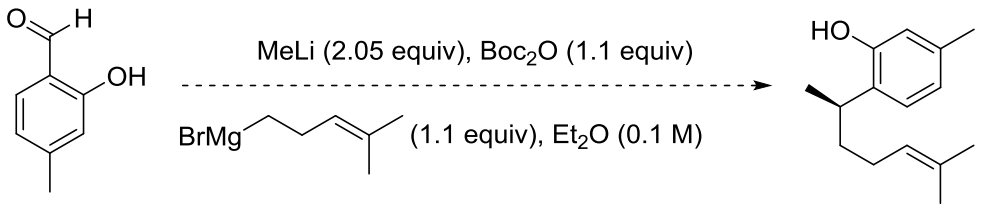

In an oven-dried schlenk flask, 2-hydroxy-4-methylbenzaldehyde (0.5 g, 3.2 mmol, 1 equiv) in Et_2O (32mL, 0.1 M) was added and stirred, then MeLi (4.1 mL, 6.5 mmol, 1.6 in Et_2O, 2.05 equiv) was subsequently added at -40 ^{o} C. After 10 min, Boc_2O (0.7 g, 3.6 mmol, 1.1 equiv) was added and allowed to stir for 2 h at -40 ^{o} C. Afterwards, 1.1 equiv of the Grignard reagent, 4-methylpent-3-enylmagnesium bromide (prepared 1 hour before the start of this reaction by stirring 5-bromo-2-methyl-2-pentene 0.5 mL (1.1 equiv.) and Mg powder 0.175 g, (2.2 equiv) in 10ml of Et_2O (0.1 equiv) under a N_2 atmosphere) was slowly added over 3 minutes. After stirring for 3 hours, the reaction was allowed to warm to room temperature. Subsequently, the reaction was quenched using 1 M aqueous NH_4Cl, the aqueous layer was extracted with Et_2O (x1), and the organic layer was dried using brine and $MgSO_4$. The resulting organic solution was filtered and concentrated under reduced pressure to afford the product. The crude reside was purified by flash-column chromatography using (5-10% ethyl acetate and 95% hexanes). Unfortunately, the result of this reaction was hard to interpret as well as not clean.[13]

2.4.1 Synthesis of phenol compound C2 with methylmagnesium bromide

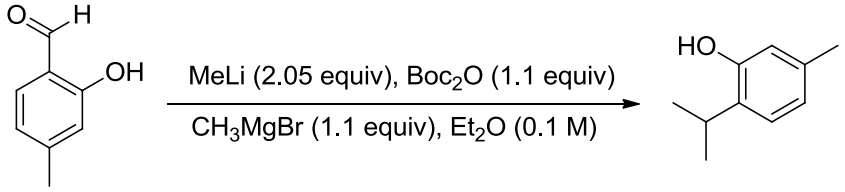

2-hydroxy-4-methylbenzaldehyde (0.3 g, 2.2 mmol, 1 equiv) was stirred in dried schlenk flask with 22 mL of Et_2O (0.1 M). The reaction was then cooled to -40 ^oC, MeLi (2.8 mL, 4.5 mmol, 1.6 M in Et_2O, 2.05 equiv) was added and stirred for 30 min, Boc_2O (0.53 g, 2.4 mmol, 1.1 equiv) was added and the reaction was allowed to stir for 2 hours at -40 ^oC. Afterwards, methylmagnesium bromide (0.8 mL, 1.1 equiv) was added slowly over 3 min at -40 ^oC, then the reaction was allowed to stir for 3 hours, and subsequently quenched with 1M aqueous NH_4Cl. The resulting solution was extracted with Et_2O (x1), then the organic layer was washed with aqueous NaCl, dried using Na_2SO_4, filtered and then concentrated in *vacuo* to afford C2 (0.2 g, 66%).

^1H NMR (300MHz, $CDCl_3$): δ 9.84 (br, 1H), 6.90 (d, J = 7.1 Hz, 1H), 6.72 (t, J = 6.9 Hz, 2H), 4.81(sex, J = 8.5 Hz, 1H), 2.20(s, 3H), 1.52 (s, 3H), 1.29 (s, 3H).

2.4.2 Synthesis of phenol compound C3 with vinylmagnesium chloride

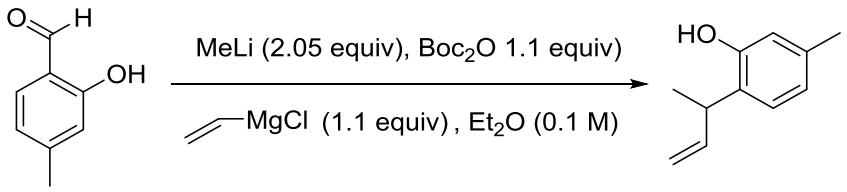

MeLi (1.88 g, 3 mmol, 1.6 M in Et_2O, 2.05 equiv) was added to a stirred solution of 2-hydroxy-4-methylbenzyldehyde (0.2 g, 1.46 mmol, 1 equiv) in Et_2O (15 mL, 0.1 M) at -40 ^oC and allowed to stir for 30 min. Afterwards, Boc_2O (0.35 g, 1.6 mmol, 1.1 equiv) was added and the reaction was allowed to stir for 3 h at -40 ^oC. Subsequently, vinylmagnesium chloride (1 mL, 1.6 M in THF) was slowly added over 2 min at -40 ^0C, and the reaction was allowed to stir for 3 h, then quenched with 1 M aqueous NH_4Cl. The resulting solution was extracted with Et_2O (x1), then the organic layer was washed with aqueous NaCl, dried using Na_2SO_4, filtered and then concentrated in *vacuo* to afford the crude product, C3 (0.9 g, 0.0069 mol, 50%).

^1H NMR (300MHz, $CDCl_3$): δ 9.8 (br, 1H), 6.90 (s, 1H), 6.72 (dd, *J* = 7.1, 6.9 Hz, 2H), 6.2 (quart, *J* = 6.6 Hz, 1H), 5.1(dddd, *J* = 7, 2H), 2.3 (s, 3H), 1.41 (d, *J* = 7.1 Hz, 1H), 1.27 (s, 3H).

2.5 Synthesis of phenol compound D

2.5.1 Synthesis of phenol compound D1 with methylmagnesium bromide

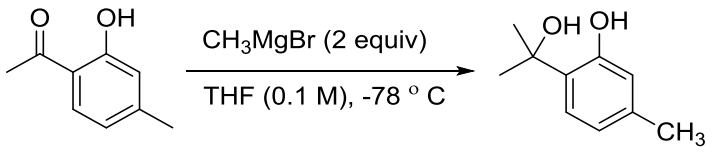

THF (6.6 mL, 0.1 M) was added into an oven-dried schlenk flask, followed by 2-hydroxy-4-methyl acetophenone (0.1 g, 0.66 mmol, 1 equiv), and the mixture was stirred in for 15 min. Afterwards, methylmagnesium bromide (0.44 mL, 3 M in diethyl ether) was added dropwise over 3 min in -78 ^{o}C. The reaction was stirred for 3 h and subsequently quenched using aqueous NH_4Cl. Afterwards, the resulting solution was extracted using THF (x1), and the organic layer were dried using brine, followed by Na_2SO_4. The resulting organic solution was filtered and concentrated in vacuo to afford compound D1 (0.05 g, 0.00033 mol, 50%).

^{1}H NMR (300MHz, $CDCl_3$): δ 12.31 (s, 1H), 7.65 (d, *J* = 7.1 Hz, 1H), 6.82-6.80 (s, 1H), 6.75 (d, *J* = 6.5 Hz, 1H), 2.65 (s, 3H), 2.48 (s, 3H), 2.31 (s, 3H), 1.70(s, 1H).

2.5.2 Synthesis of phenol compound D2 with vinylmagnesium chloride

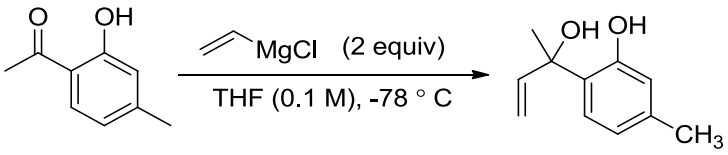

Vinylmagnisium chloride (0.8 mL, 1.6 M in THF, 2 equiv) was added to 2-hydroxy-4-methyl acetophenone (0.1 g, 0.66 mmol, 1 equiv) in THF (6.6 mL, 0.1 M) at -78 ^{o}C. The solution was stirred for 2 h and subsequently allowed to warm to room temperature, before quenching with saturated aqueous NH_4Cl. The solution was extracted with THF (x1), and the organic layer was dried with brine, followed by Na_2SO_4. The organic solution was filtered and concentrated in *vacuo* to afford compound D2 (0.04 g, 0.00026 mol, 39%).

^{1}H NMR (300MHz, $CDCl_3$): δ 8.80 (br, 1H), 6.98 (m, *J* = 7.6, 7.3 Hz, 1H), 6.74 (s, 1H), 6.22 (dd, *J* = 14,10 Hz, 2H), 5.34 (t, *J* = 6.5 Hz, 1H), 3.21 (br, 1H), 2.3 (s, 3H), 1.76 (s, 3H).

2.5.3 Synthesis of phenol compound D3 with ethylmagnesium iodide

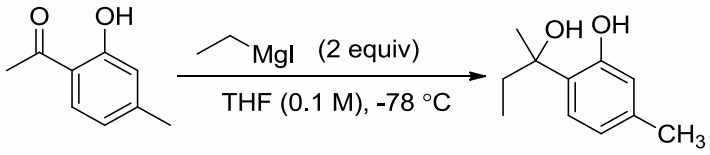

Magnesium powder (0.2 g) was added to 10 mL of THF in an oven-dried Schlenk flask under nitrogen and the mixture was stirred for 15 min. Subsequently, ethyl iodide (0.53 mL) was added dropwise over 3 min. The reaction was allowed to stir for 1 h, then cooled to -78 ^{o}C and 2-hydroxy-4-methyl acetophenone (0.5 g) in 3 mL THF was added and allowed to stir for 1 h. Subsequently, the reaction was allowed to warm to room temperature before quenching with saturated aqueous NH_4Cl. The solution was extracted with THF (x1), and the organic layer was dried with brine, followed by Na_2SO_4. The organic solution was filtered and concentrated in *vacuo* to afford compound D3 (0.3 g, 0.00199 mol, 60%).

^{1}H NMR (300MHz, $CDCl_3$): δ 6.81 (s, 1H), 6.52 (d, *J* = 8 Hz, 2H), 6.31 (d, *J* = 8 Hz, 1H), 3.92 (quart, *J* = 7.5 Hz, 2H), 3.1 (br, 1H), 1.64 (s, 3H), 1.58 (s, 3H), 1.54 (s, 3H).

2.5.4 Synthesis of phenol compound D4 with ethyl lithium iodide

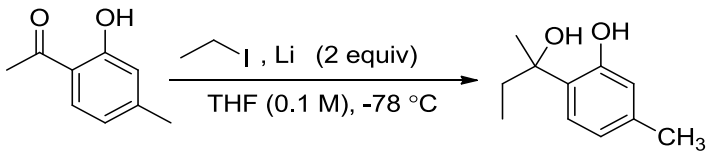

Li wire (0.057 g, 2.2 equiv.) was hammered flat, cut into thin slivers, washed 3 times with petroleum ether, and added to THF (33 mL, 0.1 M) in a dry Schlenk flask under N_2. Ethyl iodide (0.53 mL, 2 equiv.) was added dropwise over 3 min and the reaction mixture was stirred for 1 h. Afterwards, the reaction mixture was cooled to -78^{o}C and 2-hydroxy-4-methyl acetophenone (0.5 g, 1 equiv.) in 5 mL THF was added and allowed to stir for 2 h. Subsequently, the reaction was allowed to warm to room temperature before quenching with saturated aqueous NH_4Cl. The solution was extracted with THF (x1), and the organic layer was dried with brine, followed by Na_2SO_4. The organic solution was filtered and concentrated in *vacuo* to afford compound D4 (0.4 g, 0.0026 mol, 78%).

^{1}H NMR (300MHz, $CDCl_3$): δ 6.81 (s, 1H), 6.52 (d, *J* = 8 Hz, 2H), 6.31 (d, *J* = 8 Hz, 1H), 3.92 (t, *J* = 7.5 Hz, 2H), 3.1 (br, 1H), 1.64 (s, 3H), 1.58 (s, 3H), 1.54 (s, 3H).

2.5.5 Synthesis of benzyl alcohol D5 with 4-brom-1-butene

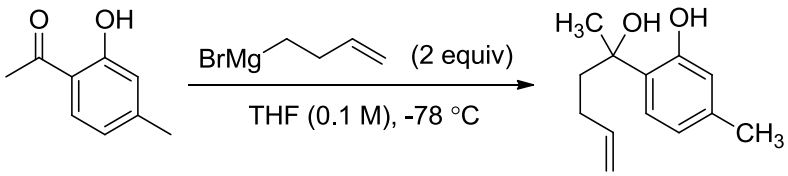

Grignard reagent (prepared by adding 4-bromo-1-butene (2.7 mL, 2 equiv) to a mixture of Mg powder (0.809g, 2.5 equiv) in THF (10 mL, 0.1 M) and stirred for 1h at room temperature under N_2) was added dropwise to 2-hydroxy-4-methyl acetophenone (2 g, 13.31 mmol, 1 equiv.) at -78 ^{o}C. The reaction was stirred for 2 h and subsequently, allowed to warm to room temperature before quenching with saturated aqueous NH_4Cl. The solution was extracted with THF (x1), and the organic layer was dried with brine, followed by Na_2SO_4. The organic solution was filtered and concentrated in *vacuo* to afford compound D5 (1 g, 0.0066 mol, 50%).

^{1}H NMR (300MHz, $CDCl_3$): δ 9.4 (br, 1H), 6.9 (s, 1H), 6.75(dd, *J* = 7.6, 7.5, 2H), 5.90(m, 1H), 5.06 (dddd, *J* = 12, 8, 6, 3 Hz, 2H), 3.10 (br, 1H), 2.32 (s, 3H), 2.1 (m, 4H), 1.70 (s, 3H).

^{13}C NMR (75 MHz, $CDCl_3$): δ 155.8, 139.9, 138.3, 127.3, 126.2, 125.9, 120.3, 118.1, 114.9, 41.7, 29.2, 28.4, 20.8.

LRMS calculated for $C_{13}H_{18}O_2$: 206.13: found –MS, 204.8

2.5.6 Synthesis of styrene acetate compound D6

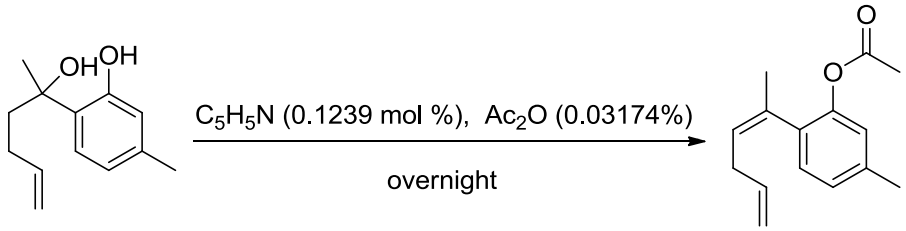

A solution of **D5** (0.2 g, 2.35 mmol), pyridine (4.12 mL, 123.9 mmol) and acetic anhydride (1.24 mL, 31.74 mmol) were allowed to stir overnight under N_2 atmosphere. Subsequently, 50 mL of Et_2O and 50 mL of H_2O were added to the solution. The organic layer was washed with 25 mL of 5% HCl (x3), 25 mL of 2N Na_2CO_3 (x3) and 25 mL of H_2O (x3). The resulting organic layer was dried using brine, followed by $MgSO_4$, and concentrated in *vacuo* to yield 0.17 g (88 %) of acetate **D6**. The product was used in the next step without purification.

^{1}H NMR (300MHz, $CDCl_3$): δ 7.17 (s, 1H), 7.08 (dd, *J* = 7.5, 5.1 Hz, 2H), 6.90 (t, *J* = 8, 2H), 5.95 (m, 1 H), 5.52 (t, *J* = 6.7 Hz, 1H), 2.95(t, *J* = 6.1 Hz, 2H), 2.5 (s, 3H), 2.02 (s, 3H), 1.89 (s, 3H).

^{13}C NMR (75 MHz, $CDCl_3$): δ 169.4, 147.5, 145.4, 138.1, 129.5, 127.5, 126.8, 123.1, 114.8, 39.1, 36.1, 32.0, 28.3, 24.2, 21.9.

2.5.7 Synthesis of curcuphenol compound D7

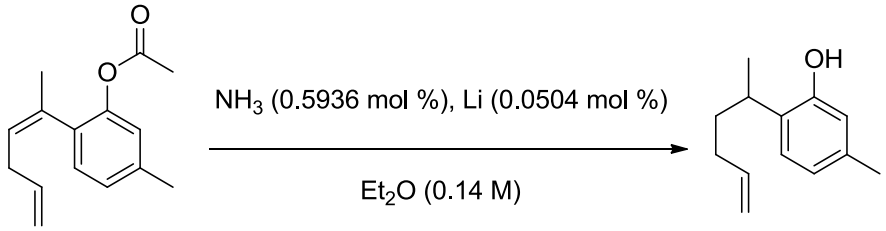

Li wire (0.77 g, 50.5 mmol) was hammered flat, cut and washed free of oil with petroleum ether, and added to 33 mL of Et_2O in a 250 mL 3-necked round bottom flask which was fitted with a Dewar condenser, under N_2. NH_3 (33 mL, 593.6 mmol) was condensed into the reaction flask for 15 min, with a subsequent change in the colour of the reaction solution from clear to blue. Subsequently, D6 (0.2 g, 0.39 mmol) was added dropwise in 2 mL of Et_2O. After 2 h, solid NH_4Cl was carefully added, and the crude product was filtered and transferred to a seperatory funnel. Et_2O and H_2O were added to the resulting solution and the organic layer was collected, dried with $MgSO_4$, filtered and concentrated in *vacuo*. The crude product was purified using silica gel chromatography (5% ethyl acetate, 95 % hexanes) to afford **D7** (0.1 g) with 85% yield.

^{1}H NMR (300MHz, $CDCl_3$): δ 7.08 (d, *J* = 8.3 Hz, 1H), 6.78 (d, *J* = 7.8 Hz, 1H), 6.62 (s, 1H), 5.90(m, 1H), 5.10 (d, *J* = 17.2 Hz, 2H), 4.70 (br, 1H), 3.10 (six, 1H), 2.32 (s, 3H), 2.08 (quart, *J*= 8.3 Hz, 2H), 1.85 (dt, *J* = 18 Hz, 2H), 1.30 (s, 3H).

^{13}C NMR (75 MHz, $CDCl_3$): δ 152.8, 139.0, 136.6, 129.8, 127.0, 121.7, 116.1, 114.4, 36.3, 31.7, 31.3, 20.9, 29.8.

LRMS calculated for $C_{13}H_{18}O$: 190.14: found – MS, 188.8

2.5.8 Synthesis of benzyl alcohol compound D8 using 5-bromo-2-methyl-2-pentene

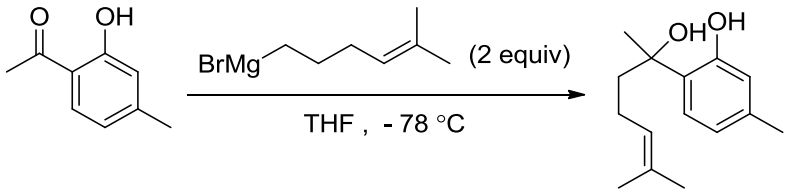

Mg powder (0.16, 6.65mmol) was added to THF (10mL, 0.1M) in an oven-dried Schlenk flask and stirred for 15 min. Subsequently, 5-bromo-2-methyl-2-pentene (0.7mL, 5.32mmol) was added to the reaction mixture over 3 min. The reaction was stirred for 1 h at room temperature and then cooled to -78 ^{o}C before adding 2-hydroxy-4-methyl acetophenone (0.4g, 2.66mmol) in 3 mL THF dropwise, over 3 min. After 2 h of stirring, the reaction was quenched using saturated aqueous NH_4Cl. Afterwards, the solution was extracted with THF (x1), and the organic layer was dried with brine, followed by $MgSO_4$. The organic solution was filtered and concentrated in *vacuo* to afford the crude product which was purified using silica gel column chromatography (10 % ethyl acetate, 90 % hexanes) to afford 0.135 g of **D8** with 78% yield.

^{1}H NMR (300MHz, $CDCl_3$): δ 7.5 (d, *J* = 7.1 Hz, 1H), 6.92 (d, *J* = 7.7 Hz, 1H), 6.71 (s, 1H), 6.1 (br, 1H), 5.20 (t, *J* = 6.3 Hz, 1H), 3.5 (br, 1H), 2.31 (s, 3H), 2.10 (dddd, *J*= 12, 8, 6, 3 Hz, 4H), 1.71 (s, 3H), 1.64(s, 3H), 1.57(s, 3H).

^{13}C NMR (75 MHz, $CDCl_3$): δ 155.9, 138.7, 133.0, 126.3, 123.7, 120.2, 118.4, 117.5, 79. 1, 42.1, 29.4, 25.7, 22.9, 20.9, 17.6.

LRMS calculated for $C_{15}H_{22}O_2$: 234: found - MS, 232.9.

2.5.9 Synthesis of styrene acetate compound D9

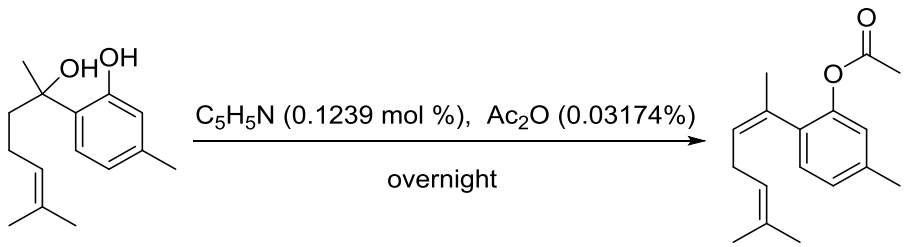

D8 **(**0.135 g, 0.576 mmol) was added to pyridine (2.3 mL, 123.9 mmol) and acetic anhydride (0.73 mL, 31.74 mmol) and stirred overnight under N_2. Subsequently, 50 mL of Et_2O and 50 mL of H_2O were added to the solution. The organic layer was washed with 25 mL of 5% HCl (x3), 25 mL of 2N Na_2CO_3 (x3) and 25 mL of H_2O (x3). The resulting organic layer was dried using brine, followed by $MgSO_4$, and concentrated in *vacuo* to yield **D9**. The product was used in the next step without purification.

^{1}H NMR (300MHz, $CDCl_3$): δ 7.32 (d, *J* = 8.2 Hz, 1H), 7.16 (d, *J* = 8.4 Hz, 1H), 6.88 (s, 1H), 2.90 (t, *J* = 5.4 Hz, 2H), 2.27 (s, 3H), 2.02 (s, 3H), 1.97 (s, 3H), 1.90 (s, 3H), 1.74 (s, 3H).

^{13}C NMR (75 MHz, $CDCl_3$): δ 169.3, 146.0, 138.4, 137.5, 129.5, 126.7, 124.6, 123.8, 114.8, 82.7, 39.8, 36.8, 27.5, 25.6, 22.7, 20.7, 17.5.

2.5.10 Synthesis of curcuphenol compound D10

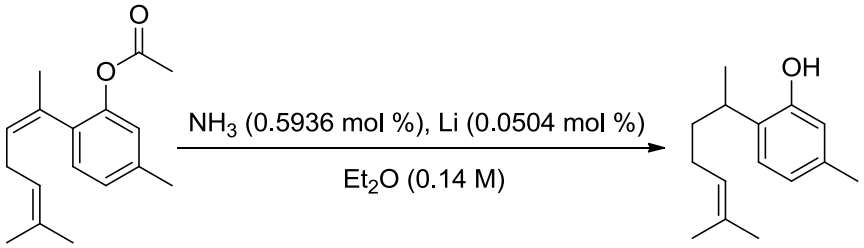

Li wire (0.29 g, 50.4 mmol) was hammered flat, cut and washed free of oil with petroleum ether, and added to (12.5 mL, 0.14 M) mL of Et_2O in an oven-dried 250 mL 3-necked round bottom flask which was fitted with a Dewar condenser, under N_2. NH_3 (12.504 mL, 953.6 mmol) was condensed into the reaction flask for 15 min, with a subsequent change in the colour of the reaction solution from clear to blue. Subsequently, D9 (0.084 g, 0.39 mmol) was added dropwise in 3 mL of Et_2O. After 2 h, solid NH_4Cl was carefully added to destroy access ammonia, and the crude product was filtered and transferred to a seperatory funnel. Et_2O and H_2O were added to the resulting solution and the organic layer was collected, dried with $MgSO_4$, filtered and concentrated in vacuo. The crude product was purified using silica gel chromatography (5% ethyl acetate, 95 % hexanes) to afford **D10**.[77]

^{1}H NMR (300MHz, $CDCl_3$): δ 7.1 (d, *J* = 8.1 Hz, 1H), 6.8 (d, *J* = 9.3 Hz, 1H), 6.6 (s, 1H), 5.5 (t, *J* = 6 Hz, 1H), 6.1 (br, 1H), 5.1 (t, *J* = 9.5 Hz, 2H), 2.5 (d, *J* = 7.7 Hz, 2H), 1.5 (s, 6H), 1.4 (s, 3H), 1.0 (s, 3H).

2.6 Synthesis of ruthenium catalyst

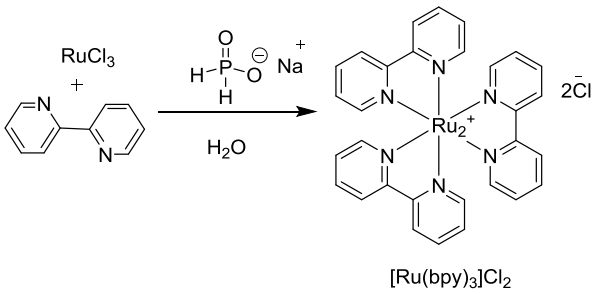

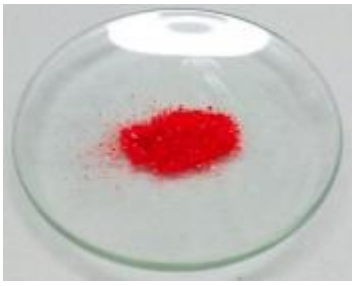

$RuCl_3$ from commercial $RuCl_3.3H_2O$

Commercial $RuCl_3.3H_2O$ purchased from Sigma Aldrich, was placed on a watch glass and heated in an oven at 130 ^oC for 3 hours to afford $RuCl_3$.[78]

NaH_2PO_2 preparation from H_3PO_2

About 10 mL of 50% phosphinic acid was measured into a beaker containing 6 mL of water. Sodium hydroxide (NaOH) pellets (3.9g) were carefully added to the solution (ensuring that previously added pellets had dissolved before adding more) until a cloudy precipitate was obtained.

2.6.1 Synthesis of $[Ru(bpy)_3]Cl_2$

Oven-dried and cooled $RuCl_3$ (0.4 g, 1.93 mmol), 2,2-bipyridine (0.9 g, 5.76 mmol), and H_2O (40 ml) were added to a 100 mL dry round-bottom flask fitted with a reflux condenser. Subsequently, 2 mL of freshly prepared NaH_2PO_2 solution was added and the mixture was heated to reflux for 30 min. During this time, the colour of the solution changed from green to brown, and finally orange. Afterwards, the solution was filtered to

remove traces of undissolved material, and potassium chloride (12.6 g) was added to the filtrate. Subsequent heating of the solution resulted in a colour change to deep-red. The solution was cooled to room temperature, yielding beautiful red crystals, which were filtered and washed with 30 mL of an ice-cold acetone-water solution. Subsequently, the crystals were air-dried to yield 1.13g (77% yield) of the product.[78]

^{1}H NMR (300 MHz, D_2O): δ 7.32 (t, *J* = 8.5 Hz, 1H), 7.99 (d, *J* = 7.7 Hz, 1H), 8.00 (t, *J* = 5.4 Hz, 1H), 8.50 (d, *J* = 6.8 Hz, 1H).

2.6.2 Synthesis of $[Ru(bpy)_3](BF_4)_2$

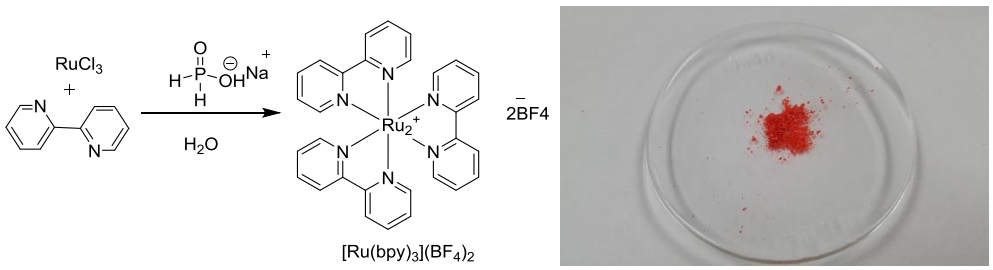

Oven-dried and cooled $RuCl_3$ (0.083 g, 0.4 mmol), 2,2-bipyridine (0.18 g, 1.204 mmol), and H_2O (8 ml) were added to a 100mL dry round-bottom flask fitted with a reflux condenser. Subsequently, 0.4 mL of freshly prepared NaH_2PO_2 solution was added and the mixture was heated to reflux for 30 min. During this time, the colour of the solution changed from green to brown and finally orange. Afterwards, the solution was filtered to remove traces of undissolved material, and $NaBF_4$ (0.33g in 2 mL of H_2O) was added to the filtrate. Solids were formed upon addition of the $NaBF_4$ solution. Subsequent heating

until solid dissolution resulted in an orange solution. The solution was cooled to room temperature, yielding beautiful orange crystals, which were filtered, washed with ethanol and subsequently dried.[78]

^{1}H NMR (300 MHz, D_2O): δ 7.32 (t, *J* = 8.5 Hz, 1H), 7.99 (d, *J* = 7.7 Hz, 1H), 8.00 (t, *J* = 5.4 Hz, 1H), 8.50 (d, *J* = 6.8 Hz, 1H).

2.7 Synthesis of iridium catalyst [Ir(dF(CF$_3$)ppy)$_2$(dtbbpy)(PF$_6$)

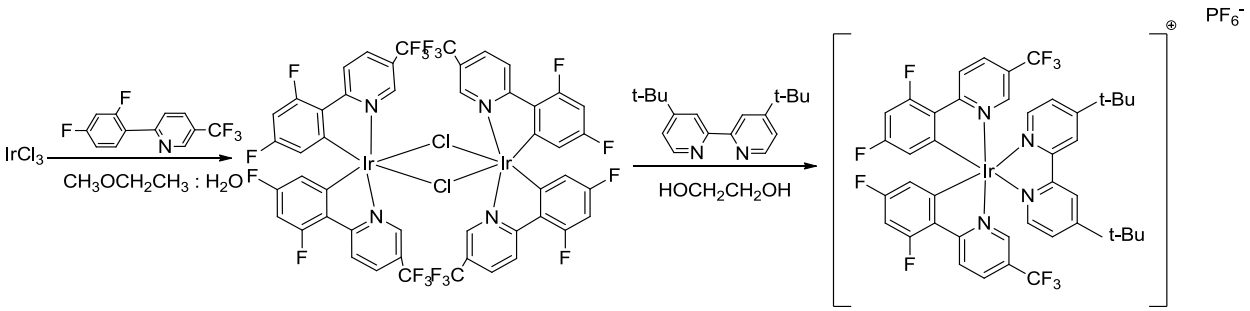

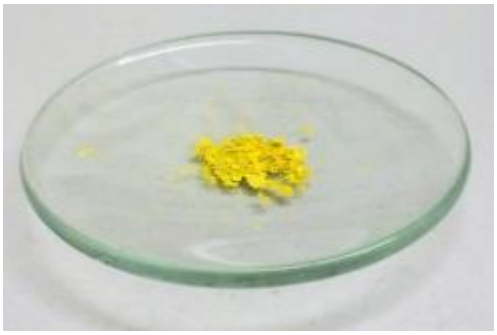

Where dF(CF$_3$)ppy is, 2-(2,4-diflurophenyl)-5-triflouro-methylpyridine, and (dtbbpy) is 4,4-di-tert-butyl-2,2-dipyridyl.

2.7.1 Synthesis of dF(CF_3)ppy (yellow-green solid).

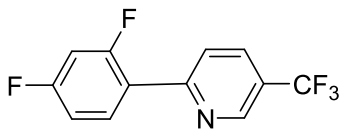

In an oven-dried Schlenk flask, a mixture of 2-chloro-5-(trifluoro-methyl) pyridine (3 mmol, 0.68 g), 2,4-difluorophenylbronic acid (3.3 mmol, 0.52 g), PdL_4 (0.07 mmol, 0.081 g) in benzene (4 mL), 2 M aqueous sodium carbonate (3 mL), and ethanol (0.75 mL) were stirred and heated to reflux at 70 ^{o}C under N_2 for 48 h. After cooling the solution to room temperature, the solution was transferred to a separatory funnel with water (3 x 25 mL) and dichloromethane (15 mL) and the organic layers were combined. The resulting organic solution was washed with 50ml of water and filtered through silica gel over a porous glass frit, using dichloromethane to elute the filtrate. Subsequently, the filtrate was dried using Na_2SO_4 and concentrated in *vacuo* to yield 0.17 g (88% yield).[79]

^{1}H NMR (300 MHz, $CDCl_3$): δ 8.99 (s, 1H), 8.09 (m, 1H), 8.01 (d, J = 9 Hz, 1H), 7.93 (d, J = 8 Hz, 1H), 7.06 (td, J = 8.1 Hz, 1H), 6.97 (t, J = 9, 1H).

2.7.2 Synthesis of [(dF(CF_3)ppy)$_2$-IrCl]$_2$ (yellow-green-powder).

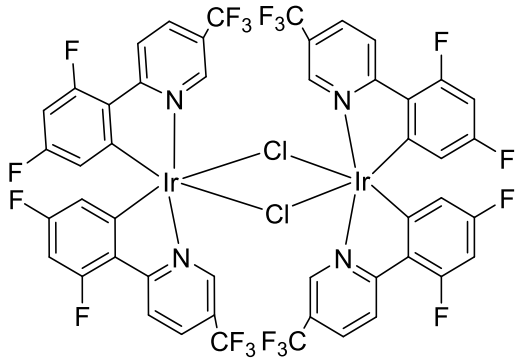

2-(2,4-diflourophenyl)-5-triflouromethylpyridine (0.68 mmol, 0.18 g) in 2-methoxyethanol (4.0 mL) and water (2.0 mL) were added to an oven-dried Schlenk flask and stirred under N_2. Subsequently, iridium (III) chloride hydrate (0.68 mmol, 0.18 g) was added and the solution was heated to reflux at 120 $^{\circ}$C under nitrogen gas for 12 h. Afterwards the reaction was cooled to room temperature and the resulting green powder was collected by filtration, washed with water (3 x 20 mL), dried and then recrystallized using a methanol : acetone (4:1) solution to yield 0.21 g (85%) of pure product.[79]

^{1}HNMR (300 MHz, $CDCl_3$): δ 9.50 (d, *J* = 5 Hz, 4H), 8.45 (dd, *J* = 9.1 Hz, 4H), 6.39 (m, 4H), 5.06 (dd, *J* = 9.3 Hz, 4H)

2.7.3 Synthesis of [Ir(dF(CF_3)ppy)$_2$(dtbbpy)(PF_6)

Ethylene glycol (6 mL) was stirred in a dried flask to which bis-chlorotetrakis (2-(4,6-difluoromethylphenyl)-pyridinato)diiridium) (0.09 mmol, 0.13 g) and 4,4-di-tert-butyl-2,2-dipyridyl (0.2 mmol, 0.0054 g) were added and then heated to reflux (150 °C) under nitrogen for 15 h. After cooling to room temperature, the solution was transferred to a separatory funnel using about (60 mL) of water, and washed with hexanes (3 x 30 mL). To remove residual hexanes, the aqueous layer was heated for 5 min at 85 °C. Subsequently, 10 mL of NH_4PF_6 solution (1 g of ammonium hexafluorophosphate in 10 mL water) was added to the reaction which produced a yellow-green precipitate that was, filtrated, dried, and recrystallized with an acetone : pentane diffusion to give the pure product [Ir(dF(CF_3)ppy)$_2$(dtbbpy)(PF_6). The yield was 1.13 g (70 %).[79]

^{1}H NMR (300 MHz, acetone-d_6): δ 8.97 (d, *J* = 2 Hz, 2H), 8.64 (dd, *J* = 9 Hz, 2H), 8.43 (dd, *J* = 9 Hz, 2H), 8.20 (d, *J* = 6 Hz, 2H), 7.83 (m, 4H), 6.89 (td, *J* = 9 Hz, 2H), 6.00 (dd, *J* = 8.8 Hz, 2H), 1.47 (s, 18H).

2.8 Oxidation of phenol using ceric ammonium nitrate (CAN)

2.8.1 Oxidation of phenol compound A

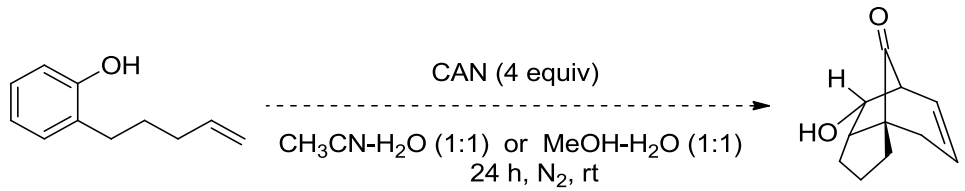

Phenol A (0.01 g, 0.06 mmol, 1 equiv), CAN (0.13 g, 0.2 mmol, 4 equiv), and 2 mL of solvent (1 mL CH_3CN : 1 mL H_2O) were stirred under nitrogen for 24 h at room temperature. The solution was quenched with saturated aqueous NH_4Cl, and the organic phase was extracted with CH_3CN, dried using brine followed by $MgSO_4$, and concentrated in *vacuo*. The same reaction was also carried out using a different solvent system; 1 mL MeOH: 1 mL H_2O.[80]

2.8.2 Oxidation of phenol compound B

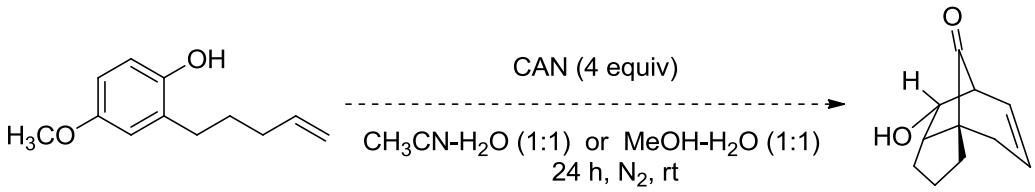

In a schlenk flask, phenol B (0.01 g, 0.05 mmol, 1 equiv), CAN (0.1 g, 0.2 mmol, 4 equiv), and 2 mL of solvent (1 mL CH_3CN : 1 mL H_2O) were stirred under nitrogen for 24 h at room temperature. The solution was quenched with saturated aqueous NH_4Cl, and the organic phase was extracted with CH_3CN, dried using brine followed by $MgSO_4$, and

concentrated in *vacuo*. The same reaction was also carried out using a different solvent system; 1 mL MeOH : 1 mL H_2O.[81]

2.9 Oxidation of phenol compound using lead acetate

2.9.1 Oxidation of phenol compounds A and B using $Pb(oAc)_4.H_2O$

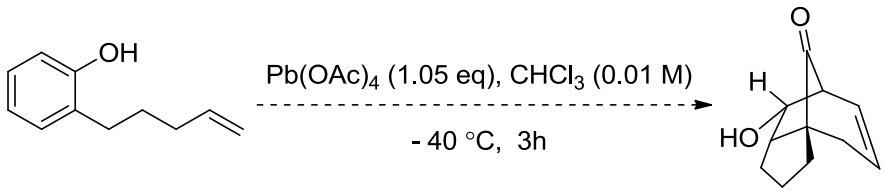

Phenol A (0.01 g, 0.06 mmol, 1 equiv), Pb(oAc)4.H_2O (0.02 g, 0.063 mmol, 1.05 equiv), and $CHCl_3$ (0.01 M) were allowed to stir for 2 h at -40 ^{0}C. Subsequently, the solution was quenched with saturated aqueous NH_4Cl, and the organic phase was extracted with $CHCl_3$, dried using brine followed by $MgSO_4$, and concentrated in *vacuo*.

2.9.2 Oxidation of phenol compounds A and B using $Pb(CH_3COO).PbO$

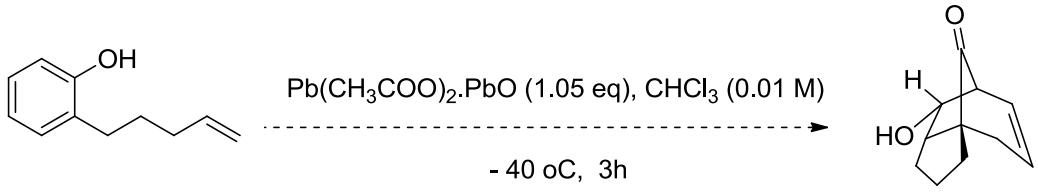

Phenol A (0.01 g, 0.06 mmol, 1 equiv), $Pb(CH_3COO)_2.PbO$ (0.04g, 0.063 mmol, 1.05 equiv) and $CHCl_3$ (0.01 M) were allowed to stir for 2 hours at -40 ^{0}C. Subsequently, the solution was quenched with saturated aqueous NH_4Cl, and the organic phase was extracted with $CHCl_3$, dried using brine followed by $MgSO_4$, and concentrated in *vacuo*.

2.10 Photocycloaddition reactions

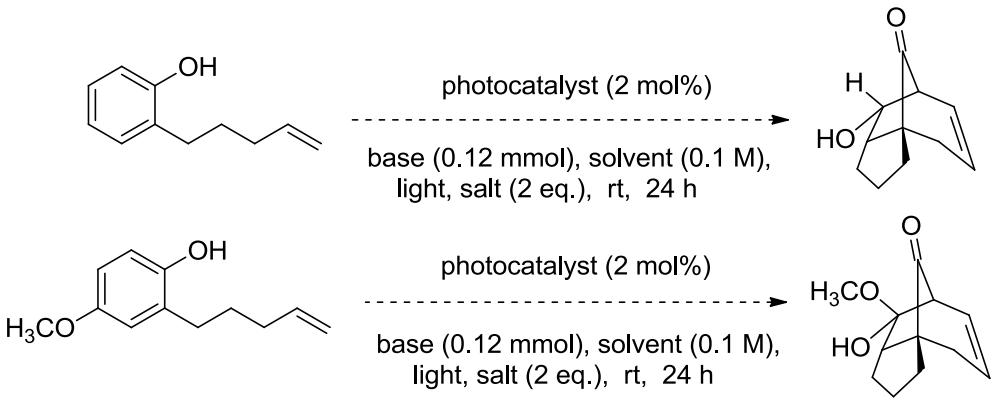

Photocycloaddition reactions were performed using different solvents, bases, salts, and light sources. All solvents for these reactions were appropriately dried before use. In addition, all glassware were oven-dried for at least 1 h before use. The various photocycloaddition experiments were performed as reported in Table 2.1, using different light types such as white light (floodlight), blue LEDs, sun light, and UV LEDs.

A dry 10 mL schlenk flask was charged with a solution of the phenol (1 equiv), $Ru(bpy)_3Cl_2.6H_2O$ (0.05 equiv.), salt (2 equiv.), base (0.12 mmol), and dry solvent (0.1 M). The reaction was then degassed using three freeze-pump-thaw cycles under nitrogen gas. The schlenk flask was then placed at a distance of 20 cm from the light source (reactions that employed sunlight were placed on a window sill for proper exposure), and irradiated using the respective light type (Table 2.1) while stirring for 24 h at room temperature. Upon completion of the various reactions, the respective products were concentrated in *vacuo* and characterised by ^{1}H NMR spectroscopy.[44,82,83,84,85,86,87]

Table 2.1: The Components of the Various Photocycloaddition Reactions Performed

Catalyst	Solvent	Light Source	Base	Salt	Time
$[Ir(df(CF_3)ppy)_2(dtbbpy)(BF_6)]$ $Ru(bpy)_3Cl_2$	Dry CH_3CN CCl_4	Blue LEDs			24h under nitrogen gas
$[Ir(df(CF_3)ppy)_2(dtbbpy)(BF_6)]$ $Ru(bpy)_3Cl_2$	WetCH_3 CN H_2O CCl_4	Blue LEDs			18h
$[Ir(df(CF_3)ppy)_2(dtbbpy)(BF_6)]$ $Ru(bpy)_3Cl_2$	CH_3N_2	Visible light (Fluorescent)			24h open to the air
$Ru(bpy)_3Cl_2$	DMF CCl_4	Visible light (floodlight)			24h
$[Ir(df(CF_3)ppy)_2(dtbbp)(BF_6)]$ $Ru(bpy)_3Cl_2$(0.05 eq.)	CH_3CN	Blue LEDs	*N*,*N*-Diisopropylethylamine	$NaBF_4$	24h under N_2
$[Ir(df(CF_3)ppy)_2(dtbbp)(BF_6)]$ (0.1eq.) $Ru(bpy)_3Cl_2$ (0.05 eq.)	CH_3CN	UV light	*N*,*N*-Diisopropylethylamine	$NaBF_4$	24h under nitrogen gas
$[Ir(df(CF_3)ppy)_2(dtbbp)(BF_6)]$ (0.1eq.)	CH_3CN DMF	UV light	N,*N*-Diisopropylethylamine	$NaBF_4$	24h open to the air
$[Ir(df(CF_3)ppy)_2(dtbbp)(BF_6)]$ $Ru(bpy)_3Cl_2$ $Ru(bpy)_3(BF_4)_2$	DCM	Blue light	Na_2CO_3		24h under N_2

[Ir(df(CF_3)ppy)$_2$ (dtbbpy)(BF_6)] Ru(bpy)$_3$$Cl_2$ Ru(bpy)$_3$($BF4$)$_2$	CH_3CN	Visible light	$(NH_4)S_2O_8$		24h
[Ir(df(CF_3)ppy)$_2$(dtbbpy)(BF_6)] Ru(bpy)$_3$$Cl_2$ Ru(bpy)$_3$(BF_4)$_2$	CH_3CN	UV light	$(NH_4)S_2O_8$		24h
[Ir(df(CF_3)ppy)$_2$(dtbbpy)(BF_6)] Ru(bpy)$_3$$Cl_2$ Ru(bpy)$_3$(BF_4)$_2$	DMF	UV light	Na_2HPO_4		24h
[Ir(df(CF_3)ppy)$_2$(dtbbpy)(BF_6)] Ru(bpy)$_3$$Cl_2$ Ru(bpy)$_3$(BF_4)$_2$	DMF	Visible light	Na_2HPO_4		24h
[Ir(df(CF_3)ppy)$_2$(dtbbpy)(BF_6)] Ru(bpy)$_3$$Cl_2$ Ru(bpy)$_3$(BF_4)$_2$	CH_3CN	Visible light	1,4-benzoquinone	$MgSO_4$	24h
[Ir(df(CF_3)ppy)$_2$(dtbbpy)(BF_6)] Ru(bpy)$_3$$Cl_2$ Ru(bpy)$_3$(BF_4)$_2$	CH_3CN	UV light	1,4-benzoquinone	$MgSO_4$	24h
[Ir(df(CF_3)ppy)$_2$(dtbbpy)(BF_6)] Ru(bpy)$_3$$Cl_2$ Ru(bpy)$_3$(BF_4)$_2$	DCM	UV light	Na_2CO_3		24h under N_2
Ir(df(CF_3)ppy)$_2$(dtbbpy)(BF_6)] Ru(bpy)$_3$$Cl_2$ Ru(bpy)$_3$(BF_4)$_2$	CH3N	Visible light	$K_2S_2O_8$		24 h
Ir(df(CF_3)ppy)$_2$(dtbbpy)(BF_6)] Ru(bpy)$_3$$Cl_2$ Ru(bpy)$_3$(BF_4)$_2$	CH3N	UV light	$K_2S_2O_8$		24 h

2.11 Preparation of Gold Nanoparticles

Gold nanoparticles were synthesized according to a controlled citrate reduction approach. In a typical procedure, a 100 mL sample of aqueous $HAuCl_4$ (0.25 mM) was put into a 250 mL three-neck flat-bottom flask. After the solution was brought to boil under reflux with stirring, 1 mL of 5% sodium citrate solution was added. The reaction solution was allowed to boil until the solution became wine red in color (about 20 min). The gold nanoparticles were then allowed to cool to room temperature.[87]

The gold nanoparticles obtained from the above procedure were centrifuged at 8000 rpm for 20 min. The supernatant was then removed and discarded, and the pellet in each Eppendorf tube was collected together and centrifuged again at 8000 rpm for 20 min to obtain the gold concentrate (gold atom concentration of 0.4 M). The electrode was allowed to dry completely after each layer deposition and prior to use, however, all electrolyte solutions were purged with Argon gas (Figure 2.1). [87]

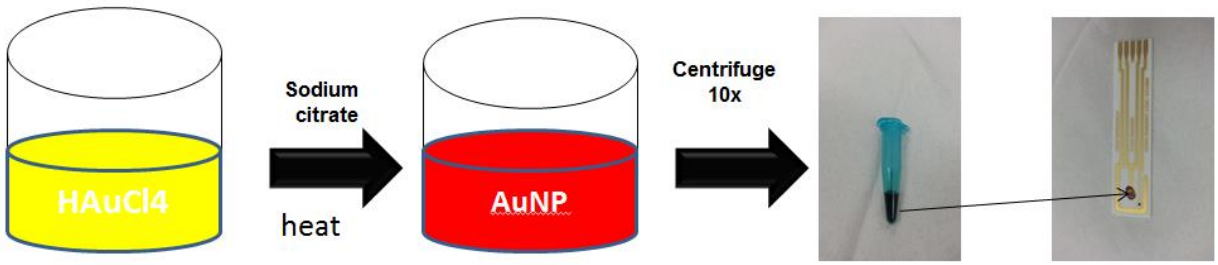

Gold colloidal "paste"

Figure 2.1: Gold Colloidal nanoparticles prepared using standard citrate reduction

2.11.1 Cyclic Voltammetry

Cyclic voltammetry was used in this project as a supplementary analysis method. It is convenient since the same electrode can be used as is used for EC-SERS measurements. In some cases, CVs were collected after the cathodic and anodic EC-SERS spectra were collected. For some measurements, a traditional three electrode electrochemical cell was used instead of the disposable screen printed carbon electrodes (SPE), modified with gold nanoparticles (AuNPs). For this method, a carbon working electrode, Ag/AgCl reference electrode, and a carbon wire counter electrode were used (Figure 2.2). The electrodes were clamped up in cell caps for ease of use. The electrochemical cell is a standard glass vial with a solvent of about 5 mL as shown in (Figure 2.2). $TBAPF_6$, which is a white powder, was dissolved in CH_3CN to make a 0.1 M solution, and ferrocene was dissolved in CH_3CN to make a 10mM solution. Both solutions were used as electrolytes. Using one electrolyte per experiment, 10 µL of phenol compound A was added to the electrolyte and a potential (-0.1 V to 1 V) was applied for 9 min while data was collected for CV analysis.[87]

Figure 2.2: The setup used for EC-SERS, including the flat-walled vial, AuNP-modified screen printed electrode, and holder for connection to the potentiostat

2.11.2 EC-SERS Raman Spectroscopy

Using this technique, the Raman spectra were collected on the AuNP modified working electrode and the first spectrum collected without an applied potential was simply a regular SERS spectrum. The laser was focused onto the working electrode of a modified SPE in the electrochemical small-volume cell, the same as CV cell with different electrolytes. For open-circuit potential, the first desired potential was applied (typically 0.0 V) while the EC-SERS spectrum was recorded. The process was repeated for the next potential (e.g. -0.1 V), and so on, until the spectrum at the final desired potential was recorded. Typically, EC-SERS spectra are collected at ocp, and then from 0.0 to -1.0 V, in 1 V increments (cathodic scan). An anodic series can be collected after, typically from -1.0 to 0.0 V in +0.1 V increments, were typically collected a SERS spectra for 30 sec.

Raman spectra must be collected in a darkened room; a diagram of this setup is shown in Figure 2.3.[88,89,90]

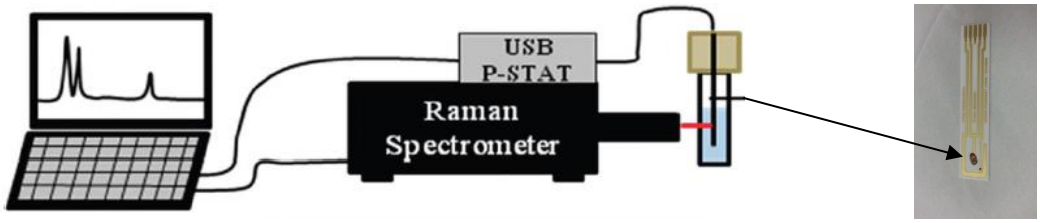

Figure 2.3: Schematic setup of the EC-SERS setup, coupling a Raman spectrometer with a portable potentiostat. The AuNPs are deposited onto the working electrode of a disposable screen printed electrode. (Adapted from ref 88)

Chapter 3: Results and discussion

This section describes attempts to perform the photoredox [5 + 2] cycloaddition reaction of phenols via ruthenium and iridium catalysis. In this section, the characterisation data of phenol compounds A, B, C and D, are presented. In addition, this section includes a summary and suggestions for future studies, as well as recommendations for obtaining better results.

This chapter includes the characterisation spectra of phenol compounds A, B, C and D. The synthesis for each of these compounds involves 3 steps, as reported in the respective sub-sections. This chapter also includes the spectra of the ruthenium and iridium catalysts. In addition, the CV and EC-SERs spectra of phenol compound A have been included. Furthermore, other phenol compounds were prepared (such as phenol C) and different synthetic methods were also explored. The results of these syntheses as well as the respective photoreaction spectra are included in the Appendix.

3.1 Phenol compound A

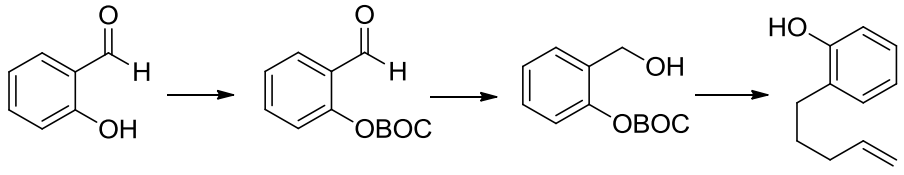

A1 **A2** **A**

Chapter 2 outlines the methods by which phenol A was synthesised. These methods involved the conversion of salicylaldehyde into the Boc_2O protected aldehyde. Subsequently, the aldehyde was converted to an alcohol, and then into phenol A. Figure 3.3 shows the NMR spectra of the intermediates and product (phenol A). The ^{1}H-NMR spectra were recorded at 300 MHz and the chemical shifts are reported in parts per million (ppm) with respect to the solvent resonance of $CDCl_3$ (7.27 ppm). In addition, ^{13}C NMR spectra were recorded at 75 MHz with a solvent resonance of $CDCl_3$ (77.23 ppm).[16]

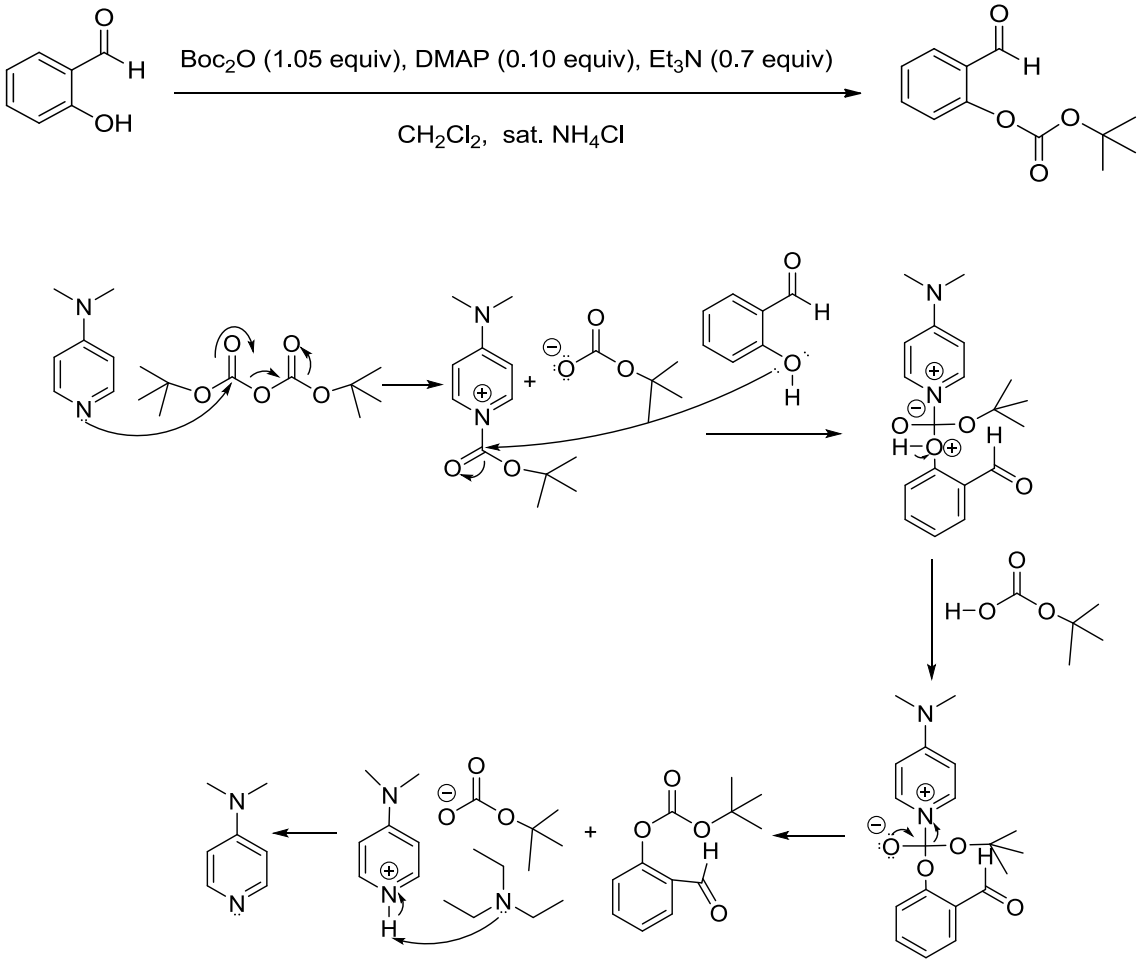

Scheme 3.1: Aldehyde compound (an intermediate in the synthesis of phenol compound A)

Scheme 3.1 depicts the first step in the synthesis of phenol compound A. The lone pair of electrons on the ring-nitrogen atom of DMAP attack a carbonyl centre of Boc_2O, forming the intermediates shown in Scheme 3.1. Subsequently, a lone pair of electrons on the oxygen atom of the alcohol attack the carbonyl centre of the pyridinium intermediate, forming a tetrahedral intermediate. Deprotonation of the intermediate and consequent breakage of the C-N bond yield the product and regenerate the catalyst. However, protonation of the catalyst occurs as a result of its reaction with the generated acid. Subsequent deprotonation by triethylamine finally regenerates the catalyst. Figure 3.1 shows the ^{1}H NMR and ^{13}C NMR of the aldehyde product.

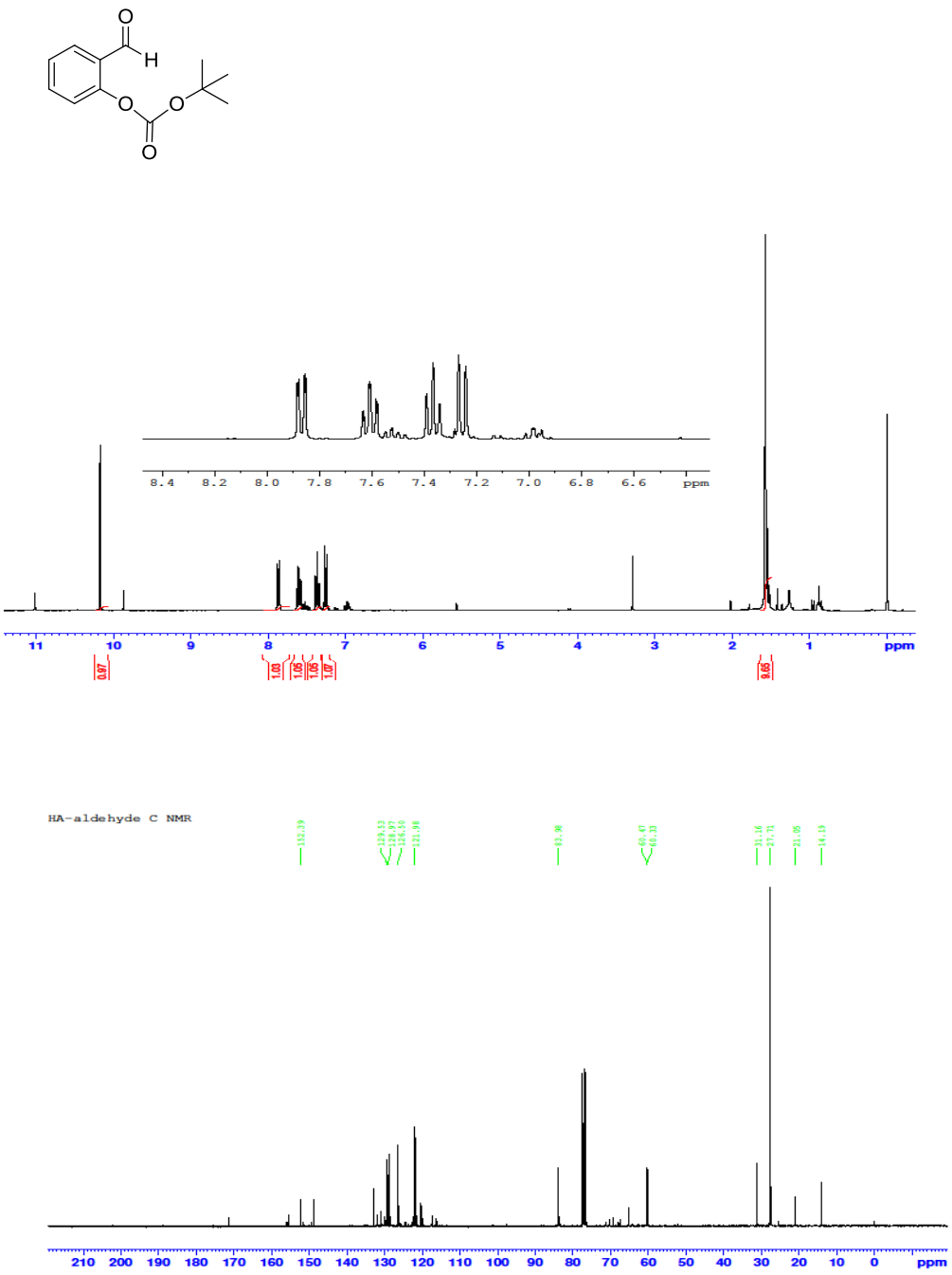

Figure 3.1: ^{1}H NMR (300 MHz, $CDCl_3$, ppm) and ^{13}C (75 MHz, $CDCl_3$, ppm) NMR spectrums of aldehyde compound (an intermediate in the synthesis of phenol compound A).

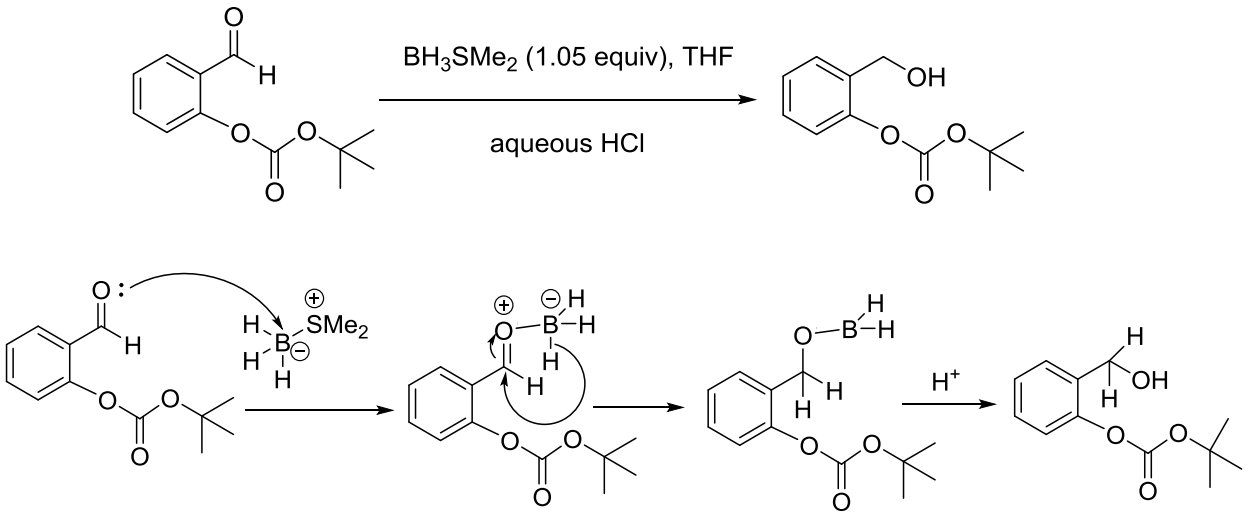

Scheme 3.2: Alcohol compound (an intermediate in the synthesis of phenol compound A)

Scheme 3.2 shows the second step in the synthesis of phenol compound A. A proposed mechanism for the reduction of the aldehyde to the alcohol involves the transfer of hydride from BH_3SMe_2, to the carbonyl carbon of the aldehyde. The subsequent transfer of an electron pair from the C=O bond to the oxygen atom results in an anionic tetrahedral intermediate. Subsequent quenching of the reaction with aqueous HCl protonates this intermediate to form the alcohol. Figure 3.2 shows the ^{1}H NMR and ^{13}C NMR of the alcohol product.[16] Prior to the use of BH_3SMe_2, the reduction of the aldehyde using $NaBH_4$ was attempted without success. A possible reason for this is shown below:

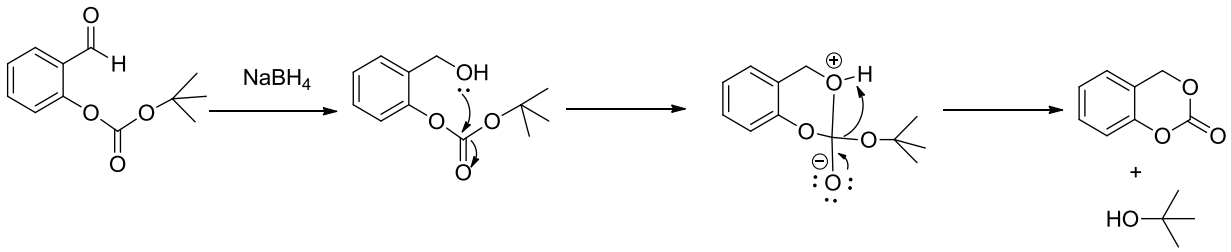

Upon the reduction of the aldehyde to the alcohol by $NaBH_4$, a lone pair of electrons on the alcohol oxygen attacked the carbonyl group to form a tetrahedral intermediate. When this intermediate collapses, the alcohol proton is abstracted by the forming tert-butoxide species, to yield the product and tert-butanol.

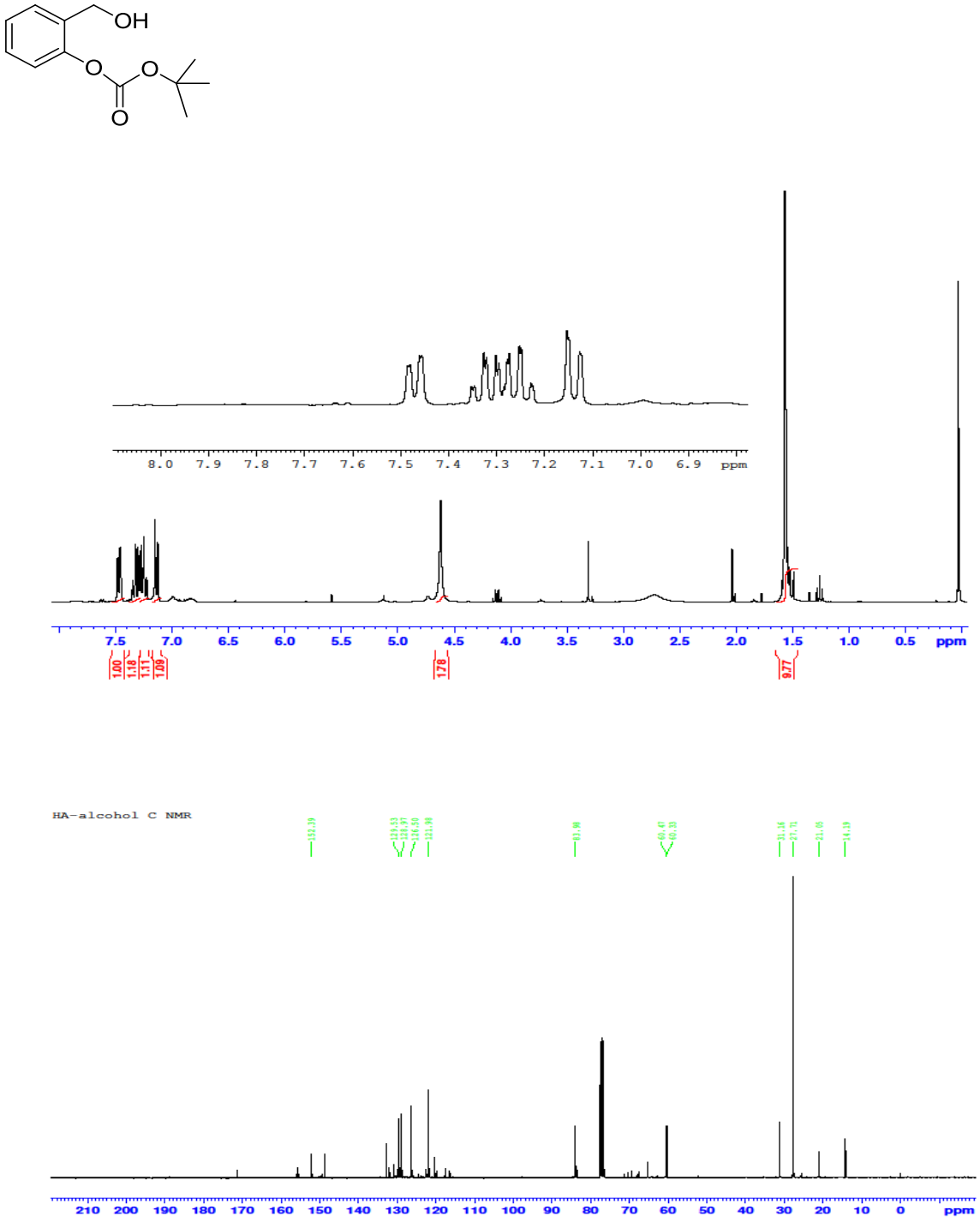

Figure 3.2: ^{1}H NMR (300 MHz, $CDCl_3$, ppm) and ^{13}C NMR (75 MHz, $CDCl_3$, ppm) spectrum of alcohol compound (an intermediate in the synthesis of phenol compound A).

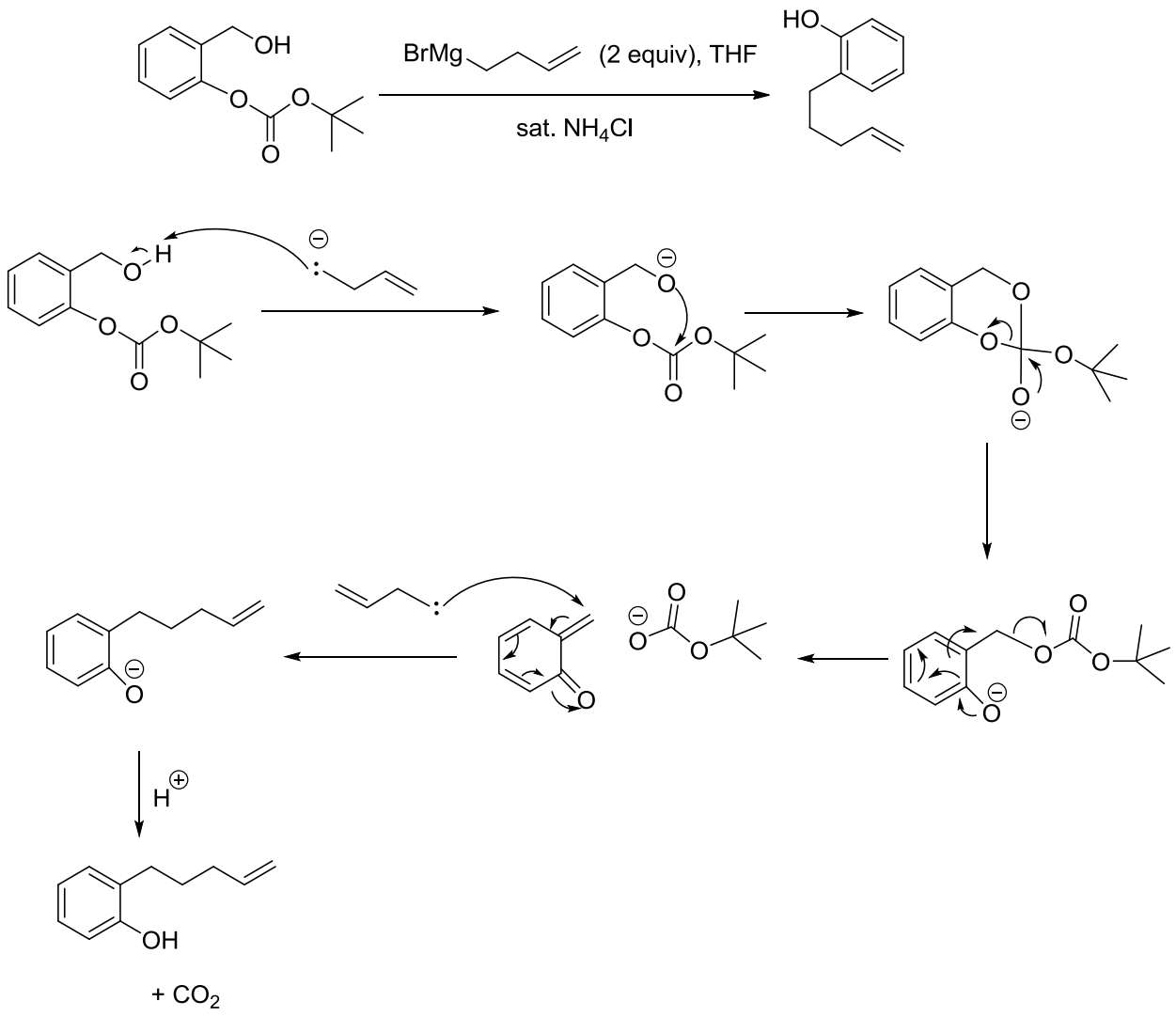

Scheme 3.3: Phenol compound A

The final step in the synthesis of phenol compound A, was the reaction of the alcohol intermediate with 2 equivalents of the Grignard reagent, $BrMg(CH_2)_2CHCH_2$ as shown in scheme 3.3. A Grignard reagent has the general formula RMgX, where X is a halogen, and R is an alkyl or aryl group. The Grignard reagent used in the final synthetic step of

phenol compound A, was made by adding magnesium to 4-bromo-1-butene in diethyl ether. The carbon-magnesium bond of the resulting Grignard reagent is polar covalent, with carbon bearing the negative charge.

The first equivalent of Grignard reagent deprotonates the alcohol proton. The negatively charged oxygen of the resulting anionic species then attacks the carbonyl moiety to form a cyclic intermediate. Upon re-establishment of the C=O bond, the cyclic intermediate is opened to form an anionic species. Establishment of a meta-C=O bond enables the movement of electrons in the aromatic ring, causing the favourable loss of the $^{-}OCO_2C(CH_3)_3$ leaving group. The subsequent Grignard attack on the sp^2 hybridized carbon, forms the phenoxide. Subsequent quenching of the reaction with aqueous NH_4Cl protonates this intermediate to form the phenol. Figure 3.3 shows the ^{1}H NMR and ^{13}C NMR of the phenol product.[16]

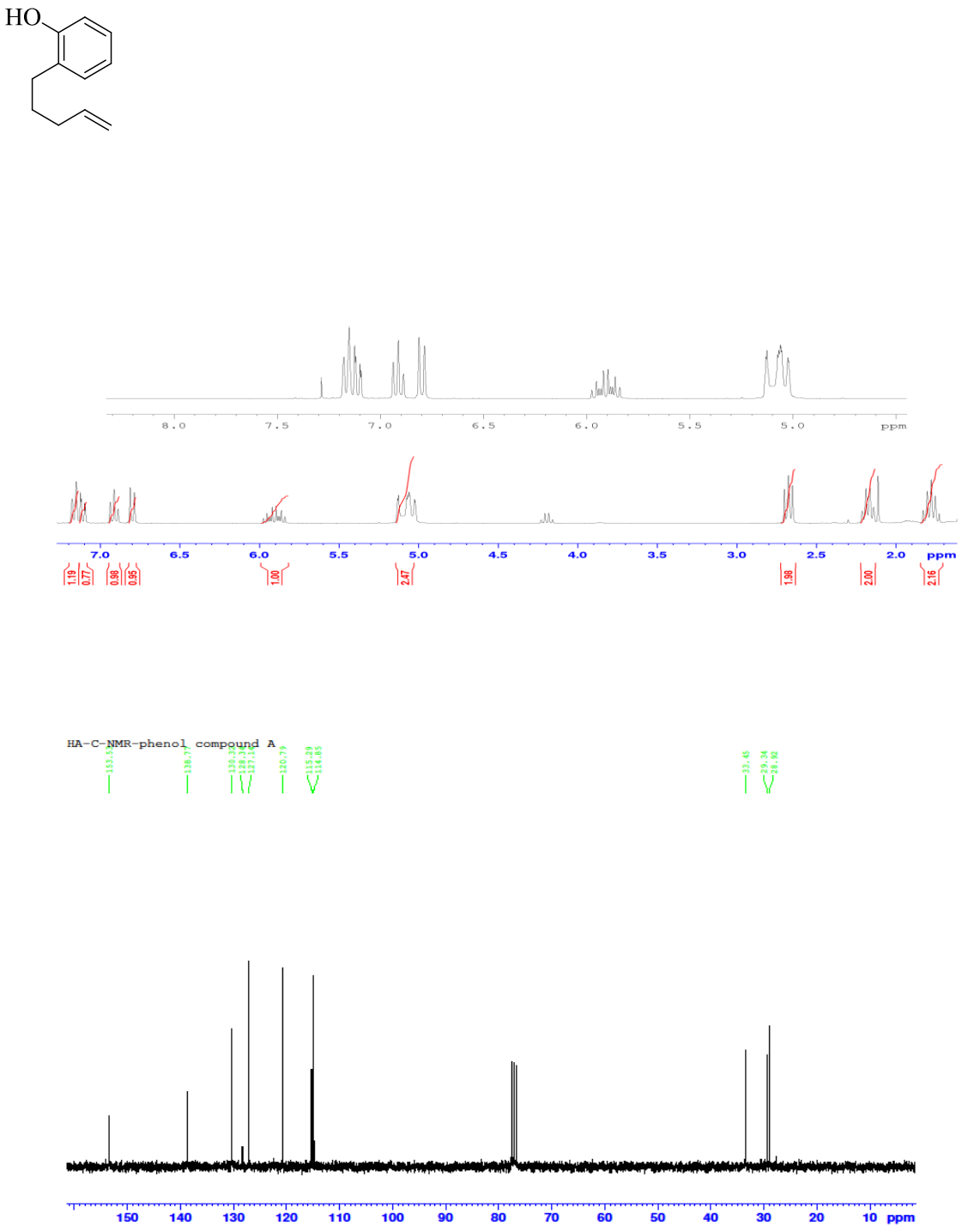

Figure 3.3: ^{1}H NMR (300 MHz, $CDCl_3$, ppm) and ^{13}C NMR spectrum of phenol compound A.

3.2 Phenol compound B

Phenol B was synthesised with a methoxy group para to the hydroxyl group. The rationale for this synthesis was to stabilize the cationic intermediate formed during cycloaddition, via the electron donating effect of a methoxy group.[74] The activating properties of the methoxy group stabilize the resonance hybrid. Thus, the radical cation is further stabilized by the electron donating properties of the methoxy group.

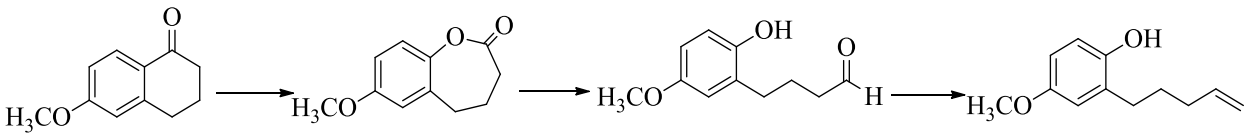

B1 **B2** **B**

The synthesis of compound B, as reported in Chapter 2, involves 3 steps. First, 6-methoxy-1-tetralone was reacted with mCPBA to yield the lactone intermediate which was used without purification. Next, the aldehyde was prepared by reacting the crude lactone with DIBAL-H in toluene at –78 °C. Finally, the final product (phenol B) was afforded by the reaction of Ph_3PCH_3Br with the aldehyde and KOt-Bu, in an ice bath. The spectra for these intermediates as well as the final product are presented below.[74]

The first step in the synthesis of phenol compound B involves the conversion of 6-methoxy-1-tetralone to B1. This step is a Baeyer-Villiger oxidation, used for the conversion of ketones to esters by C-C bond cleavage of the carbonyl group and introduction of an oxygen atom via a peroxyacid. As shown in Scheme 3.4, this step

involved the reaction of 6-methoxy-1-tetralone with the oxidizing agent, mCPBA to afford the lactone, B1.

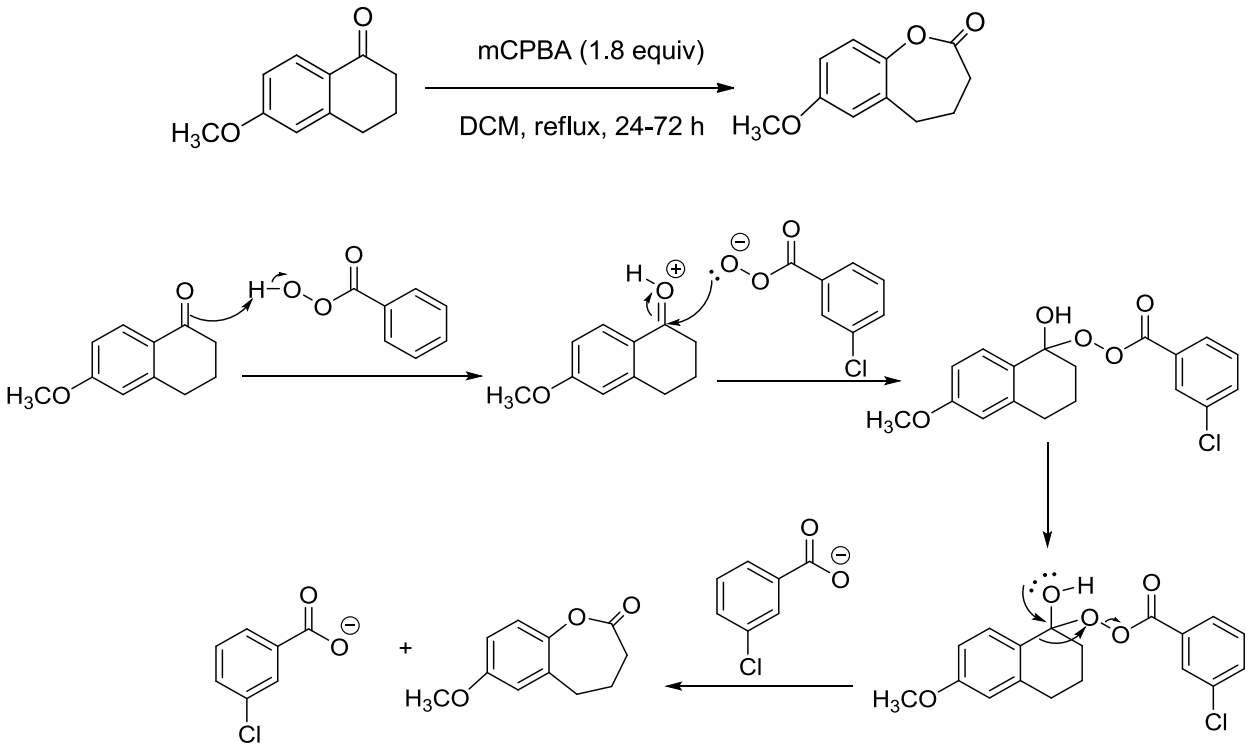

Scheme 3.4: Lactone compound (an intermediate in the synthesis of phenol compound B)

Upon deprotonation of the peroxyacid by the ketone, the resulting nucleophilic species attacks the carbonyl group of the activated ketone, forming the tetrahedral intermediate. Once the tetrahedral intermediate collapses, carbon migration occurs, benzoate is eliminated and the lactone is formed. The addition of aqueous NH_4Cl as the proton source generates p-chlorobenzoic acid as the byproduct. Figure 3.4 shows the ^{1}H-NMR and ^{13}C-NMR spectra of the synthesised lactone.

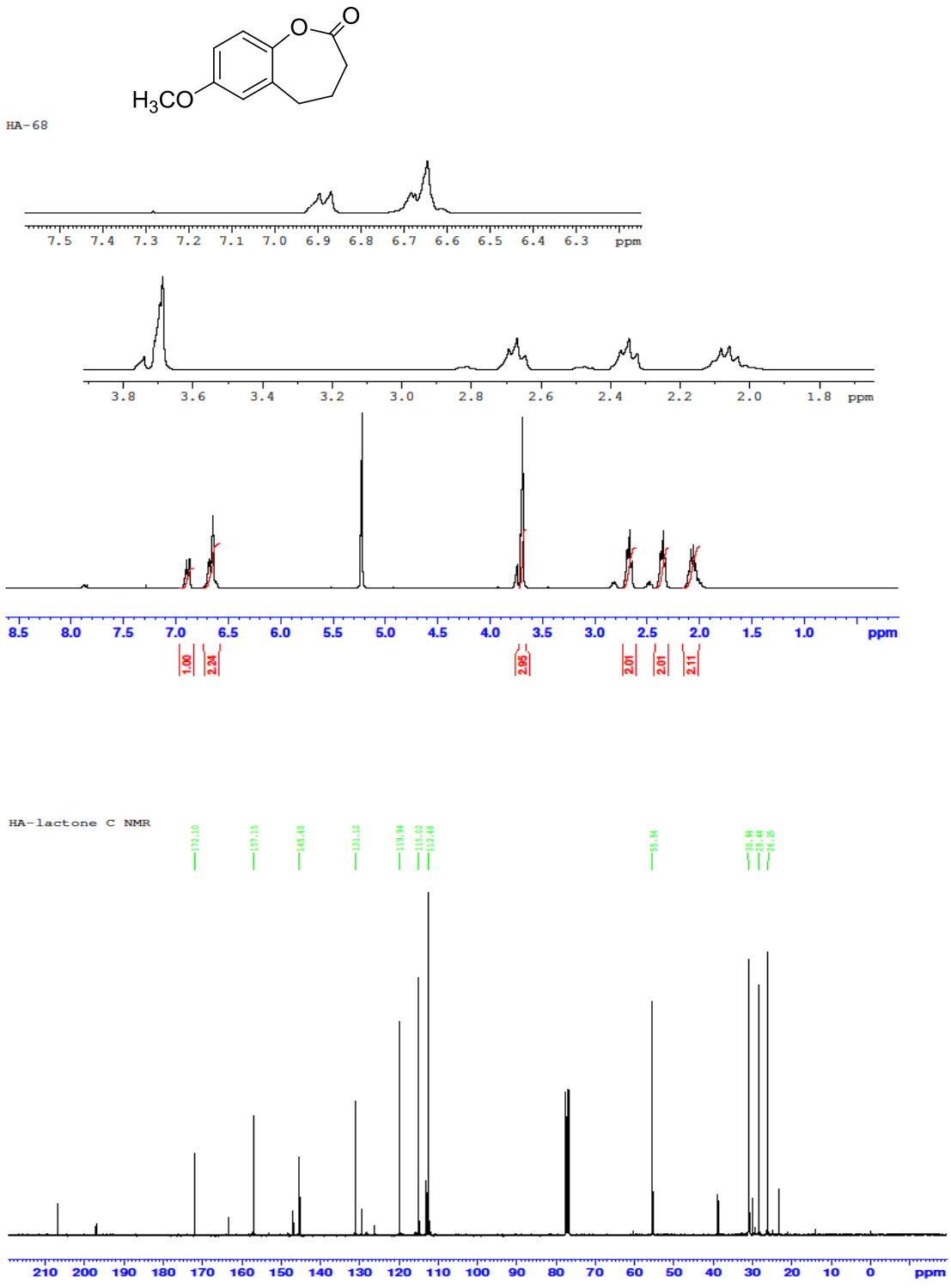

Figure 3.4: ^{1}H NMR (300 MHz, $CDCl_3$, ppm) and ^{13}C NMR (75 MHz, $CDCl_3$, ppm) spectrum of lactone compound (an intermediate in the synthesis of phenol compound B).

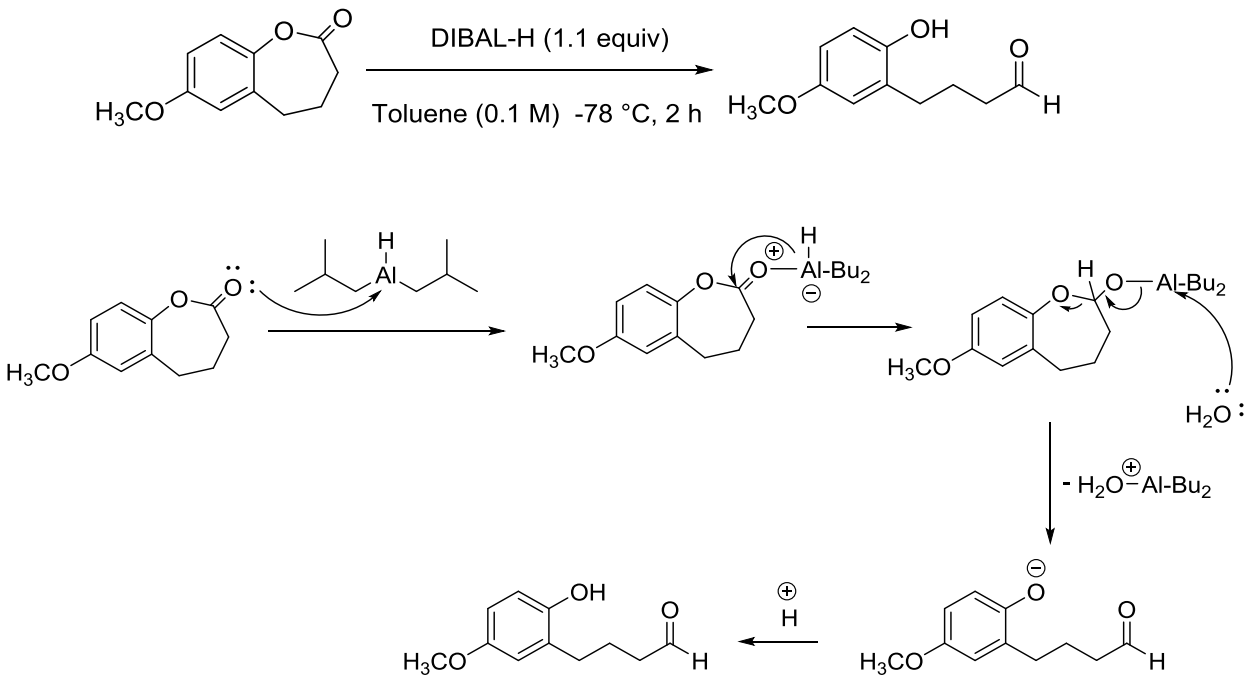

Scheme 3.5: Aldehyde compound (an intermediate in the synthesis of phenol compound B)

The synthesis of the aldehyde intermediate was the second step in the overall synthesis of phenol compound B, as shown in Scheme 3.5. This reaction involved the use of DIBAL-H, which is a strong reducing agent, to reduce the lactone to an aldehyde. This procedure did not reduce the aldehyde further, such as to the alcohol, because only one equivalent was added. A proposed mechanism for this reaction involves the donation of a lone pair of electrons from the carbonyl oxygen of the lactone, to the Lewis acidic aluminum atom of DIBAL-H, to form an anionic intermediate. A subsequent hydride transfer from the

aluminum atom to the carbonyl carbon results in a tetrahedral hemiacetal intermediate. Saturated ammonium chloride solution was used as a proton source to quench the reaction and afford the aldehyde and $AlH(t\text{-}Bu)_2$ as a by-product. This aldehyde was purified by column chromatography and subsequently used as the starting material in the third step of the synthesis of phenol compound B. Figure 3.5 shows the ^{1}H NMR and ^{13}CNMR spectra of the purified aldehyde.[74]

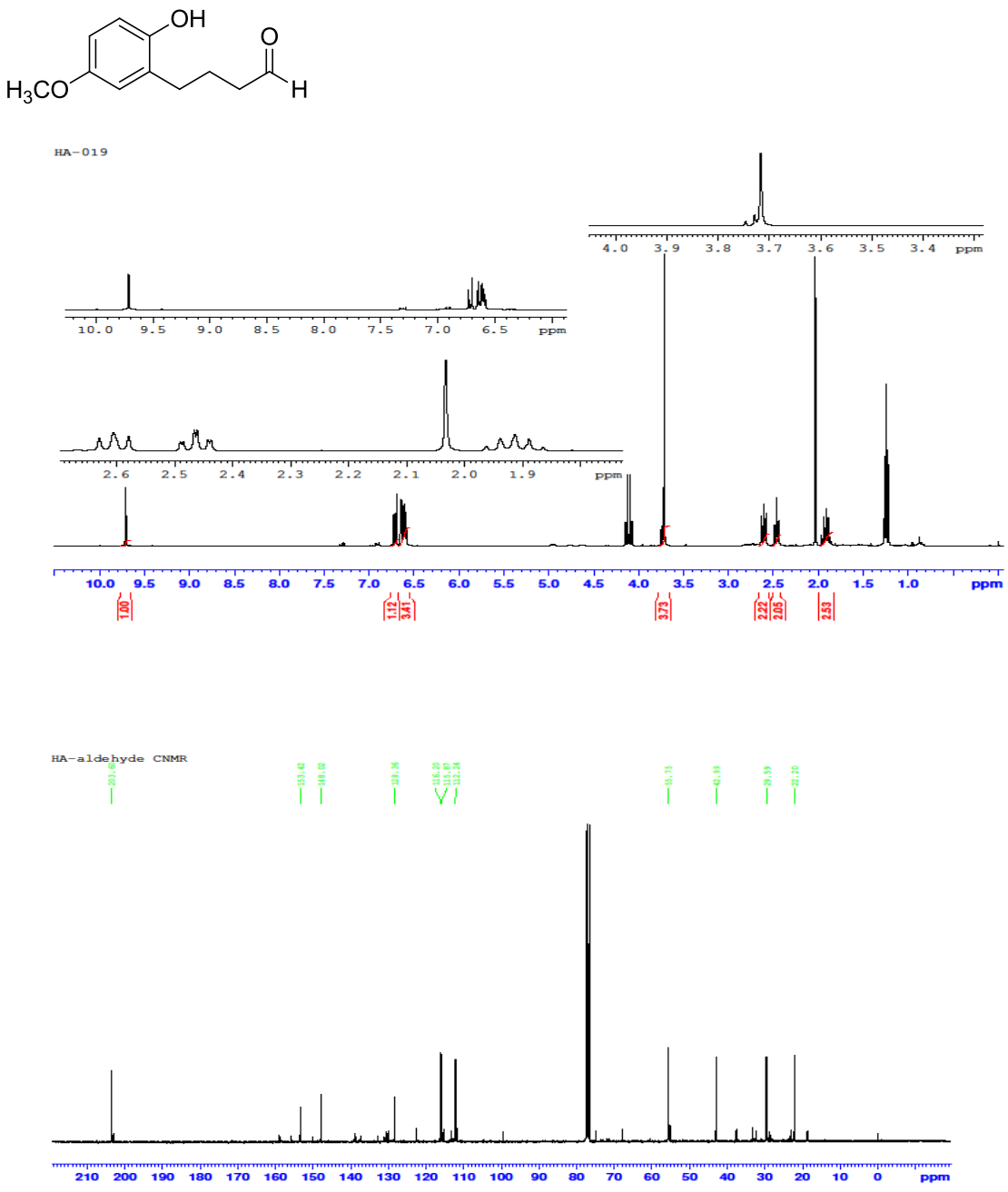

Figure 3.5: ^{1}H NMR (300 MHz, $CDCl_3$, ppm) and ^{13}C NMR (75 MHz, $CDCl_3$, ppm) spectrum of aldehyde compound (an intermediate in the synthesis of phenol compound B).

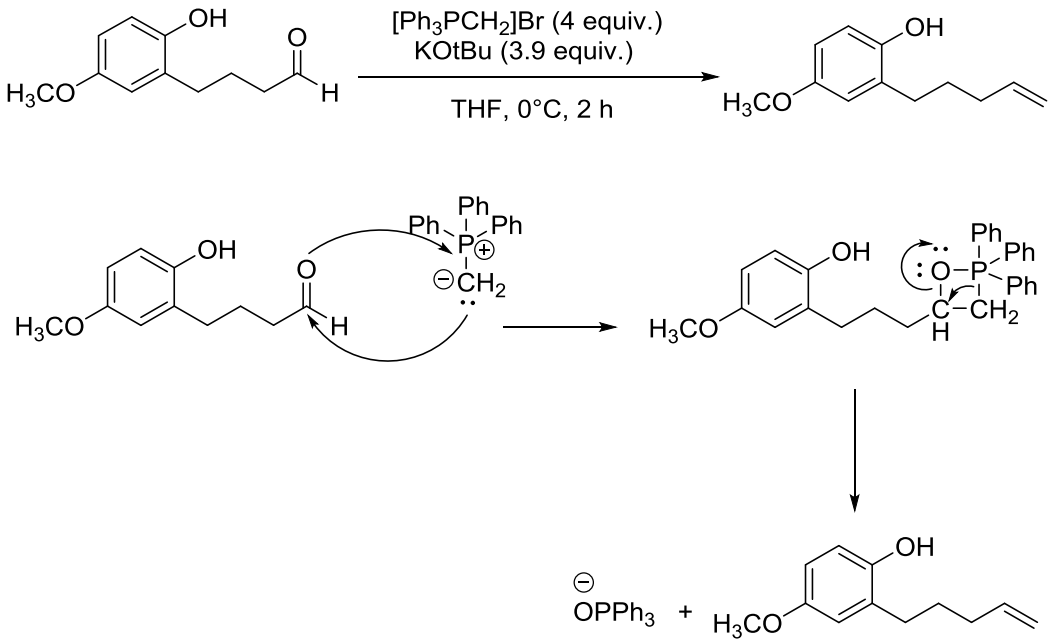

Scheme 3.6: Phenol compound B

This last step in the synthesis of phenol compound B involved the conversion of the aldehyde obtained from the second step into an alkene via the Wittig reaction shown in Scheme 3.6. While $[PPh_3CH_2]Br$ served as the nucleophile in this reaction, KOtBu acted as the base. A Wittig reaction involves the reaction of an aldehyde with an alkyl triphenyl phosphonium yield to give an alkene and triphenylphoxide. First, KOtBu was added to Ph_3PCH_2Br, deprotonation resulted in the formation of a nucleophilic phosphine anion. The nucleophilic addition of the phosphine anion to the carbonyl carbon of the aldehyde resulted in the formation of a betaine intermediate. Subsequently, a four-membered heterocyclic oxaphosphatane was formed. Finally, the cleavage of bonds in the oxaphosphatane heterocycle resulted in the formation of the alkene and a phosphine oxide by-product. Figure 3.6 shows the ^{1}H NMR and ^{13}C NMR of the alkene.

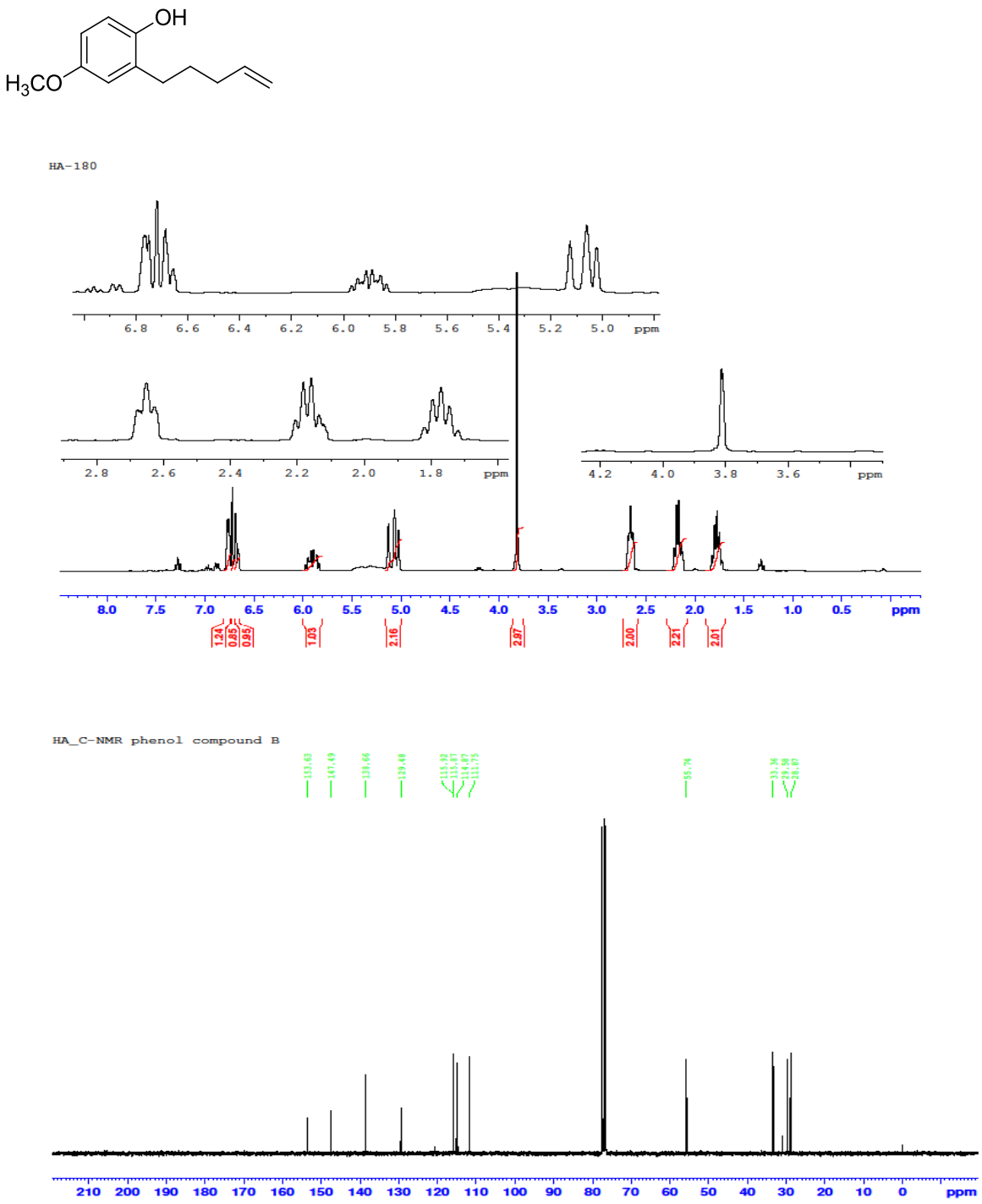

Figure 3.6: ^{1}H NMR (300 MHz, $CDCl_3$, ppm) and ^{13}C NMR (75 MHz, $CDCl_3$, ppm) spectra of phenol compound B.

3.3 Phenol compound D7

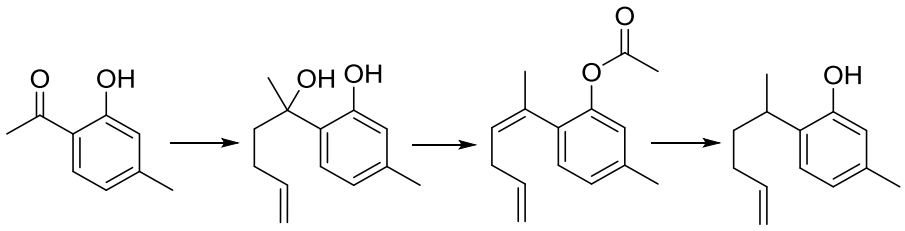

D5 **D6** **D7**

The ^{1}H NMR, and ^{13}C NMR of phenol compound D7, as well as those of the intermediates, are presented below. Via the Grignard reaction of 3-butenylmagnesium bromide with the starting ketone at -78 $^{\circ}C$, the benzyl alcohol (D5) was afforded. Styrene acetate (D6) was prepared by reacting D5 with pyridine and acetic anhydride. Finally, the reaction of Li and NH_3 with D6 generated the final product, D7.

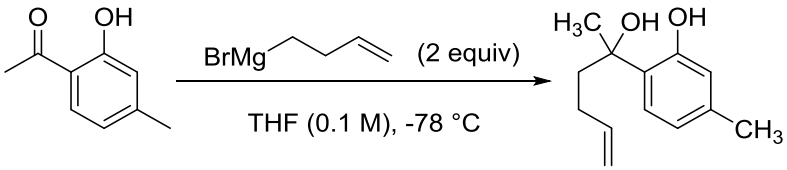

Scheme 3.7: Benzyl alcohol D5 (an intermediate in the synthesis of phenol compound D7)

The synthesis of benzyl alcohol (D5) was the first step in the synthesis of phenol compound D7, as shown in Scheme 3.7. This reaction involved the conversion of 2-hydroxy-4-methyl acetophenone to compound D5, via the addition of Grignard reagent $MgBr(CH)_2CHCH_2$. The Grignard reagent is a good nucleophile, as it readily reacted with the electrophilic carbonyl group of the acetophenone, to form a new carbon-carbon bond.

In addition, the Grignard reagent also acted as a strong base, as a second equivalent deprotonated the acidic hydrogen of the phenol compound. Subsequent quenching with aqueous NH_4Cl afforded D5. Figure 3.7 shows the ^{1}H NMR and ^{13}C NMR spectra of compound D5.

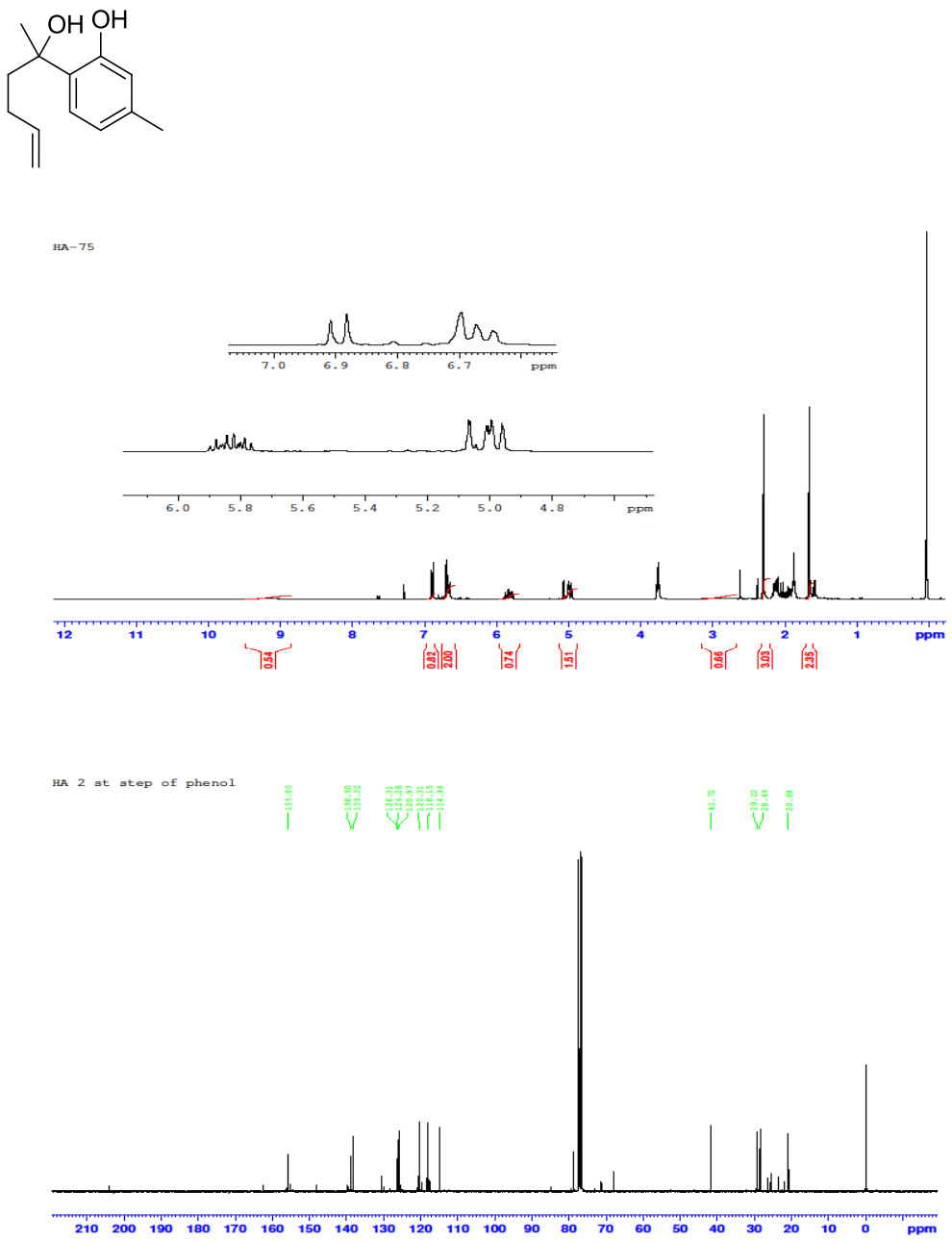

Figure 3.7: ^{1}H NMR (300 MHz, $CDCl_3$, ppm) and ^{13}C NMR (75 MHz, $CDCl_3$, ppm) spectrum of benzyl alcohol D5 (an intermediate in the synthesis of phenol compound D7).

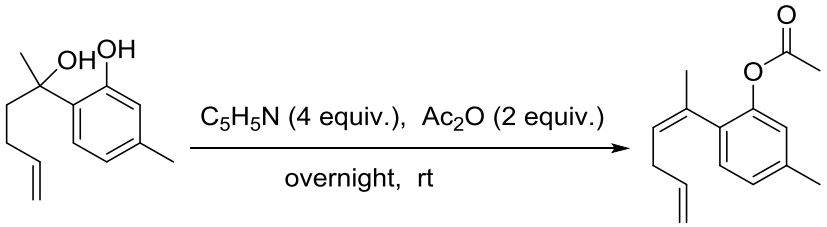
OH
OH
C5H5N (4 equiv.), Ac2O (2 equiv.)
overnight, rt
O
O

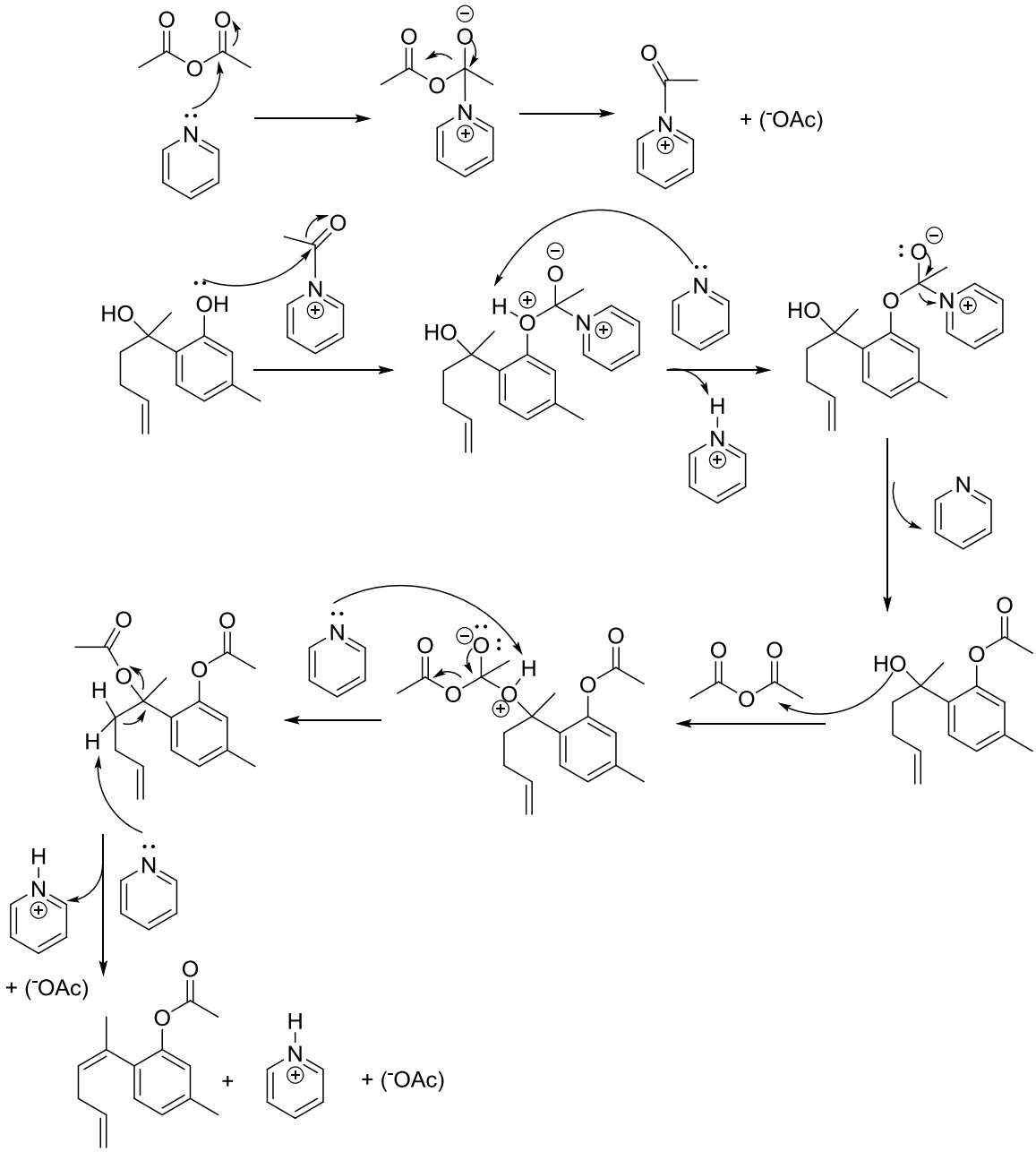

Scheme 3.8: Styrene acetate compound D6 (an intermediate in the synthesis of phenol compound D7)

The second step in the synthesis of phenol compound D7, was the conversion of benzyl alcohol D5 into styrene acetate, D6, as shown in Scheme 3.8. This step involved the

reaction of 1 equivalent of D5 with 4 equivalents of pyridine and 2 equivalents of acetic anhydride, to afford styrene acetate. First, pyridine reacted with acetic anhydride via nucleophilic addition, to form a N-C=O bond with the elimination of $^{-}$OAc. Subsequently, the nucleophilic addition of benzyl alcohol to the carbonyl group of the intermediate, resulted in the formation of a new tetrahedral intermediate. Another pyridine molecule abstracted a proton from the alcohol moiety of this intermediate, followed by the elimination of the pyridine moiety. Subsequently, the oxygen atom of the alcohol on the chain attacked another acetic anhydride molecule, which was followed by 2 pyridine mediated deprotonation steps. These steps resulted in the formation of D6, 2 equivalents of $^{-}$OAc and 2 equivalents of protonated pyridine. Figure 3.8 shows the ^{1}H NMR and ^{13}C NMR spectra of compound D6. These spectra show the presence of two isomers. This is expected, as the start compound, D5, possesses double bond. Thus, the formation of E and Z styrene acetate isomers, as shown in the spectra, was expected.

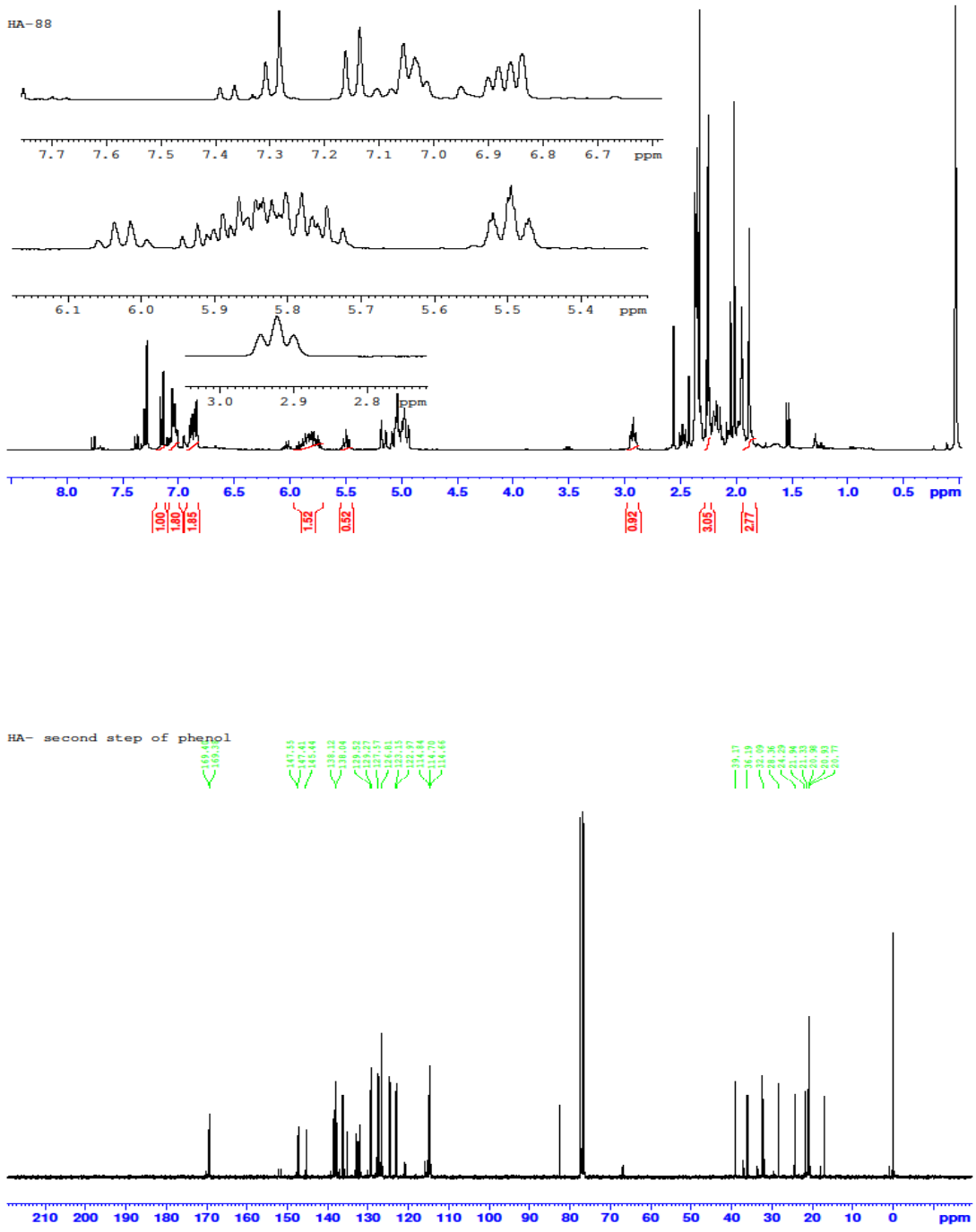

Figure 3.8: ^{1}H NMR (300 MHz, $CDCl_3$, ppm) and ^{13}C NMR (75 MHz, $CDCl_3$, ppm) spectrum of styrene acetate compound D6 (an intermediate in the synthesis of phenol compound D7).

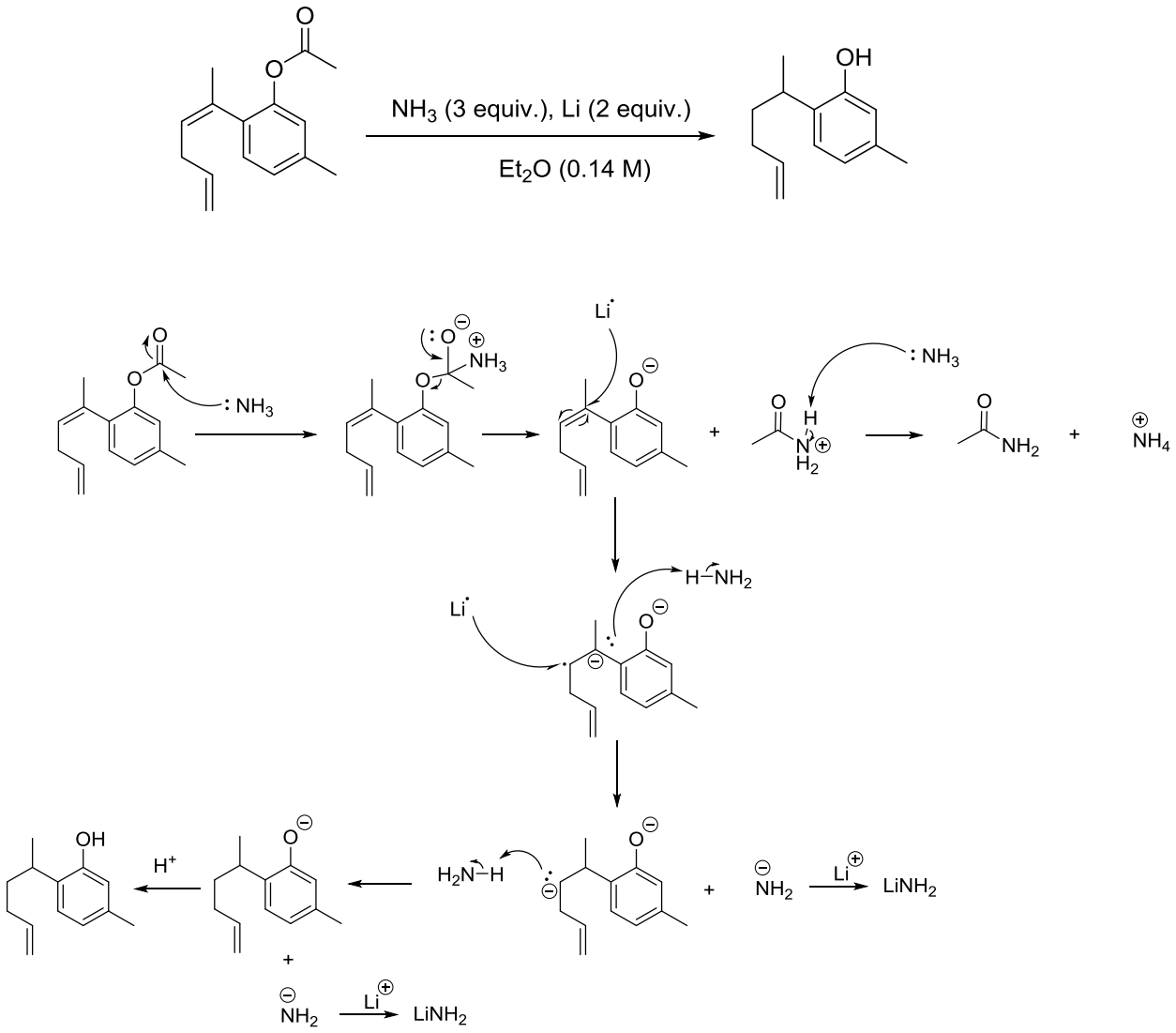

Scheme 3.9: Phenol compound D7

Phenol compound D7 was prepared from the reaction of 1 equivalent of compound D6 with 3 equivalents of NH_3 and 2 equivalents of lithium, as shown in Scheme 3.9. The first step in this mechanism involved the nucleophilic addition of ammonia to the carbonyl group of D6, with the subsequent elimination of NH_2COCH_3 and the formation of an

alcohol. Next, an electron was transferred from a lithium atom to a carbon atom of the alkene arm, resulting in the formation of one radical carbon and an anionic carbon. The lone pair of electrons on the anionic species deprotonated an ammonia molecule, with the formation of $LiNH_2$ as a by-product. This process was repeated, with another molecule of Li to form an anionic species. Subsequent abstraction of a proton from another molecule of NH_3, afforded compound D7 and another molecule of $LiNH_2$ as a by-product. Figure 3.9 shows the ^{1}H NMR and ^{13}C NMR of the successfully synthesised compound D7.

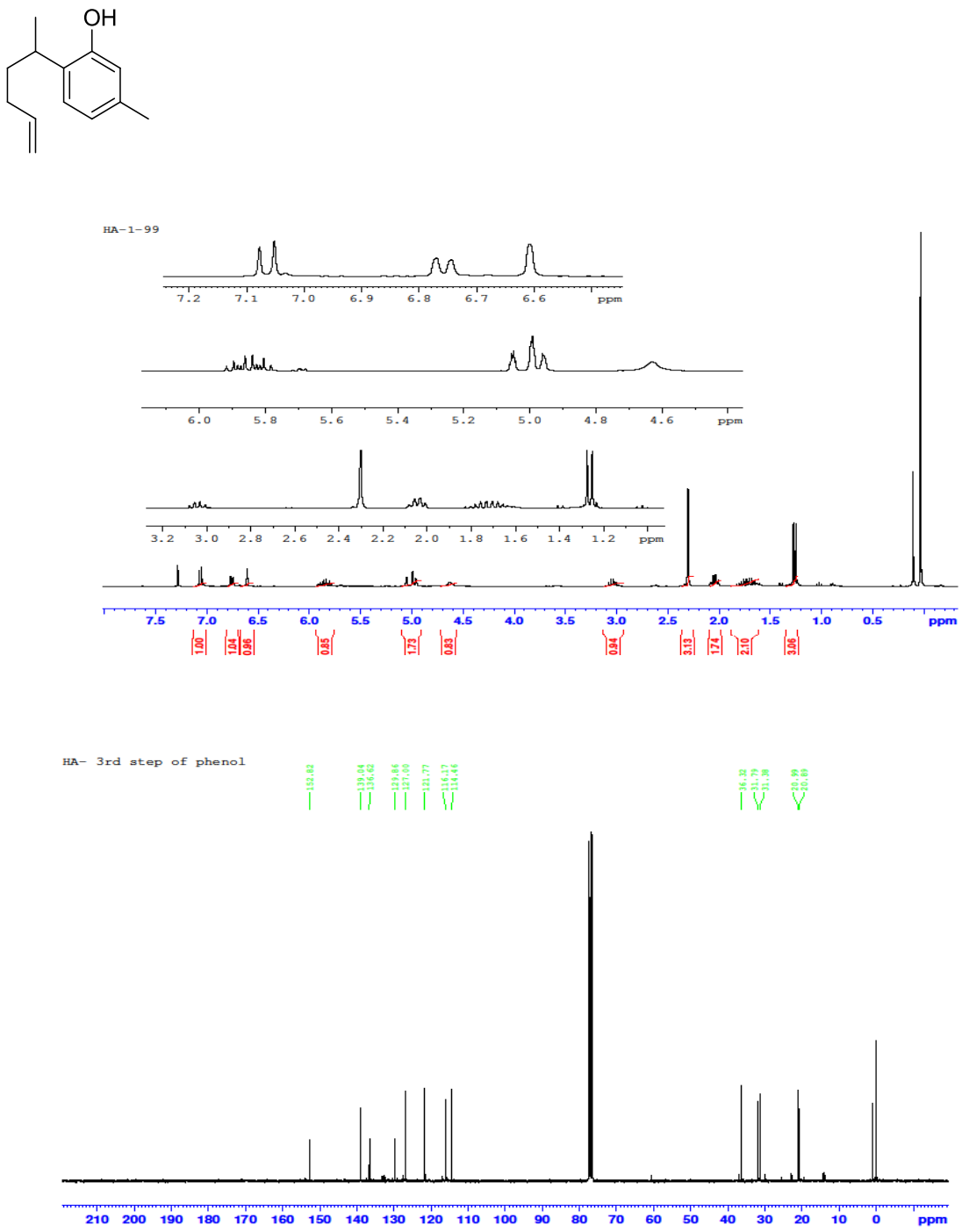

Figure 3.9: ^{1}H NMR (300 MHz, $CDCl_3$, ppm) and ^{13}C NMR (300 MHz, $CDCl_3$, ppm) spectrum of phenol compound D7

3.4 Phenol compound D10

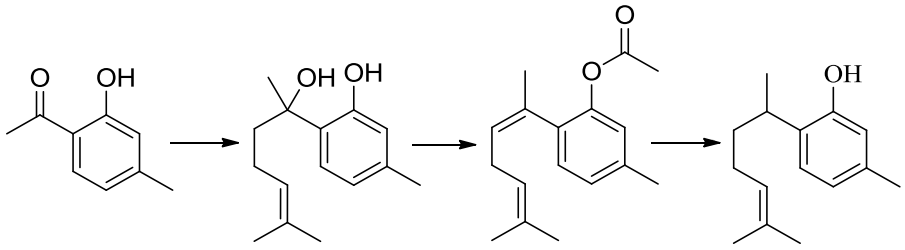

D8 **D9** **D10**

The ^{1}H NMR and ^{13}C NMR of phenol compound D, as well as those of the intermediates, are presented below: Via the Grignard reaction of 4-methylpent-3-enylmagnesium bromide with the starting ketone at -78 ˚C, the benzyl alcohol (D8) was afforded. Styrene acetate (D9) was prepared by reacting D8 with py and Ac_2O. Finally, the reaction of Li and NH_3 with D9 generated the final product, D10. [75]

This reaction has the same three steps as the similar phenol compound D7 except the alkyl halide used for preparation of the Grignard reagent, where was used 5-bromo-2-methyl-2-pentene.

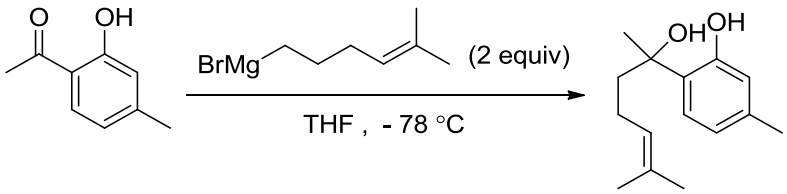

Scheme 3.10: Benzyl alcohol compound D8 (an intermediate in the synthesis of phenol compound D10)

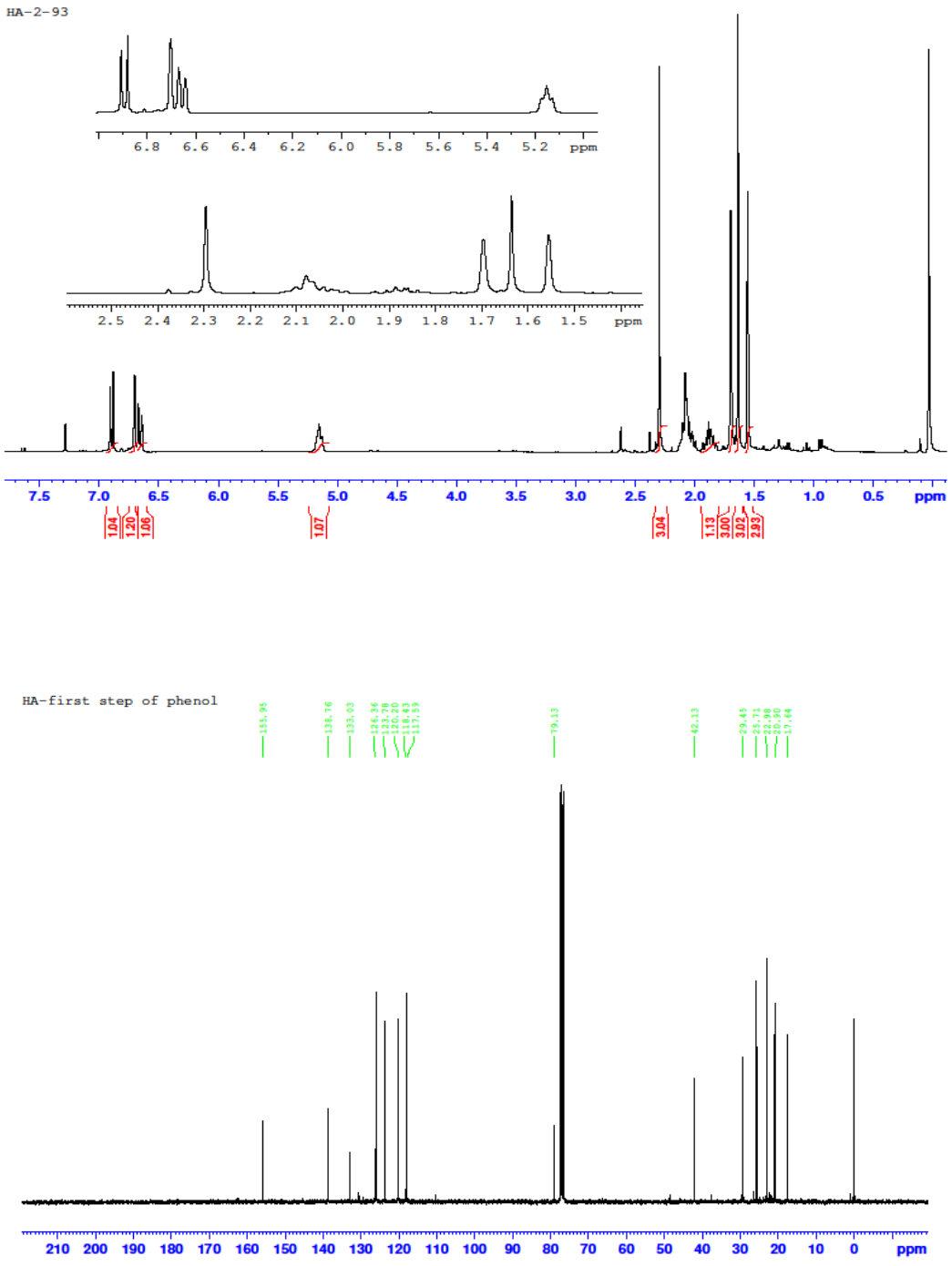

Figure 3.10: ^{1}H NMR (300 MHz, $CDCl_3$, ppm) and ^{13}CNMR (75 MHz, $CDCl_3$, ppm) spectrum of benzyl alcohol compound D8 (an intermediate in the synthesis of phenol compound D10).

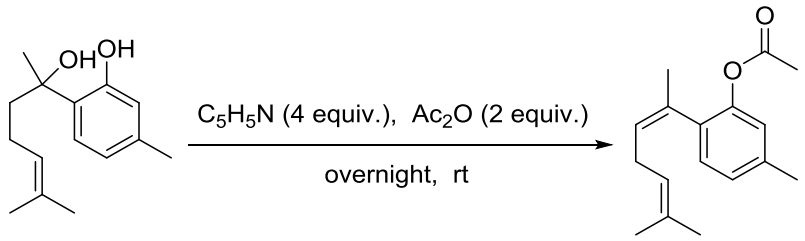

Scheme 3.11: Styrene acetate compound D9 (an intermediate in the synthesis of phenol compound D10)

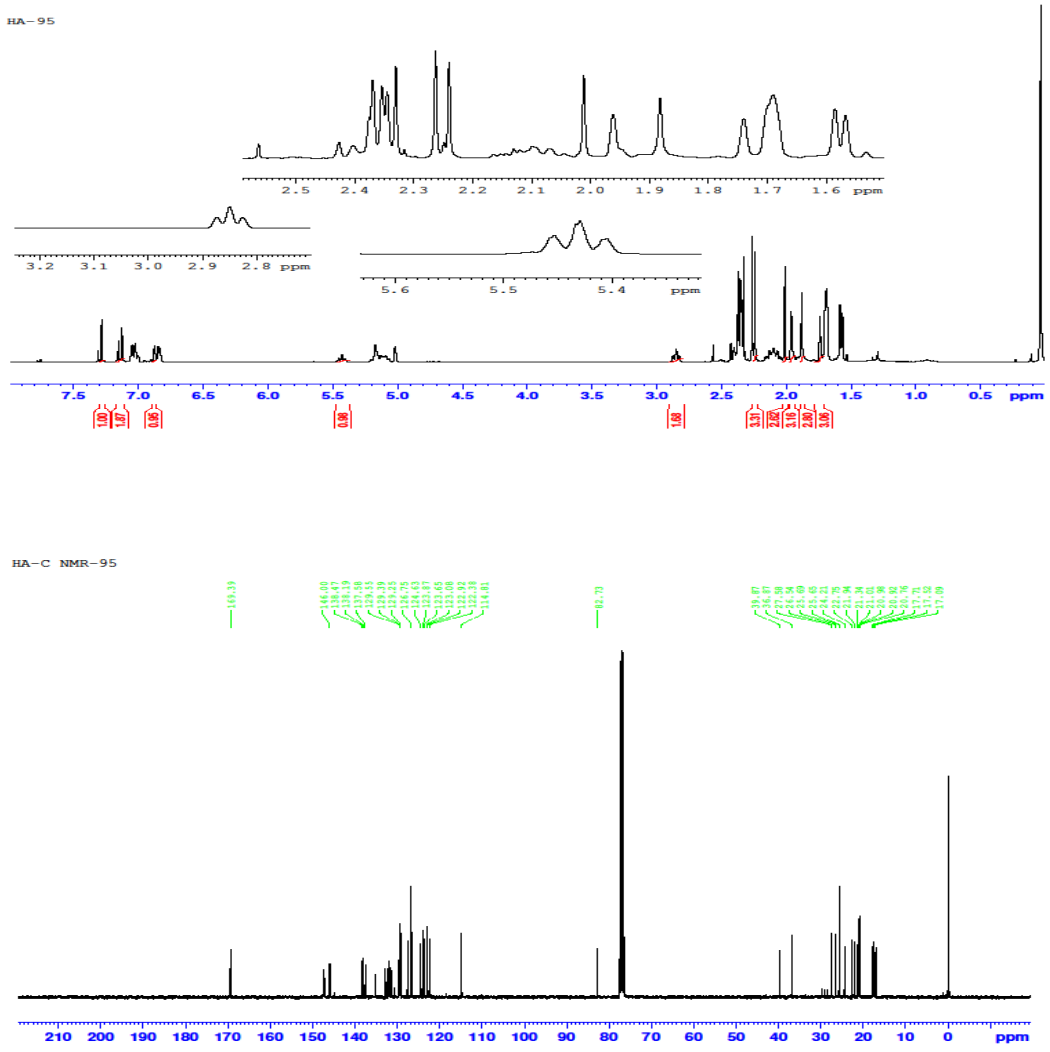

Figure 3.11: ^{1}H NMR (300 MHz, $CDCl_3$, ppm) and ^{13}C NMR (75 MHz, $CDCl_3$, ppm) spectra of styrene acetate compound D9 (an intermediate in the synthesis of phenol compound D10)

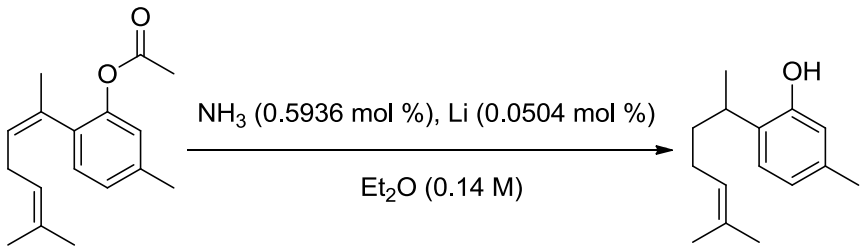

Scheme 3.12: Phenol compound D10

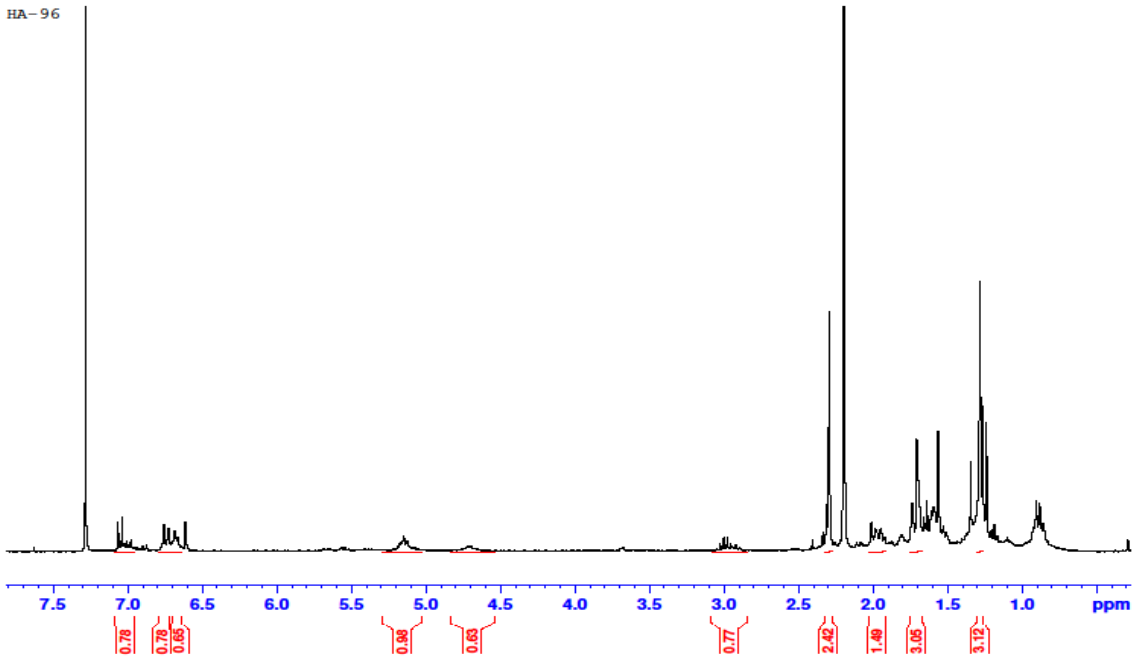

Figure 3.12: ^{1}H NMR (300 MHz, $CDCl_3$, ppm) spectrum of phenol compound D10.

3.5 Ruthenium catalyst

The $Ru(bpy)_3Cl_2$ and $Ru(bpy)_3BF_4$ complexes were synthesized using bipyridyl ligand (as reported in Section 2.6), with 70% and 75% yields, respectively. After recrystallization, the resulting crystals were washed with H_2O to afford the pure catalysts. It is clear that both $Ru(bpy)_3Cl_2$ and $Ru(bpy)_3BF_4$ exhibit similar ^1H NMR spectra, as shown in (Figure 3.13) because they both have the same ligand.[76]

A proposed mechanism for the synthesis of $Ru(bpy)_3Cl_2$ involves the displacement of the chloride ions of $RuCl_3$ by 3 equivalents of the bidentate ligand, bipy.

$$RuCl_3 + 3bpy \longrightarrow [Ru(bpy)_3]^{+3} + 3Cl^-$$

The reaction of phosphonate with water results in the formation of electrons which reduce the Ru^{3+} metal centre to Ru^{2+}.[91]

$$H_2PO_2^- + H_2O \longrightarrow HPO_3^- + 2H^+ + e^-$$

$$Ru^{+3} + e^- \longrightarrow Ru^{+2}$$

The complex was then precipitated via the common ion effect, by adding excess Cl^- (KCl).

$$[Ru(bpy)_3]^{2+} + 2Cl^- + 6H_2O \rightleftharpoons [Ru(bpy)_3]Cl_2.6H_2O$$

The procedure and mechanistic pathway in the synthesis of the $Ru(bpy)_3BF_4$ complex is similar to that of $Ru(bpy)_3Cl_2$. However, excess $NaBF_4$ instead of KCl, was used to elicit the common ion effect in the synthesis of this catalyst.

$$[Ru(bpy)_3]^{2+} + BF_4^- + 6H_2O \rightleftharpoons [Ru(bpy)_3]BF_4.6H_2O$$

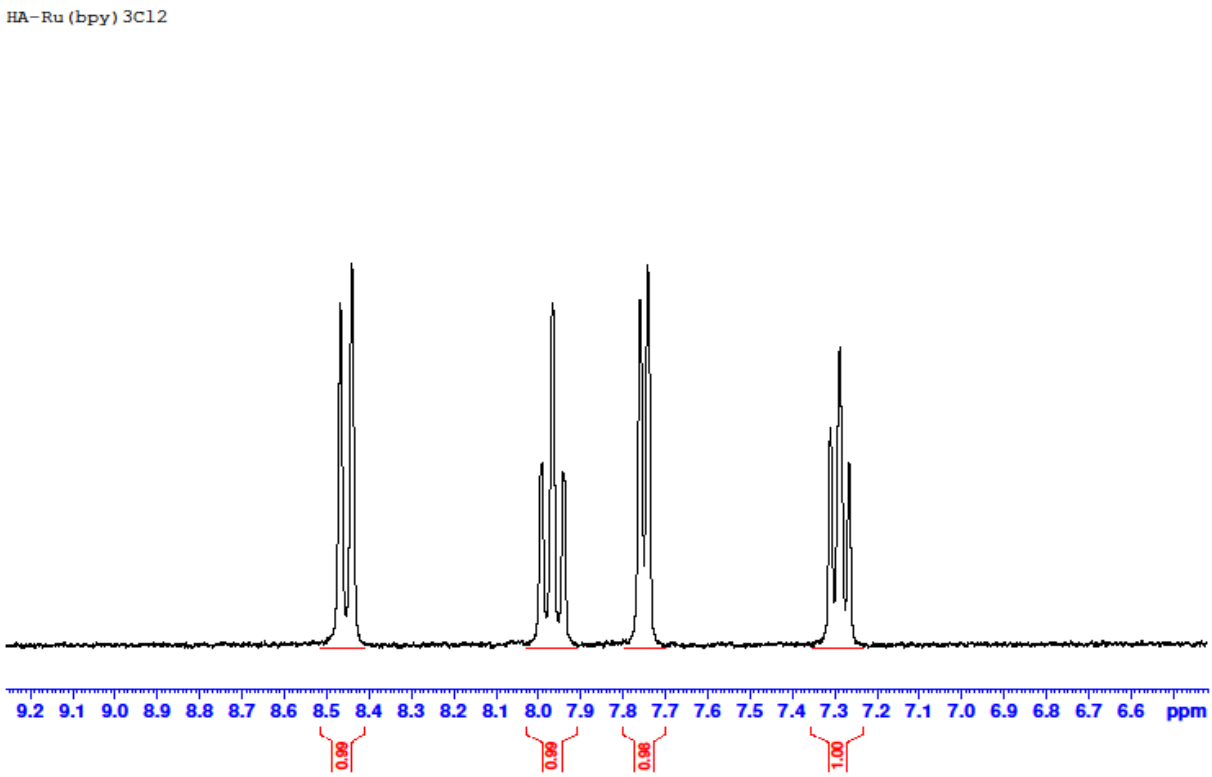

Figure 3.13: ^{1}H NMR (300 MHz, $CDCl_3$, ppm) spectrum of ruthenium catalyst $[Ru(bpy)_3]Cl_2$ and $[Ru(bpy)_3BF_4]$

3.6 Iridium catalyst

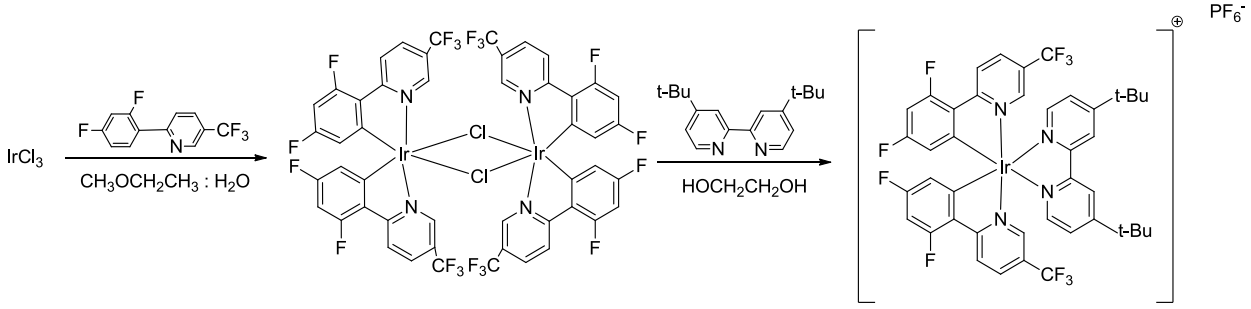

Scheme 1.13: Iridium catalyst [Ir(dF(CF_3)ppy)$_2$(dtbbpy)(PF_6)

The first step in the synthesis of dF(CF_3)ppy involved the coupling of 2-chloro-5-(trifluoromethyl)pyridine with 2,4-difluorophenylboronic acid in the presence of a palladium catalyst (tetrakis(triphenylphosphine)palladium (0)) (PdL_4), via a Suzuki pathway, leading to the formation of a new carbon-carbon bond. Excess arylboronic acid was removed from the reaction mixture by aqueous extraction. Subsequently, the remaining catalyst was separated by filtering the sample through silica gel with dichloromethane, thus completing without purification. Subsequently, two eq. of the dF(CF_3)ppy ligand and one eq. of the dtbbpy ligand (4,4′-di-tert-butyl-2,2′-dipyridyl) were added to an iridium (III) metal center according to the synthetic procedure reported in (Section 2.7). The final addition of $^{-}PF_6$ yielded the complex, which was then recrystallized to afford a yellow-green powder.[77]

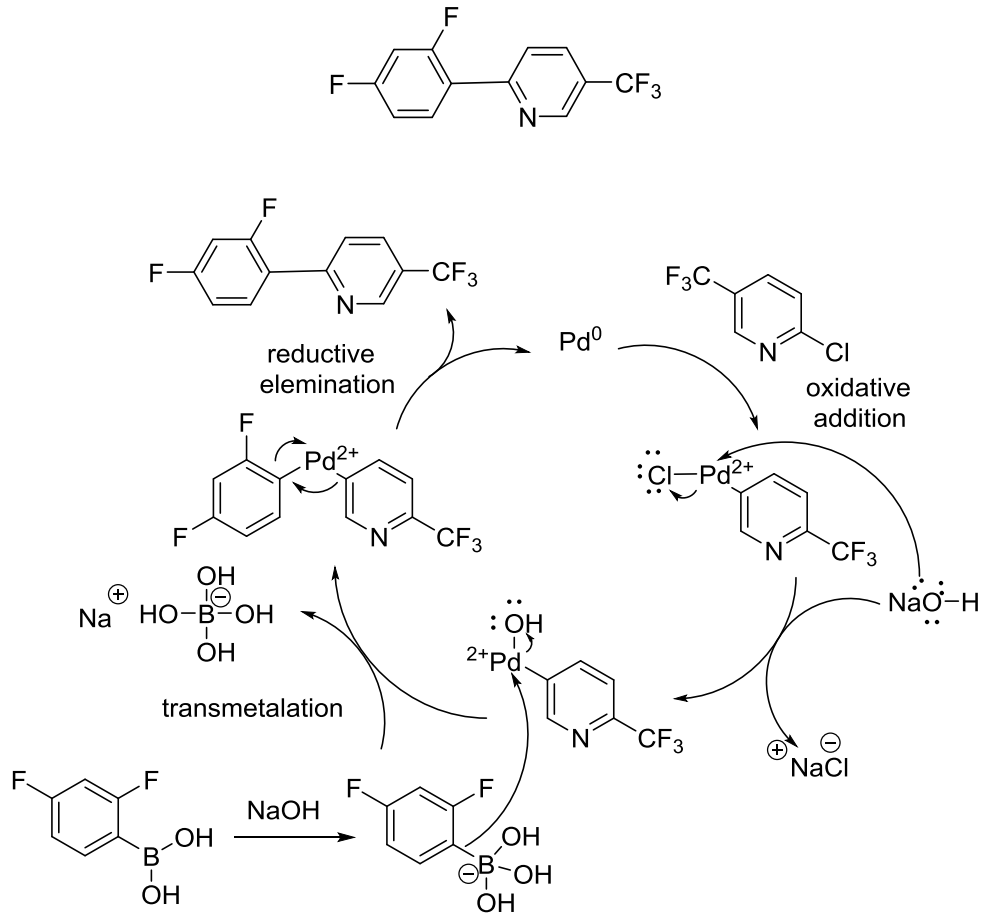

Figure 3.14: dF(CF_3)ppy (an intermediate in the synthesis of iridium catalyst)

The ligand, dF(CF_3)ppy was prepared via Suzuki cross-coupling, as shown in Figure 3.14. The first step of the proposed mechanism involves the oxidative addition of Pd(0) to the aryl halide, 2-chloro-5-trifluromethylpyridine to yield the Pd(II) organopalladium complex. A molecule of the hydroxide or alkoxide base then replaced the halide on the

palladium complex, while another was added to the organoborane to form a borate making its R group more nucleophilic. Transmetalation with the borate then follows where its R group replaces the halide anion on the palladium complex. Reductive elimination then gives the final coupled product, which regenerates the palladium catalyst, and the catalytic cycle can begin again.[92,93,94]

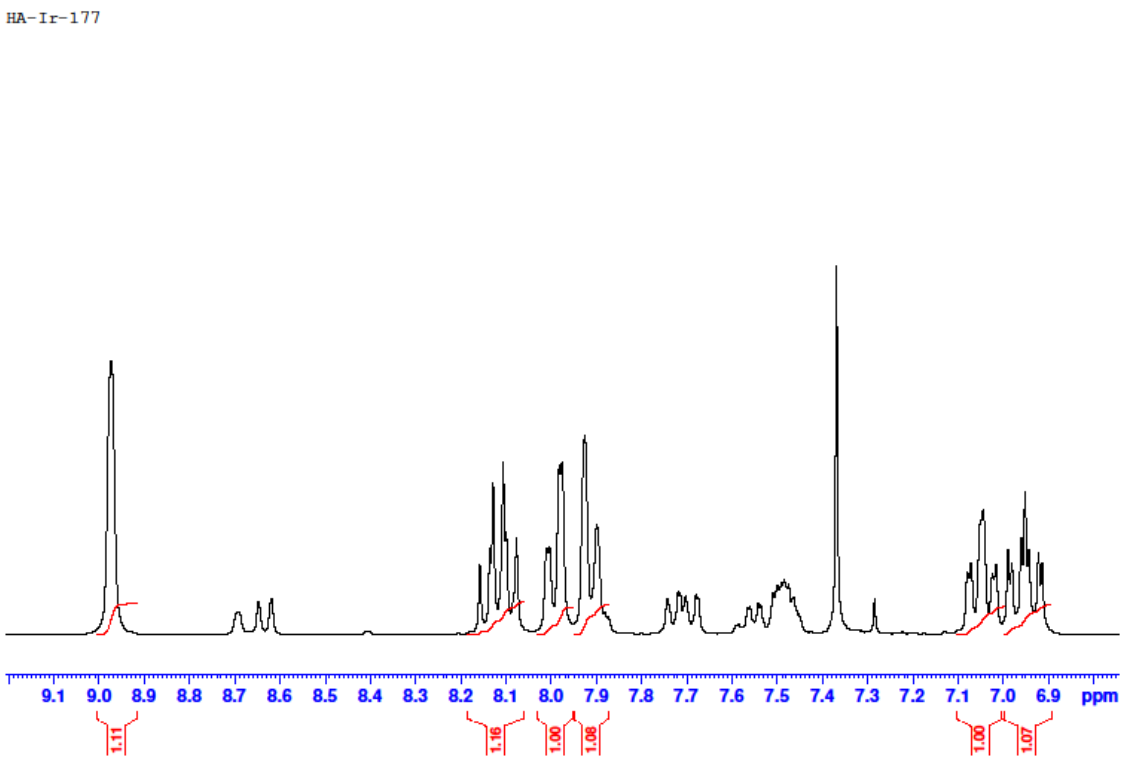

Figure 3.15: ^{1}H NMR (300 MHz, $CDCl_3$, ppm) spectrum of dF(CF_3)ppy ((an intermediate in the synthesis of iridium catalyst)

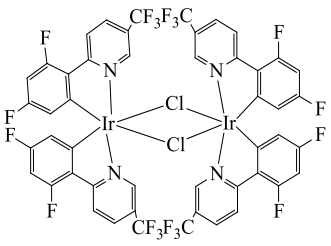

Figure 3.16: $[(dF(CF_3)ppy)_2\text{-}IrCl]_2$ (an intermediate in the synthesis of ridium catalyst)

The second step in the synthesis of the Ir catalyst involved the reaction of iridium trichloride with the $dF(CF_3)ppy$ ligand, as shown in (Scheme 3.14). Figures 3.16 and 3.17 show the ^1H NMR spectra of the dimer and monomer respectively. The chloro-bridged dimer was formed by cyclometalation with phenyl pyridine. Following the this step was the reaction of the dimer with 4,4′-di-t-butyl-2,2′-bipyridine (dtbbpy) to give monocationic iridium (III). Finally, NH_4PF_6 was added, resulting in an anion exchange of Cl^- for PF_6^-, to afford the Ir catalyst, $[Ir(dF(CF_3)ppy)_2(dtbbpy)^+(PF_6)^-$ complex.

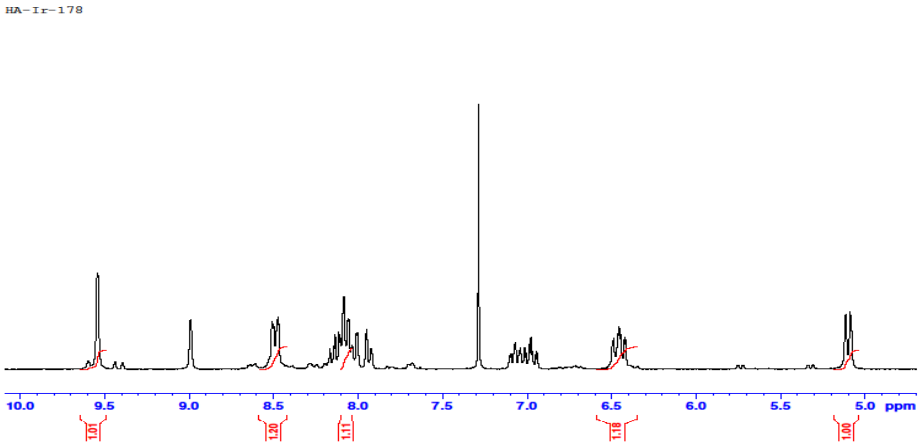

Figure 3.16: ^1H NMR (300 MHz, $CDCl_3$, ppm) spectrum of $[(dF(CF_3)ppy)_2\text{-}IrCl]_2$ (an intermediate in the synthesis of ridium catalyst)

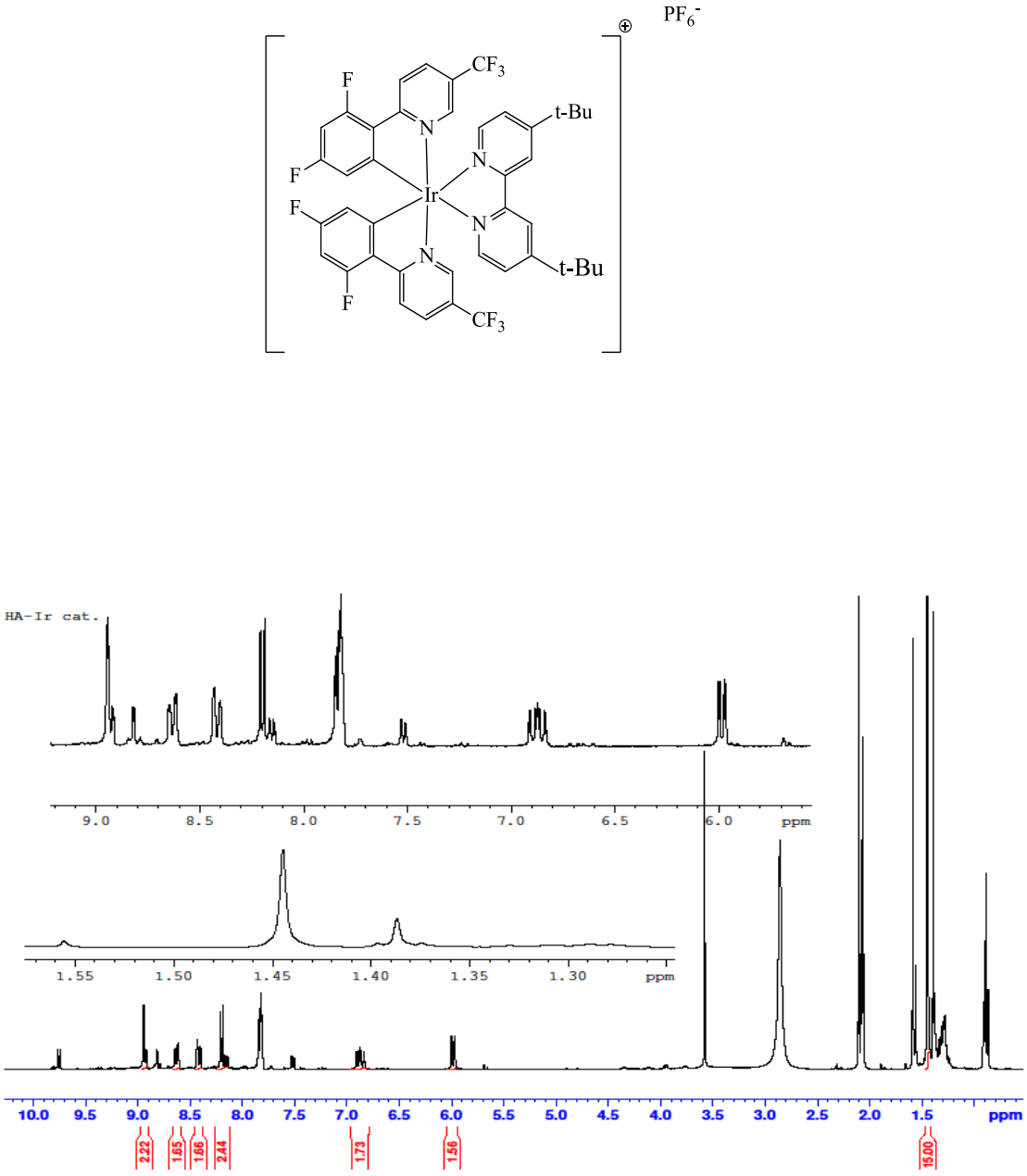

Figure 3.17: ^{1}H NMR (300 MHz, *d*-acetone, ppm) spectrum of [Ir(dF(CF$_3$)ppy)$_2$(dtbbpy)(PF$_6$)

3.7 Photoredox catalyst

Ru and Ir complexes are the most well-known transition metal photoredox catalysts in terms of long lifetimes of their visible-light-excited state. The possible mechanism of the proposed photocatalytic [5+2] cycloaddition reaction of phenol compound and ruthenium catalysis shown in (Scheme 3.15). Although the cycloaddition of phenol compound A was attempted using Ru and Ir catalysts (as well as various solvents, bases, and light sources: as reported in Chapter 2, table 2.1), the expected cycloadduct was not obtained. Also the cycloaddition of phenol compound B was attempted using Ru and Ir catalysts (as well as various solvents, bases and light sources: as reported in Chapter 2), the expected cycloadduct was not obtained. Thus, a new phenol compound called curcuphenol had to be prepared. This phenol possesses a trisubstituted alkene, with two of the substituents being terminal methyl groups. In order to stabilize the cation formed after the first cyclization step, the alkene has to be terminally substituted.

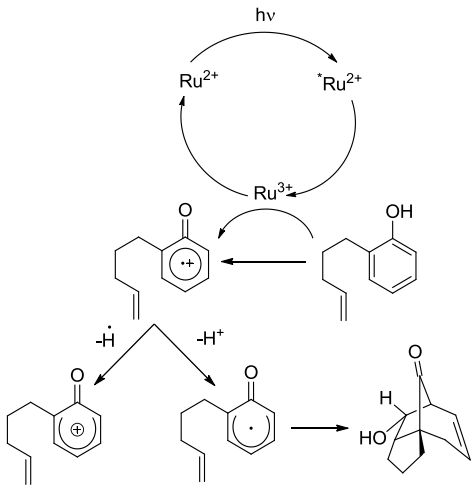

Scheme 3.18: The possible mechanism of the [5+2] cycloaddition reaction of phenol compound

Phenol compound C was prepared using methylmagnesium bromide, and vinylmagnesium chloride as different Grignard reagents, also were tried different concentrations of MeLi, Boc_2O, and the Grignard reagents. As a result, the synthesis of phenol compound D was suggested. A plausible reason for the inability to oxidise phenol compounds A and B, is the mono-substituted nature of these alkenes. This substitution pattern could have led to the instability of the primary cation, which must be stabilised in order to follow the proposed mechanism.

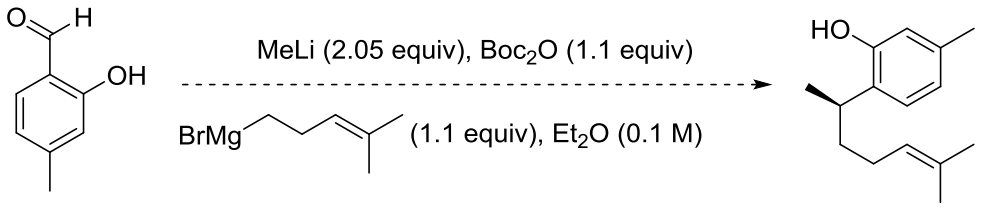

The first step of a photoredox catalysis is the absorption of a photon from visible or UV light. This results in the promotion of an electron from a low-energy orbital to higher-energy orbital, producing an excited state molecule.[4] In the instance of Ru or Ir bipyridine complexes, one electron is promoted from the metal-center to a ligand-centered π^* orbital (MLCT), producing long-lived photoexcited species that can be either reduced or oxidized, depending on the properties of the reactive materials, which can be oxidizing reagent or reducing reagents.

The energy of the light (E) is related to wavelength (λ), light speed (c), and Planck's constant (h), by the relationship $E = hc/\lambda$. Thus, the longer wavelengths of the electromagnetic spectrum in the visible light range (400 to 800 nm) are less energetic (70 to 40 kcal/mol) than those in the UV light range (200 nm to 400 nm; 150 to 70 kcal/mol).

As a result, UV light is most often used in photochemical reactions. Care should be taken when using lamps for photoreaction. The glassware being used for the photoreaction should be transparent to the light from the lamp. There are different types of glass used in photoreactions. One common type is quartz glass, which absorbs at wavelengths shorter than 170 nm. As a result, quartz glass was used in the UV photoreaction phase of this thesis. In addition, Pyrex glass was used in visible light photoreactions, since this glass absorbs at wavelength longer than 275 nm. The common solvents used in photoreactions are non-polar hydrocarbons. Toluene is a preferred solvent because of its high boiling point of about 110 °C. Solvents with low boiling points are not usually ideal because the heat from the light source may cause evaporation.

In addition to isolated sources of UV and visible light (LED and floodlights), sunlight was also explored as a viable light source for photocatalysis. This was achieved by placing the reaction vessel on a window sill, with proper sun illumination. Sunlight was used because its polychromatic nature may provide a combination of both UV and visible light, thus increasing the potential for a photoredox reaction.

The photoreaction experiments performed in this thesis were carried out at room temperature. While low temperatures may provide insufficient heat for the reaction, high temperatures may lead to the degradation of substrates. In addition, UV/Visible light sources caused the heating of the reaction above room temperature. Hence, a water bath for temperature control is useful in such situations.

In the photocycloaddition of phenols, $NaBF_4$ was added to the reaction mixture in order to aid catalyst dissolution. The addition of $LiBF_4$ produces a homogeneous reaction mixture, probably due to the increased solubility of the catalyst. $NaBF_4$ was used instead, due to availability.

The photocatalytic oxidations of phenol compounds A and B were tried under visible light from the sun and using CCl_4 and wet CH_3CN as solvents. A proposed mechanism for the catalytic cycle is reported by Stephenson and co-workers.[83] Upon irradiation with visible light, the ground state Ir(III) is excited to Ir(III)*. Subsequently, the oxidative quenching of Ir(III)* using CCl_4 yields Ir(IV) and the trichloromethyl radical. The electron-deficient Ir(IV) complex then oxidizes the phenol, forming the arene radical cation and regenerating the Ir(III) photocatalyst. The water in the wet solvent donates it to the trichloromethyl radical, forming trichloromethane and OH radical. This radical is incorporated as a substituent of the 7-membered cycloadduct. A possible reason for this reaction is shown below:

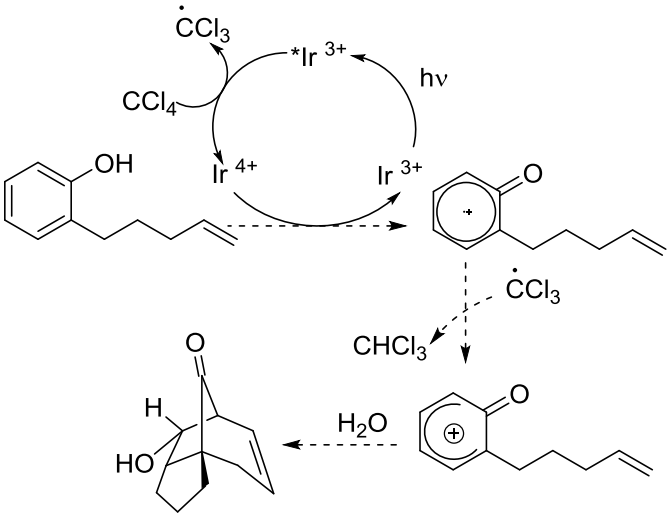

Also, the photocatalytic oxidations of phenol compounds A and B were tried under a light bulbs (white, UV, and blue light) using 1,4-benzoquinone. A proposed mechanism from the catalytic cycle is reported by Yoon and co-workers.[39] The photogenerated Ru^{+3} complex was generated upon light bulb irradiation of Ru^{+2} in presence of 1,4-benzoquinone. Subsequently, the electron-deficient Ru^{+3} complex then oxidizes the phenol, forming the arene radical cation and regenerating the Ru^{+2} photocatalyst and formation of [5 + 2] cycloadducts.

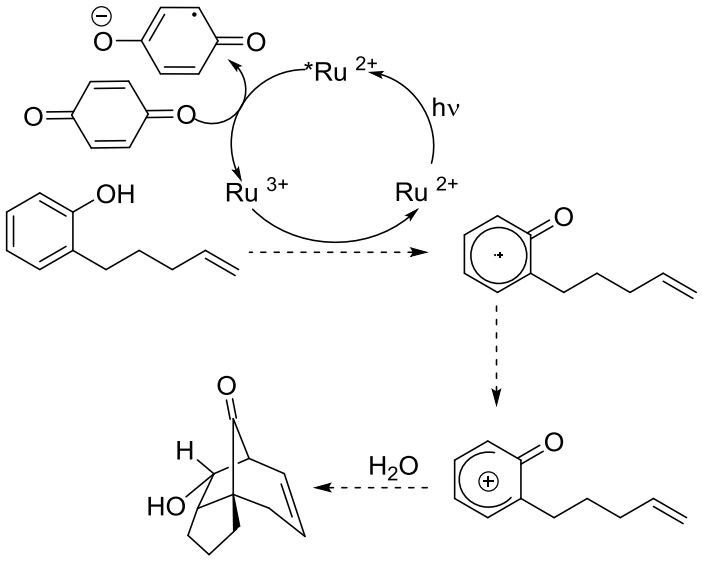

In the photocatalytic oxidations of phenol compounds A, B, and D were tried under light bulb using $K_2S_2O_8$, and $(NH_4)_2S_2O_8$. A proposed mechanism from the catalytic cycle is reported by Yoon and co-workers (as reported in Chapter 1, Scheme 1.10**)**.[84] Upon irradiation with light bulb, the ground state Ru^{+2} is excited to $^{*}Ru^{+2}$. Subsequently, the oxidative quenching of $^{*}Ru^{+2}$ using $(NH_4)_2S_2O_8$ yields Ru^{+3} and a sulfate radical. The

oxidation of phenol generates the corresponding radical cation, which can be further oxidized to generate a resonance-stabilized phenoxonium to afford [5+ 2] cycloaddition reaction.

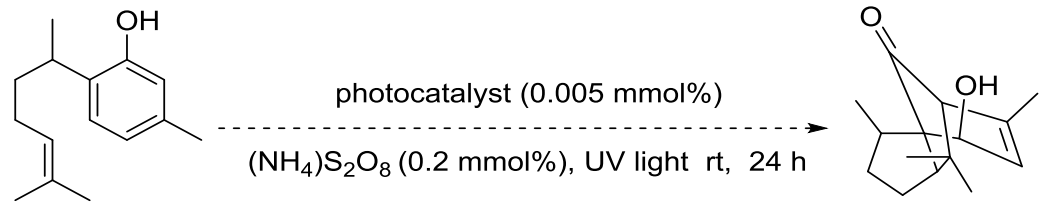

Photoreaction included lead acetate a strong oxidizing agent with the ability to form organolead compounds and act as an acetyloxy moiety source. A proposed mechanism from the catalytic cycle is reported by Pettus and co-workers (as reported in Chapter 1, Scheme 1.4). Reactions of phenols with lead acetate afford cationic intermediates which eventually yield [5 + 2] cycloaddition adducts, after appropriate work-up procedures. As such, lead acetate was used in an attempted [5 + 2] cycloaddition of phenol compounds A and B. Although oxidation reactions of these phenol compounds were tried with different lead acetate salts, inconclusive results were obtained, most likely due degradation of the Pb(OAc) compound.[16]

Electrochemical oxidation of phenol

The electrochemical oxidation of phenol to perform a [5 + 2] cycloaddition reaction was achieved before by Yamamura and coworkers in 1980.[14] Phenols with a double bond at the side chain are subjected to anodic oxidation under various conditions to give tricyclic

compounds depending on functional groups attached to the double bond (as reported in Scheme 1.3). Therefore the electrochemical oxidation of phenol was tried using phenol compound A, cyclic voltammetry and EC-SERS. First, cyclic voltammetry (CV) was performed to determine if the electrode was working properly and whether there was a compact layer formed on the AuNP surface in 0.1 M $TBAF_6$ electrolyte, as seen in (Figure 3.17). CV is used as a qualitative method to determine whether an oxidation and reduction of phenol compound A is formed on an electrode surface. This can be shown by the resultant current measured for the experiment. It was clear that the electrode with the adsorbed phenol compound showed a large increase in the current with scan rate. This result indicates that the phenol compound A was absorbed on the surface of the AuNP, and can be carried forward to do EC-SERS.

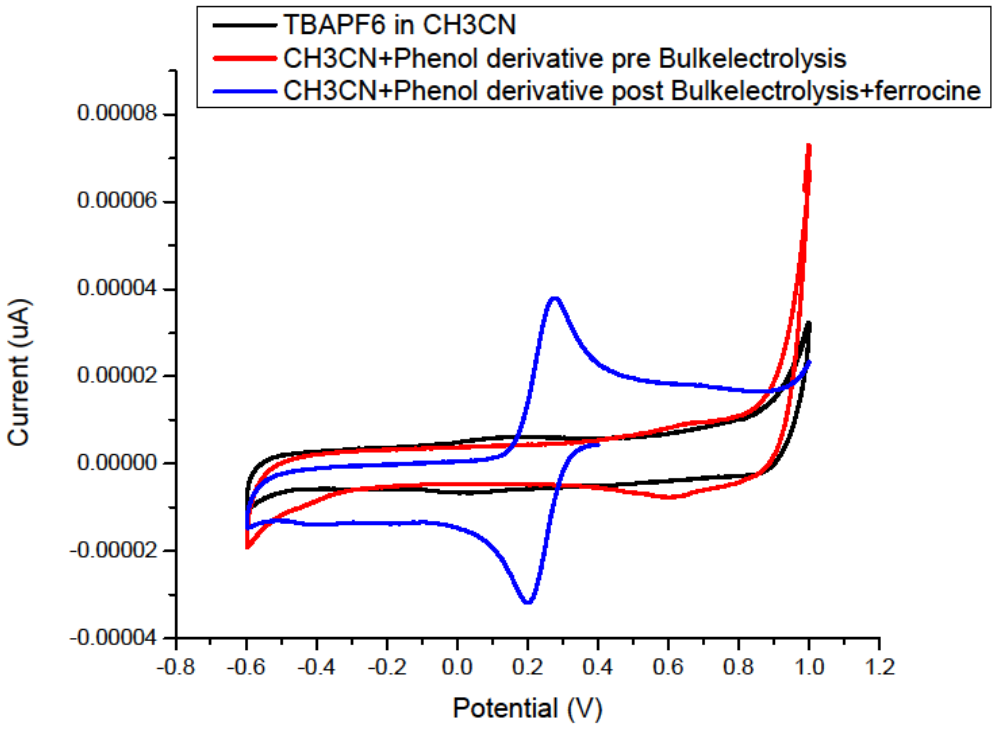

Figure 3.18: CV of phenol compound A before and after bulk electrolysis, and 0.1 M $TPAPF_6$ in CH_3CN. Applied potential (- 0.1, 1 V), collection time = 9 min, on AuNP modified screen printed electrode.

The normal Raman spectra of phenol compound A in (Figure 3.18) was recorded using the 532 nm lasers prior to conducting the EC-SERS measurement in order to identify the prominent Raman bands for this molecule. The bands of phenol compound A are located at 788 cm^{-1}, 1300 cm^{-1}, 1639 cm^{-1}, 1639 cm^{-1}, correspond to the aromatic ring, OH group, and C=C bond of the chain respectively. EC-SERS measurements of phenol compound A were conducted on a screen printed electrode after the carbon working electrode had been modified with gold nanoparticles, in 0.1 M TBAPF6 as a supporting electrolyte. The

signals were recorded at open circuit potential (ocp), and over the potential range of 0.0 to -0.6 V to 1V. The only observable signals were located at 925 and 1380 cm^{-1} of CH_3CN.

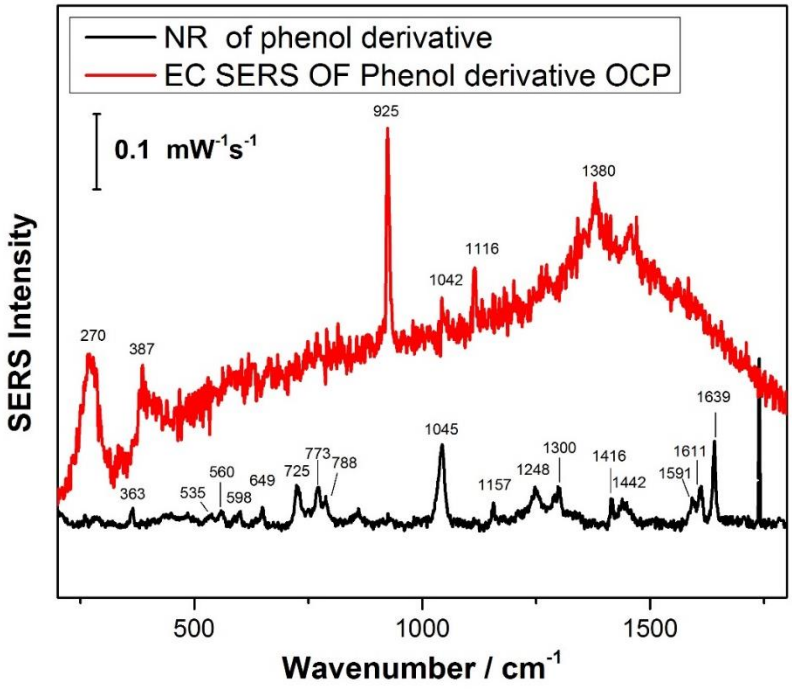

Figure 3.19: Raman spectra of phenol command A using 532 nm (3 mW, 30 s), and Enhanced SERS signal as a result of oxidation in phenol 10 µL, and 0.1 M $TBAPF_6$ was electrolyte in CH_3CN, applied potential (0.0 to - 0.6), increments 1 V, collection time = 60 s. Laser wavelength= 780 nm.

Conclusion

The scope of the novel ring-constrained [5 + 2] cycloaddition reaction using ruthenium and iridium catalysts has been explored and somewhat expanded. The successful synthetic routes of the $[Ru(bpy)_3Cl_2]$, $[Ru(bpy)_3BF_4]$, and $[Ir(dF(CF_3)ppy)_2(dtbbpy)](PF_6)$ catalysts have been demonstrated. However, even with the use of such strong tools, the photocatalytic oxidation of phenols A and B to yield [5 + 2] cycloaddition products was not achieved. While the synthesis of phenol compounds D7 and D10 was successful, not enough of these compounds was available to proceed to the [5 + 2] cycloaddition step. According to the proposed mechanism, in order to stabilize the cation formed after the first cyclization step, the alkene has to be terminally substituted. The phenol compounds D7 and D10 possess a trisubstituted alkene, with two of the substituents being terminal methyl groups. This leads us to believe that the photocatalytic [5+2] cycloaddition reaction of the phenol compounds D7 and D10 will be fruitful, and this could also be a plausible reason for the inability to oxidise phenol compounds A and B because of the mono-substituted nature of these alkenes. It is hoped that in the future the photocatalytic [5 + 2] cycloaddition reactions of the phenol compounds D7 and D10 can be proved feasible using ruthenium and iridium catalysis.

While initial electrochemical and luminescence studies of phenol compound A have been disappointing, it is hoped that as part of the future work, electrochemical methods using EC-SERS and CV on the phenol compounds can be further investigated using electrolytes other than $TBAPF_6$ in CH_3CN.

Appendix

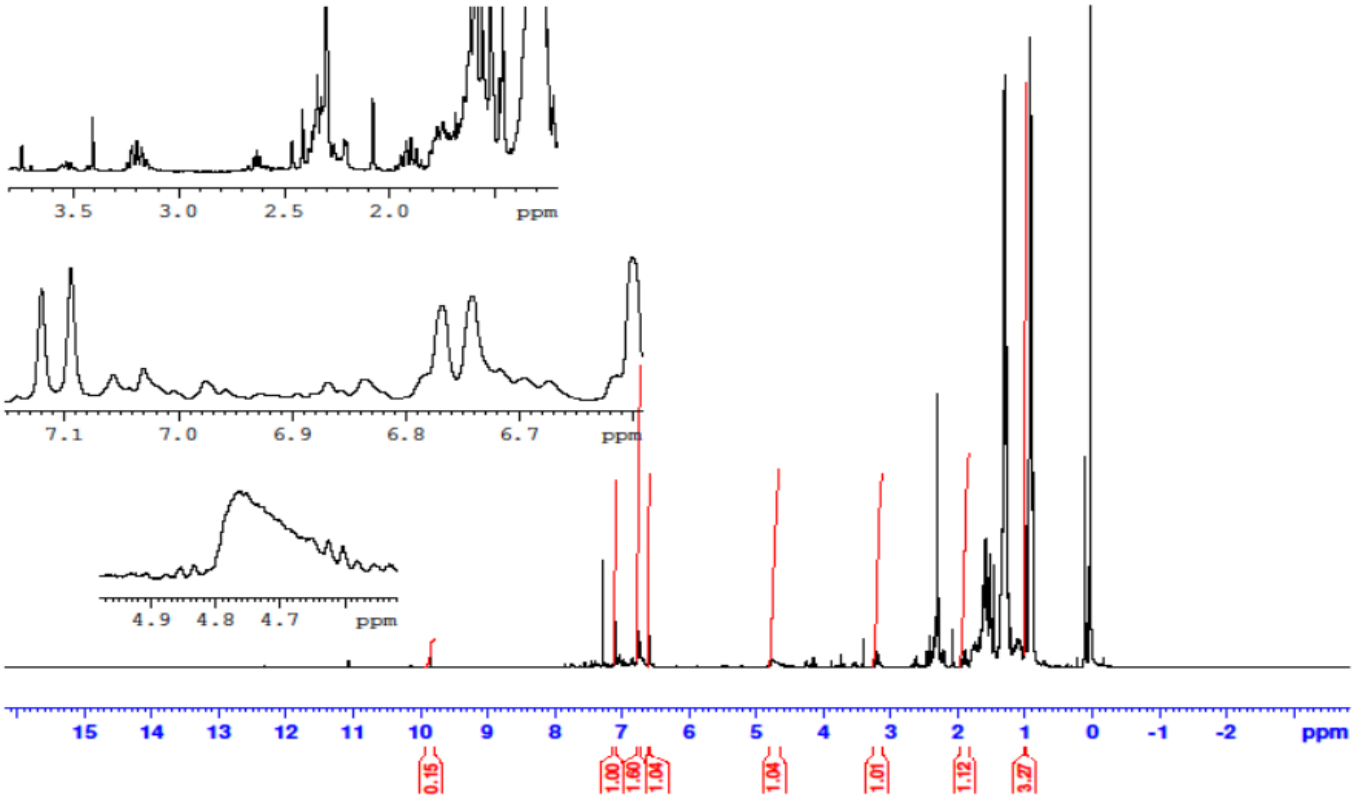

Figure 49: 1H NMR spectra of phenol compound C1 using 4-methymagnesium bromide.

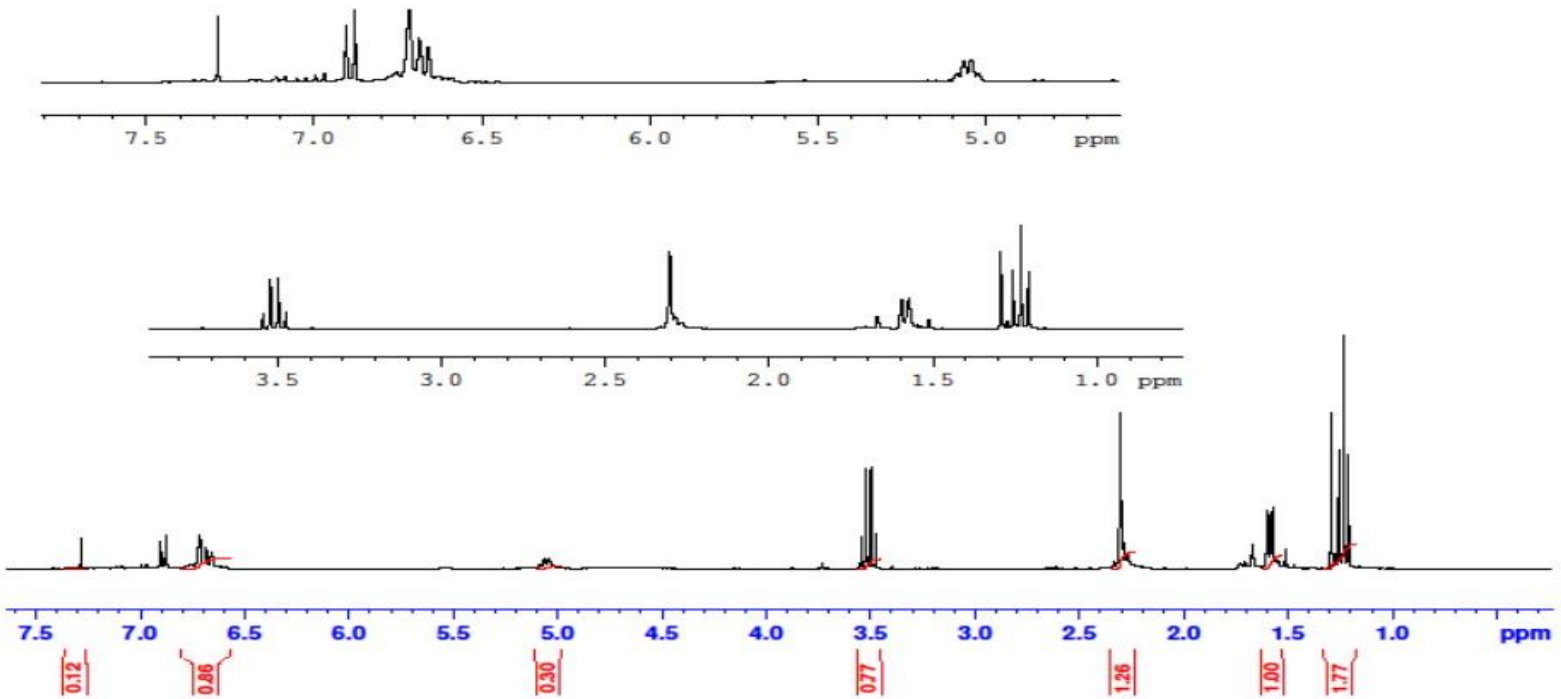

Figure 50: ^{1}H NMR spectra of phenol compound C1 using 4-methymagnesium bromide, and acsses BOC_2O.

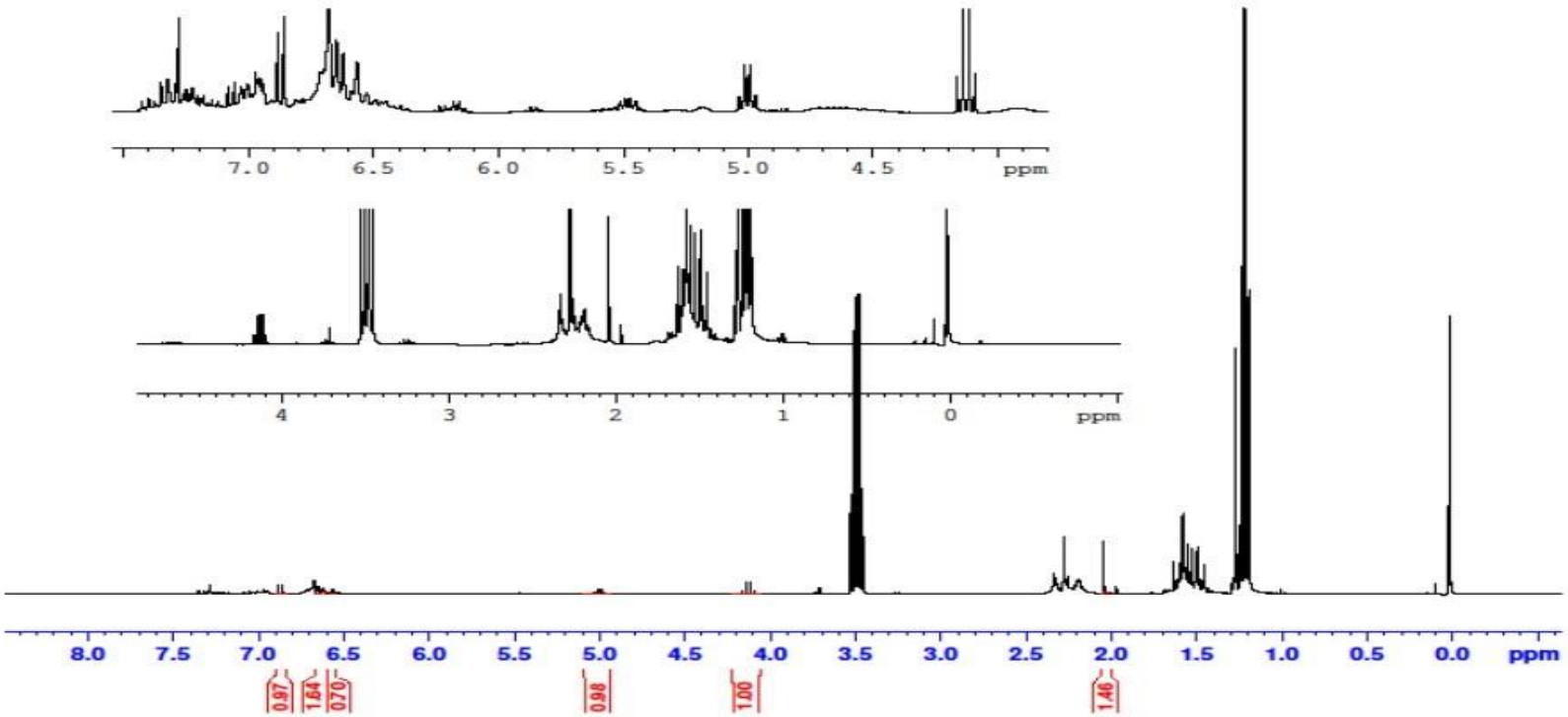

Figure 51: ^{1}H NMR spectra of phenol compound C1 using 4-methymagnesium bromide, and acsses CH_3MgBr.

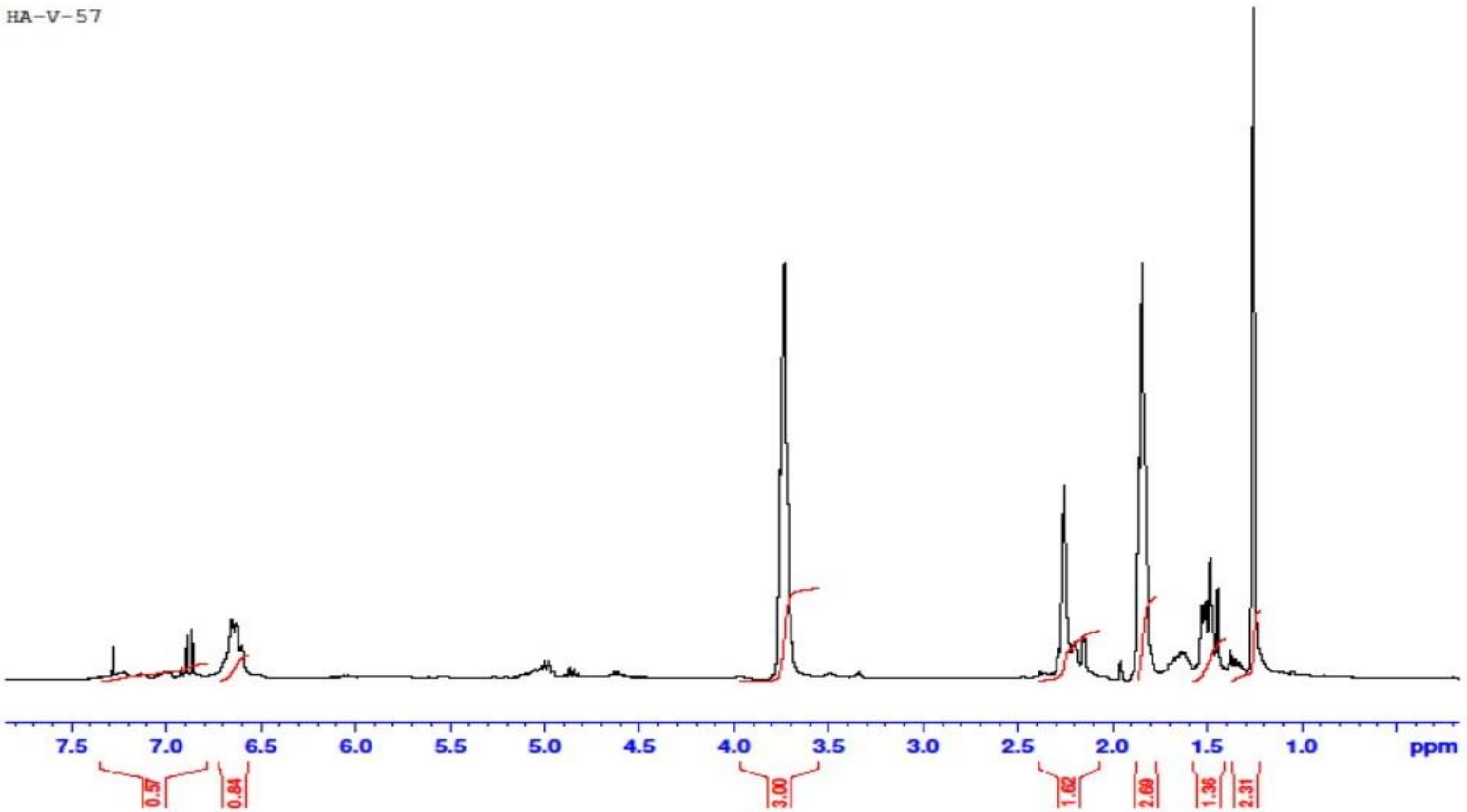

Figure 52: ^{1}H NMR spectra of phenol compound C1 using vinyl magnesium chloride.

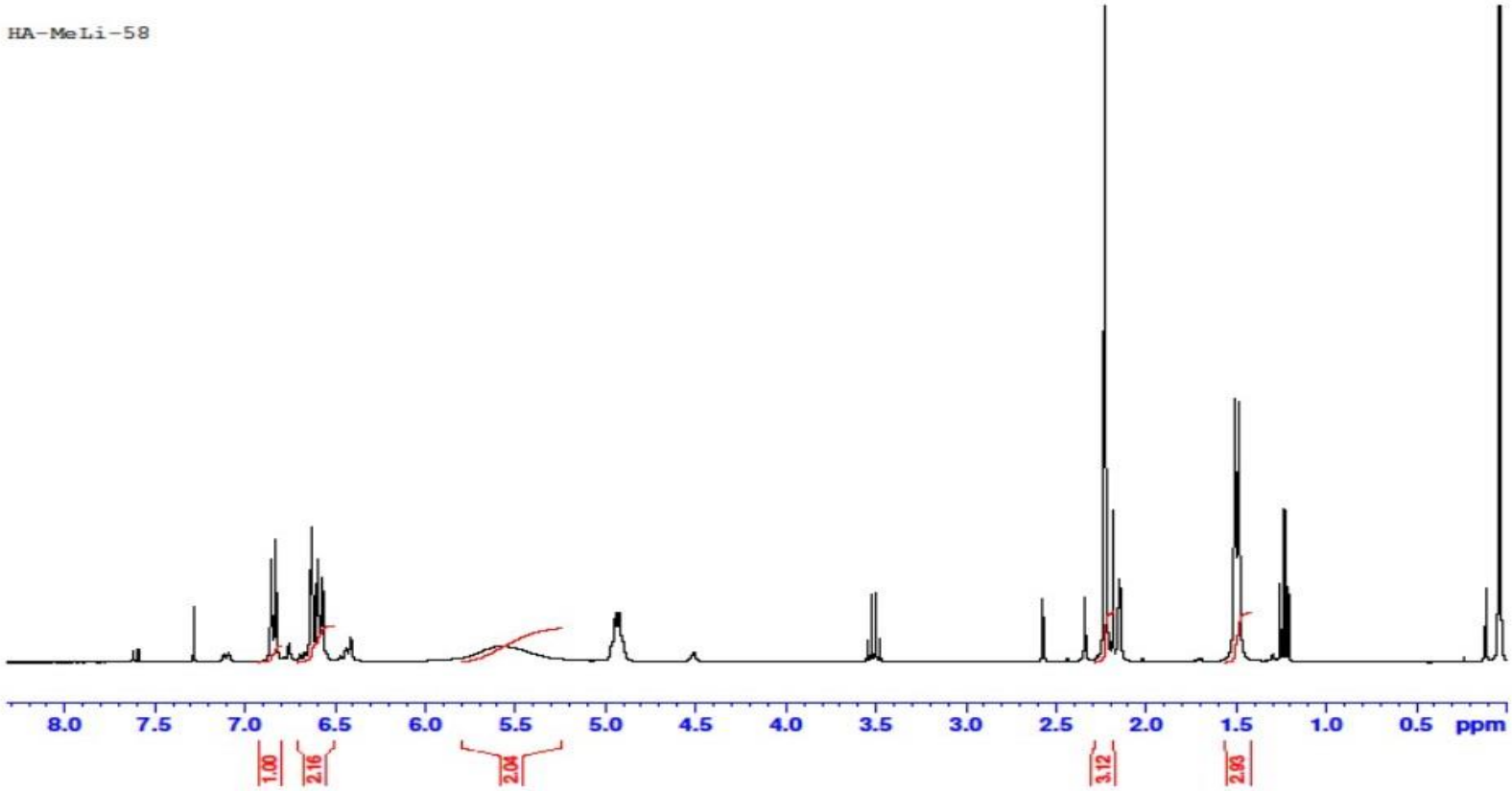

Figure 53: ^{1}H NMR spectra of phenol compound C1 using MeLi.

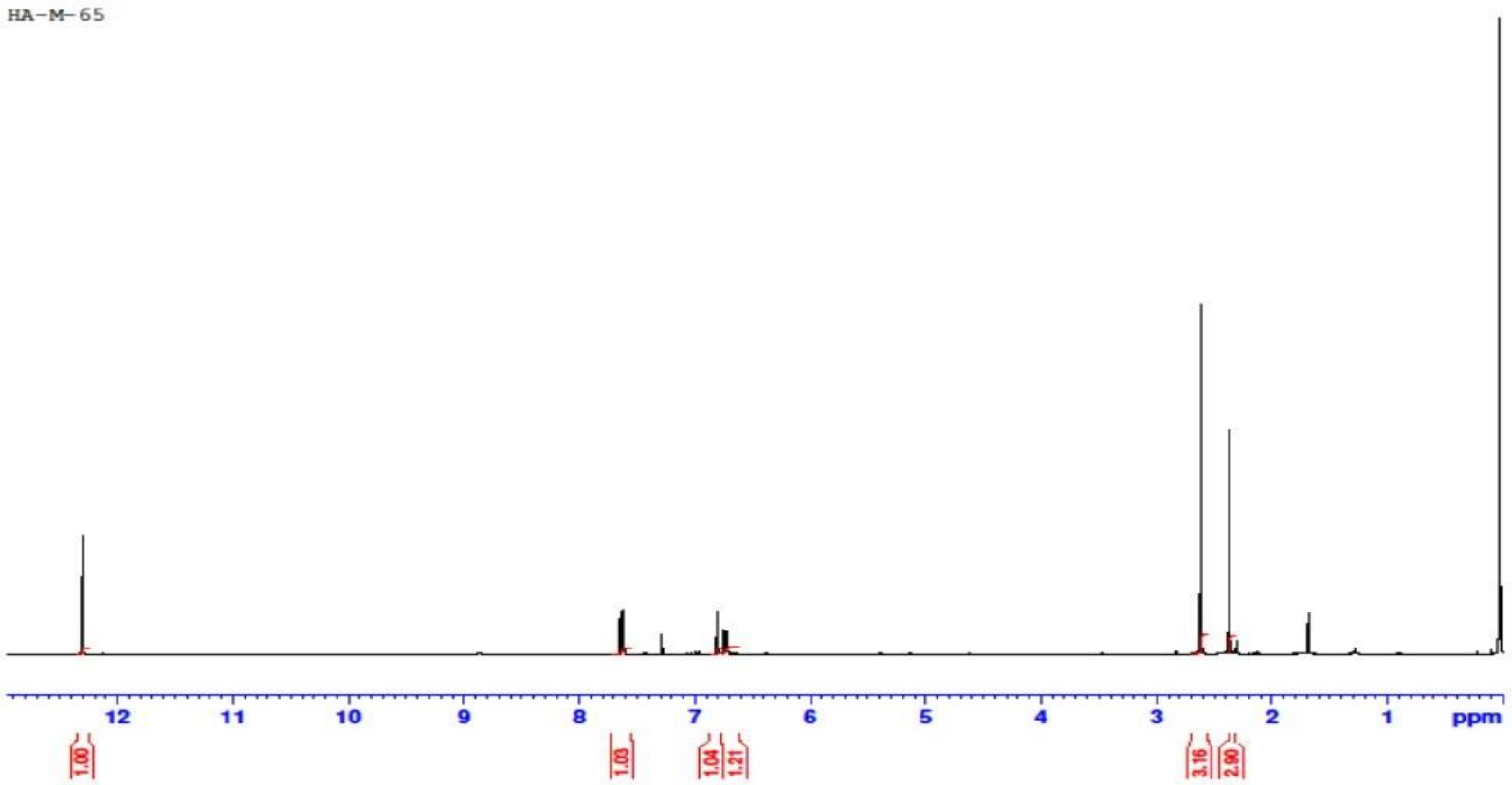

Figure 56: ^{1}H NMR spestra of phenol compound D1 with methylmagnesium bromide.

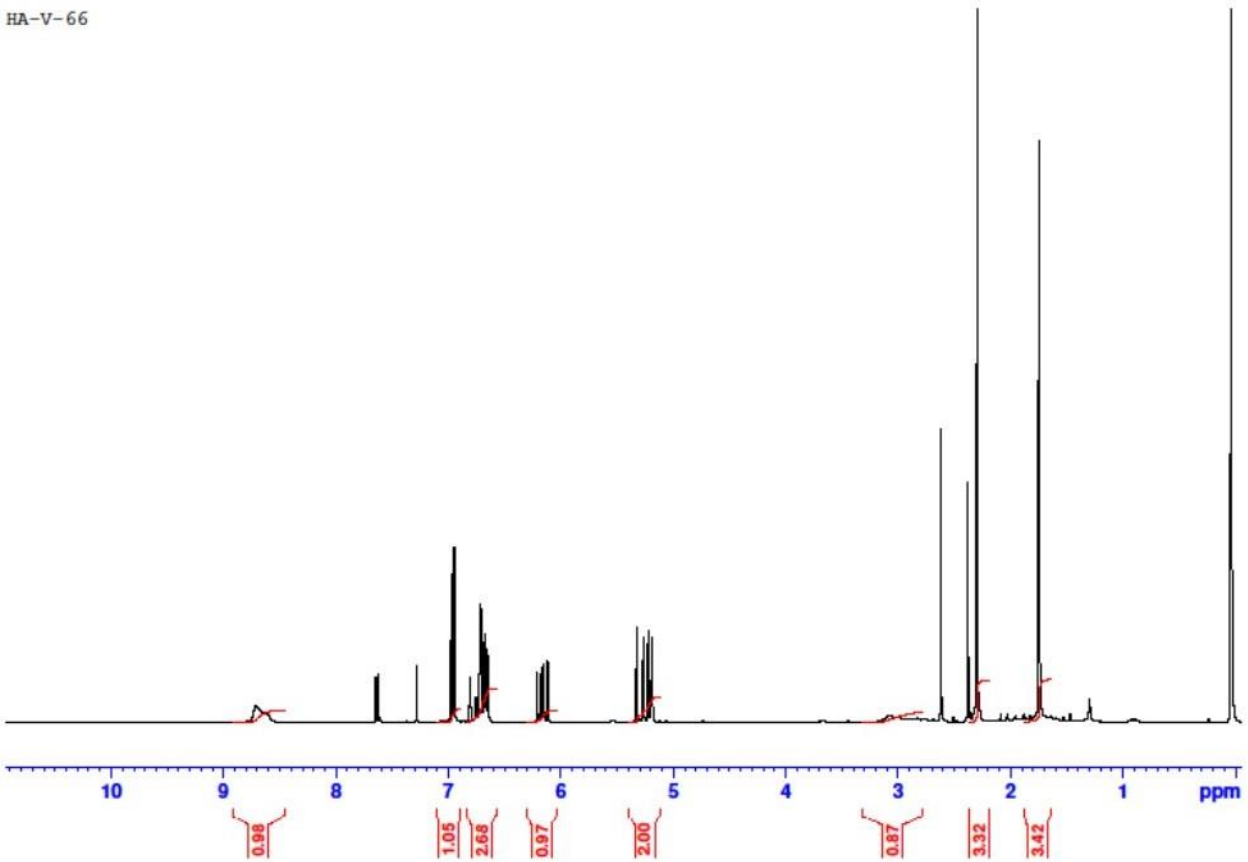

Figure 57: ^{1}H NMR spestra of phenol compound D2 with vinylmagnesium chloride.

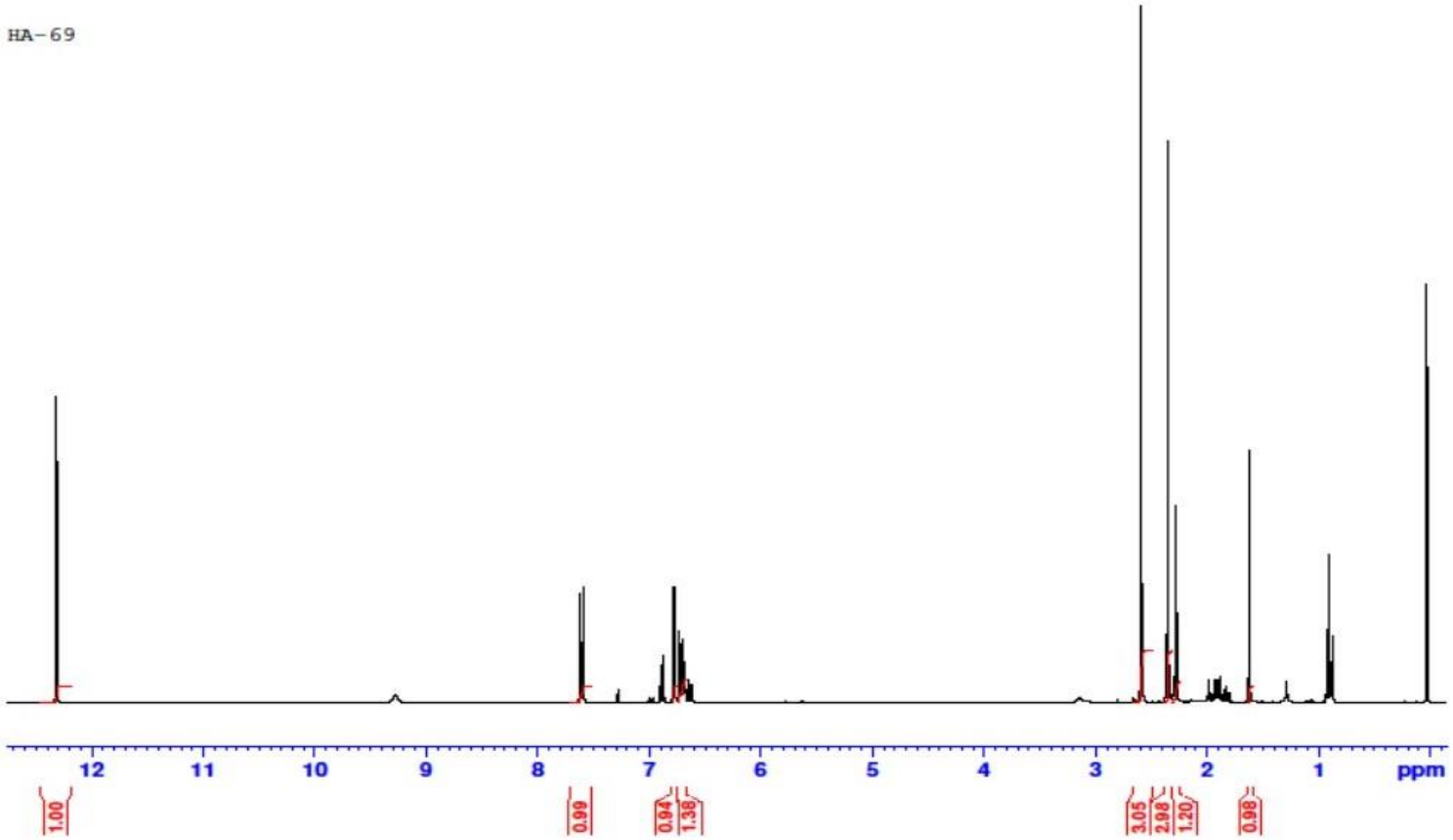

Figure 58: ^{1}H NMR spestra of phenol compound D3 with ethylmagnesium iodide.

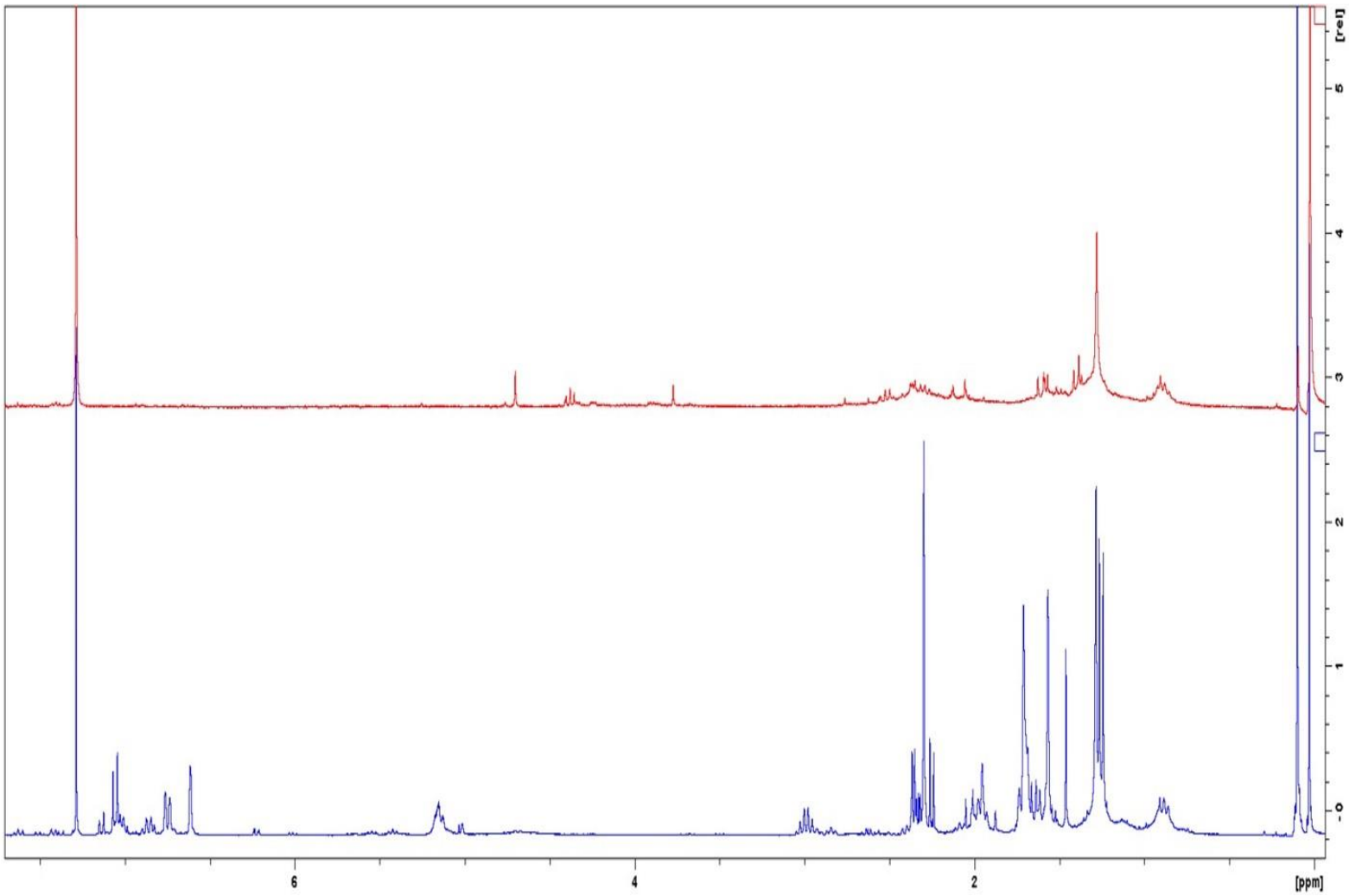

Figure 59: 1 H NMR spectra of photocycloaddition reaction of phenol compound D10 (curcuphenol)

References

1. McNaught, D., & Wilkinson, A. Compendium of Chemical Terminology, 2nd ed. The Cold Book. Wlilkinson. Blackwell Scientific Publication, Oxford, **1997**.

2. Klemperer., & William. *J. Am. Chem. Soc*, **1964**, 86, 5705–5706.
3. Soo Bong., & Han, *Am. Chem. Soc*, **2010**, 132, 15559-15561.

4. Bandara, H. M., Dhammika., & Shawn C. Burdette. *Chem. Soc. Rev*, **2012**, 41, 1809-1825.

5. Quideau, S., L. Pouys-gu, D. Deffieux, C. *Org. Chem*. **2004**, 8, 113-148.
6. Takakura, H., Toyoda, K., Yamamura, S. *Tetrahedron Lett*, **1996**, 37, 4043.
7. Anschutz, R., Leather, W. *Chem. Ber.* **1885**, 18, 715-719.
8. Joseph-Nathan, P., Mendoza, V., Garcia, E. *Tetrahedron*., **1977**, 33, 1573
9. Ylijoki, K. E. O., & Stryker, J. M. *Chem Rev*, **2012**, 113, 3, 2244-2266.

10. (a) Shizuri, Y., Nakamura, K., Yamamura, S. J. *Chem. Soc., Chem. Commun*, **1985**, 530. (b) Maki, S., Suzuki, T., Kosemura, S., Shizuri, Y., Yamamura, S. *Tetrahedron Lett*, **1991**, 32, 4973. (c) Maki, S., Toyoda, K., Kosemura, S., Yamamura, S. *Chem. Lett*, **1993**, 1059. (d) Takakura, H., Yamamura, S. *Tetrahedron Lett*. **1998**, 39, 3717. (26) (a) Shizuri, Y., Yamamura, S. *Tetrahedron Lett*. **1983**, 24, 5011. (b) Shizuri, Y., Suyama, K., Yamamura, S. J. *Chem. Soc., Chem. Commun*. **1986**, 63. (c) Shizuri, Y., Okuno, Y., Shigemori, H., Yamamura, S. *Tetrahedron Lett*. **1987**, 28, 6661. (d) Shizuri, Y., Maki, S., Ohkubo, M., Yamamura, S. *Tetrahedron Lett*. **1990**, 31, 7167. (e) Yamamura, S., Shizuri, Y., Shigemori, H., Okuno, Y., Ohkubo, M. *Tetrahedron*, **1991**, 47, 635. Takakura, H., Toyoda, K., Yamamura, S. *Tetrahedron Lett*. **1996**, 37, 4043. (g) Takakura, H., Yamamura, S. *Tetrahedron Lett*, **1999**, 40, 299.
11. Rossi, M. H., Yoshida, M., & Maia, J. G. S. *Phytoch*, **1997**, 45, 1263-1269.
12. Thoppil, R. J., & Bishayee, A. *World J Hepatol*, **2011**, 3, 228-249.
13. Green, J. C., & Pettus, T. R. R. *J. Am. Chem. Soc*, **2011**, 133, 1603.
14. Ito, Y., R, Kato., K, Hamashima., Y Kataoka., Y Oe., Ohta, T., & Furukawa, I. *Org. Chem*, **2007**, 692, 691-697.

15. Patil, A. D., Freyer, A. J., Killmer, L., Offen, P., Carte, B., Jurewicz, A. J., & Johnson, R. K. *Tetrahedron*, **1997**, 53, 5047-5060.
16. Hoppe, W., Brandl, F., Strell, I., Röhrl, M., Gassmann, I., Hecker, H., Bartsch, G., Kreibich, G., & Szczepanski, C. *Angew. Chem. Int. Ed.* **1967**, 6, 809-810.

17. Brady, S. F.; Singh, M. P.; Janso, J. E.; & Clardy, J. *J. Am. Chem. Soc*, **2000**, 122, 2116-2117.
18. Kim, S., & Winkler. *J. Chem. Soc. Rev.* **1997**, 26, 387-399.
19. a) Grubbs, R. H.; Miller, S. J.; & Fu, G. C. *Acc. Chem. Res.* **1995**, 28, 446-452. b) Boyer, F.-D. Hanna, I., & Ricard, L. *Org. Lett*, **2004**, 6, 1817-1820.
20. Iimura, S., Overman, L. E., Paulini, R., & Zakarian, A. *J. Am. Chem. Soc.* **2006**, 128, 13095-13101.
21.Trost, B. M., Hu, Y., & Horne, D. B. *J. Am. Chem. Soc*, **2007**, 129, 11781-11790.
22. Stroumsa, G. G., & Kingsley, P. Ancient Philosophy, Mystery, and Magic: Empedocles and Pythagorean Tradition. **1997**

23. Smith, J. D. *The Mathematical Gazette*., **1992**, 76, 189-198.

24. Sarkar, T. K., Mailloux, R., Oliner, A. A., Salazar-Palma, M. *History of wireless*. Vol. 177. John Wiley & Sons, **2006.**
25. Einstein, A. *Annalen der Physic*, **1905**, 322, 132-148.
26. Dhar, N. R., & Mukerji, B. K. *Trans. Faraday Soc.*, **1926**, 21, 489-493
27. Esser, P., Pohlmann, B., & Scharf, H. D. *Angew. Chem. Int. Ed. Engl*, **1994**, 33, 2009-2023.
28. Coyle, J. D. *Introduction to organic photochemistry*. John Wiley & Sons. **1986**.

29. Michalet, X., Shimon W., & Marcus, J. *Chem. Rev.***2006**, 106.5, 1785-1813.

30. Mulhern, D., Brooker, S., Görls, H., Rau, S., & Vos, J. G. *Dalton Trans.*, **2006**, 1, 51-57.

31. Mulhern, D., Lan, Y., Brooker, S., Gallagher, J. F., Görls, H., Rau, S., & Vos, J. G. *Inorg. Chim. Acta*, **2006**, 359, 736-744.
32. Esboui, M., & Nejmeddine, J. *Photochem. Photobiol. Sci* , **2015**, 14, 1127-1137.
33. Lakowicz, J. R., Ray, K., Chowdhury, M., Szmacinski, H., Fu, Y., Zhang, J., & Nowaczyk, K. *Analyst*, **2008**, 133, 1308-1346.

34. Montalti, M., Credi, A., Prodi, L., & Gandolfi, M. T. *Handbook of photochemistry*. CRC press.**2006**. p. 71.

35. Zimmermann, J., Zeug, A., & Röder, B. *Phys. Chem. Chem. Phys*, **2003**, 5, 2964-2969.

36. Balzani, V., Bergamini, G., Campagna, S., & Puntoriero, F. Photochemistry and photophysics of coordination compounds: overview and general concepts. In *Photochemistry and Photophysics of Coordination Compounds I* Springer Berlin Heidelberg. **2007**. p. 1-36.
37. G. Ciamician, *Science*, **1912**, 36, 385–394.

38. Koike, T., & Akita, M. *Inorg. Chem. Front*., **2014**, 1, 562-576.
39. Hopkinson, M. N., Sahoo, B., Li, J. L., & Glorius, F. *Chem. Eur. J*, **2014**, 20, 3874.
40. T. Koike and M. Akita, *Top. Catal*., **2014**, 57, 967.
41. Nicewicz, D. A., & MacMillan, D. W. C. *Science*, **2008**, 322, 975; (b) Nagib., D. A., Scott., M. E. & MacMillan, D. W. C., J. *Am. Chem. Soc*, **2009**, 131, 10875; (c) Shih, H.-W., Vander Wal, M. N., Grange, R. L. & MacMillan, D. W. C. *J. Am. Chem. Soc*, **2010**, 132, 13600.

42. (a) Yoon, T. P., & Du, J., *J. Am. Chem. Soc*, **2009**, 131, 14604 (b) Ischay., Lu, M. A., & Yoon, T. P. *J. Am. Chem. Soc*, **2010**, 132, 8572; (c) Shen, Z. Lu., M., & Yoon, T. P., J. *Am. Chem. Soc*, **2011**, 133, 1162.

43. (a) Narayanam, J. M. R., Tucker, J. W., & Stephenson, C. R. J. *J. Am. Chem. Soc*, **2009**, 131, 8756 (b) Tucker, J. W., Narayanam, J. M. R., Krabbe, S. W., & Stephenson, C. R. J. *Org. Lett*, **2010**, 12, 368 (c) Tucker, J. W., Nguyen, J. D., Narayanam, J. M. R., Krabbe, S. W., & Stephenson, C. R. J. *Chem. Commun*, **2010**, 46, 4985 (d) Furst, L., Matsuura, B. S., Narayanam, J. M. R., Tucker, J. W., & Stephenson, C. R. J., *Org. Lett*., **2010**, 12, 3104 (e) C. Dai, J. M. R. Narayanam and C. R. J. Stephenson, Nature Chem., **2011**, 3, 140; (f) J. D. Nguyen, J. W. Tucker, M. D. Konieczynska and C. R. J. Stephenson, J. *Am. Chem. Soc*, **2011**, 133.

44. (a) Chen, Y., Kamlet, A. S., Steinman, J. B., & Liu, D. R. *Nature Chem*, **2011**, 3, 146 (b) Rueping, M., Vila, C., Koenigs, R. M., Poscharny, K., & Fabry, D. C. *Chem. Commun*, **2011**, 47, 2360 (c) Maji, T., Karmakar, A., & Reiser, O *J. Org. Chem*, **2011**, 76, 736 (d) Andrews, S. R., Becker, J. J., & Gagne´, M. R. *Angew. Chem, Int. Ed*, **2010**, 49, 7274 (e) Borak, J. B., & Falvey,D. E. *J. Org. Chem*, **2009**, 74, 3894 (f) DeClue, M. S., Monnard, P. A., Bailey, J. A., Maurer, S. E., Collis, G. E., Zoick, H. J., Ramussen, S., & Boncella, J. M. *J. Am. Chem. Soc*, **2009**, 131, 931 (g) Koike, T., & Akita, M. *Chem. Lett*, **2009**, 38, 166.

45. Sun Y., Hudson, Z. M., Rao, Y., & Wang, S. *Inorg. Chem*, **2011**, 50, 3373.
46. Dixon, I. M., Lebon, E., Sutra, P., & Igau, A. *Chem. Soc. Rev*, **2009**, 38, 1621.

47. Burstall F.H., *J. Chem. Soc*, **1936**, 173.

48. Paris, J.P., & Brandt, W.W. *J. Am. Chem. Soc*, **1959**, 81, 5001-5002.

49. Kalyanasundaram K., *Photochemistry of Polypyridine and Porphyrin Complexes*, Academic Press, London, **1992**.

50. Balzani V., & Scanola F., *Photochemical and photophysical devices*, in: Reinhoudt D.N., Atwood J.L., Davies J.E.D., MacNicol D.D., Vögtle F. (Eds.), Comprehensive Supramolecular Chemistry, Pergamon Press, Oxford, **1996**, Vol. 10, . 687-746.

51. Sauvage, J. P., Collin J. P., Chambron J. C., Guillerez, S., & Coudret, C. *Chem. Rev*, **1994**, 94, 993-1019.

52. Denti G., Serrani S., Campagna S., Ricevuto V., & Balzani V. *Chem. Rev*, **1991**, 111, 227-236.

53. Cano-Yelo H., & Deronzier A. *J. Chem. Soc*, **1984**, 2, 1093.

54. Elofson , R. M., & Gadallah, F. F. *J. Org. Chem*., **1971**, 36,1769-1771.

55. Kim, S., Rojas-Martin, J., & Toste, F. D. *Chem. Sci*, **2016**, 7, 85-88.

56. Cano-Yelo, H., & Deronzier, A. *Tetrahedron Lett*. **1984**, 25, 5517-5520.

57. Roh, Y., Jang, H. Y., Lynch V., Bauld, N. L., & Krische, M. J. *Org. Lett*. **2002**, 4, 611-613.

58. Yang, J. K., Felton, G. A. N., Bauld, N. L., & Krische, M. J. *J. Am. Chem. Soc.* **2004**, 126 , 1634-1635.

59. Ischay M. A., Anzovino, M. E., Du, J., & Yoon, T. P. *J. Am. Chem. Soc*, **2008**, 130, 12886.

60. Ischay, M. A., Lu, Z., & Yoon, T. P. *J. Am. Chem. Soc*, **2010**, 132, 8572.

61. Crabtree, R. *Acc. Chem. Res.* **1979**, 12, 331.

62. Brown, J.M. *Angew. Chem. Int. Ed.Engl.* **1987**, 26, 190.

63. Yang, D.-Q., Liang, X., Long,Y.-H., Li, X., Fang, S., Wang, S., & Li, C-R. *Organometallics*, **2012**, 31, 3113.

64 (a) Takeuchi, R., Tanaka, S., & Nakaya, Y. *Tetrahedron Lett.* **2001**, 42, 2991. (b) Kezauka, S., Tanaka, S., Ohe, T., Nakaya, Y., & Takeuchi, R. *J. Org. Chem.* **2006**, 71, 543. (c) Matsuda, T., Kadowaki, S., Goya, T., & Murakami, M. *Org. Lett.* **2007**, 9, 133.

(d) Takeuchi, R., & Nakaya, Y. *Org. Lett.* **2003**, 5, 3659 (e) Farnetti, E., & Marsich, N. *J. Organomet. Chem.* **2004**, 689, 14.
65 a) Shibata, T., & Takagi, K. *J. Am. Chem. Soc.* **2000**, 122, 9852 (b) Shibata, T., Toshida, N., Yamazaki, M., Maekawa, S., & Takagi, K. *Tetrahedron*, **2005**, 61, 9974. (c) Jeong, N., Kim, D. H., & Choi, J. H. *Chem. Commun.* **2004**, 1134. (d) Shibata, T., Kadowaki, S., Hirase, M., & Takagi, K. *Synlett*, **2003**, 573.
66. Zhao, Y., Chen, J. R., & Xiao, W. *J. Organic Letters*. **2016**, 18, 6304-6307.
67. Stothers, J. *Carbon-13 NMR Spectroscopy: Organic Chemistry, A Series of Monographs*. Vol. 24. Elsevier, **2012**.

68. Cavanagh, J., Fairbrother, W. J., Palmer, A. G., Skelton, N. J. *Protein NMR spectroscopy: principles and practice*. Academic Press, **1995**.

69. Neuhaus, D., & Williamson, M, P., *The Nuclear Over hauser Effect in Structural and Conformation Analysis*, VCH, New York, **1989**.
70. Snyder, J. P. *J. Am. Chem. Soc*, **1989**, 111, 7630-7632.

71. Vékey, K., Telekes, A., & Vertes, A. *Medical applications of mass spectrometry*. Amsterdam: Elsevier. **2008**.
72. Siuzdak, G. *Mass spectrometry for biotechnology*. San Diego, Calif: Academic Press. **1996**.
73. Ferraro, J. R., & Nakamoto, K. *Introductory Raman spectroscopy*. Boston: Academic Press.**1994**.
74. Wang, J. *Analytical Electrochemistry,* 2nd ed.; John Wiley & Sons: New York, **2000**.
75. Harroun, Scott G., & Christa L. Brosseau. *Development of an Electrochemical Surface-Enhanced Raman Spectroscopy Dna Aptamer Biosensor for Rapid Detection of Protein Biomarkers of Disease*. Halifax, N.S: Saint Mary's University, **2014**.
76. Ammann, S. E., Rice, G. T., & White, C. M. *J. Am. Chem. Soc*, **2014**, 136 , 10834-10837
77. McEnroe, F. J., & William F. *Tetrahedron*. **1978**, 1661-1664.
78. Charles, G., Broom. & A., Johan, R. *Reagents for transition metal complex and organometallic syntheses*. **2007**, 28, 17.p 338-340.
79. Lowry, M. S., & Bernhard, S. *Chem. Eur. J*, **2006**, 12, 7970-7977.
80. Tohma, H., Morioka, H., Harayama, Y., Hashizume, M., & Kita, Y. *Tetrahedron Lett*, **2001**, 42, 6899-6902.
81. Nair, V., & Deepthi, A. *Chem Rev*, **2007**, 107, 1862-1891.

82. Blum, T. R., Zhu, Y., Nordeen, S. A., & Yoon, T. P. *Angew. Chem. Int. Ed*., **2014**, 53, 11056-11059.
83. Condie, A. G., González-Gómez, J. C., & Stephenson, C. R. *J. Am. Chem. Soc*, **2010**, 132, 1464-1465.
84. Ischay, M. A., Anzovino, M. E., Du, J., & Yoon, T. P. *J. Am. Chem. Soc*, **2008**, 130, 12886-12887.
85. Freeman, D. B., Furst, L., Condie, A. G., & Stephenson, C. R. *Org. Lett.*, **2012**, 14, 94-97.
86. Blum, T. R., Zhu, Y., Nordeen, S. A., & Yoon, T. P. *Angew. Chem. Int. Ed.* **2014**, 53, 11056-11059.
87. Tucker, J. W., Narayanam, J. M., Shah, P. S., & Stephenson, C. R. *Chem. Commun.* **2011**, 47, 5040-5042.
88. Robinson, A. M., Harroun, S. G., Bergman J., & Brosseau, C. L. *Anal. Chem*. **2012**, 84, 1760-1764.
89. Harroun, S. G., & Brosseau, C. L. *Development of an Electrochemical Surface-Enhanced Raman Spectroscopy Dna Aptamer Biosensor for Rapid Detection of Protein Biomarkers of Disease*. Halifax, N.S: Saint Mary's University, **2014**.
90. J. Wang. *Analytical Electrochemistry*, 2nd ed.; John Wiley & Sons: New York, **2000**.
91. Bolton, E., & Richter, M. M. *J. Chem. Educ*, **2001**, 78, 47.
92. Miyaura, N., Yamada, K., Suzuki, A. *Tetrahedron Letters*, **1979**, 20, 3437-3440.
93. Ali, N. M., McKillop, A., Mitchell, M. B., Rebelo, R. A., & Wallbank, P. J. *Tetrahedron.* **1992**, 48, 8117.
94. Watanabe, T., Miyaura, N., &Suzuki, A. *Synlett*, **1992**, 3, 207-210.